

Supplementary Material for

Molecular architecture of the *Saccharomyces cerevisiae* activated spliceosome

Reinhard Rauhut, Patrizia Fabrizio, Olexandr Dybkov, Klaus Hartmuth, Vladimir Pena, Ashwin Chari, Vinay Kumar, Chung-Tien Lee, Henning Urlaub, Berthold Kastner,*
Holger Stark,* Reinhard Lührmann*

*Corresponding author. Email: b.kastner@mpi-bpc.mpg.de (B.K.); hstark1@gwdg.de (H.S.);
reinhard.luehrmann@mpi-bpc.mpg.de (R.L.)

Published 25 August 2016 as *Science* First Release
DOI: 10.1126/science.aag1906

This PDF file includes:

Materials and Methods
Figs. S1 to S19
Tables S1 to S3
Full Reference List

Other Supplementary Material for this manuscript includes the following: (available at www.sciencemag.org/content/science.aag1906/DC1)

Movies S1 and S2

Materials and Methods

Yeast growth

The *Saccharomyces cerevisiae* 3.2.AID/CRL2101 strain (*MATalpha, prp2-1, ade2, his3, lys2-801, ura3*) carrying the G360D substitution in the helicase domain of Prp2 (53) was kindly provided by Ren-Jang Lin. This mutation renders Prp2 temperature-sensitive at 35 °C. Yeast spliceosomes assembled in the presence of this temperature-sensitive Prp2 mutant stop at the stage of the B^{act} complex. Yeast was grown in yeast extract/peptone medium (Formedium™) in a 100 L fermenter to a density of OD₆₀₀ 4. Biomass was collected by centrifugation. Cell pellets were washed with cold water and resuspended in a volume of 1 ml per g cells in AGK buffer (20 mM HEPES-KOH pH 7.5 4°C, 200 mM KCl, 1.5 mM MgCl₂, 10% v/v glycerol, 0.5 mM DTT, 0.5 mM PMSF) containing protease inhibitors (Roche). Drops of this slurry were frozen in liquid nitrogen.

Whole-cell extract preparation

Frozen beads were ground at 18,000 rpm in a Retsch ZM200 nitrogen mill. The yeast powder was thawed at room temperature and then centrifuged at 4 °C for 30 min in an A27-8x50 rotor (Thermo-Scientific). The supernatant was then centrifuged for 1 hour at 4 °C in a T647.5 rotor (Thermo Scientific) at 42,000 rpm. The clear middle phase in each tube was collected (ca. 60–70% of total volume) and dialyzed three times for 2 hours against 5 L each of buffer D (20 mM HEPES-KOH pH 7.5 4°C, 50 mM KCl, 0.2 mM EDTA, 20% (v/v) glycerol, 0.5 mM DTT, 0.5 mM PMSF), using SnakeSkin™ dialysis tubing (7000 MW cut-off, Thermo Scientific). After a final centrifugation in an F14-14x50cy rotor (Thermo-Scientific) (10 min at 9500 rpm) aliquots were frozen in liquid

nitrogen and stored at –80 °C.

Aptamer-tagged pre-mRNA substrate

For affinity purification of B^{act} complexes, cap-free wild-type actin pre-mRNA tagged with three MS2 RNA aptamers (M3-actin) was prepared by T7 runoff transcription in the presence or absence of α-[³²P]-labeled UTP (2). Actin pre-mRNA substrate comprises the end of exon 1, the intron and the 5' end of exon 2 of the yeast actin gene. B^{act} complexes assembled on actin pre-mRNA in the presence of MS2-MBP fusion protein were then purified on amylose affinity columns.

Splicing reaction and affinity purification of B^{act} complexes

Splicing reactions were performed in a volume of 36 ml or multiples thereof. Dialyzed prp2-1 extract was thawed in cold water and then incubated at 35 °C for 30 min to heat-inactivate the Prp2 protein. For a standard 36 ml reaction a mixture of 0.85 pmol [³²P]-labeled pre-mRNA and 65 pmol unlabeled actin pre-mRNA (the total pre-mRNA concentration in the reaction was ~1.8 nM, with a specific activity of ~160 cpm/fmol) was pre-incubated with a 15-fold molar excess of MS2-MBP protein in 1.5 ml HEPES-KOH buffer (pH 7.3 4°C) on ice for 30 min. The splicing reaction mixture contained 60 mM K-phosphate buffer, pH 7.25 20°C, 0.3% (w/v) PEG8000, 2.5 mM MgCl₂, 2 mM spermidine, 1.8 nM pre-mRNA, 27 nM MS2-MBP, 2 mM ATP and 14.4 ml dialyzed prp2-1 extract. The reaction was allowed to proceed for 1 hour at 23 °C. Thereafter the reaction mixture was centrifuged for 10 min at 9000 rpm in a F14-14x50cy rotor (Thermo Scientific) and the supernatant was applied directly to a 0.6 ml column of Amylose Resin™ affinity matrix (NEB), equilibrated with G75 buffer (20 mM HEPES-KOH pH

7.3 4°C, 1.5 mM MgCl₂, 75 mM KCl, 0.01% NP-40 (v/v), 5% glycerol (v/v), 0.5 mM DTT and 0.5 mM PMSF). After loading under hydrostatic pressure, the matrix was washed with 10 volumes of G75 buffer. B^{act} was eluted from the column with G75 buffer containing 100 mM maltose. HEPES-KOH buffer at pH 7.3 4°C had been identified as an optimum buffer for B^{act} complex stability in a thermofluor experiment performed according to Chari *et al.* (54).

Binding of the dominant negative Prp2 G551N protein to the B^{act ΔPrp2} complex

Unlike the prp2-1 ts-mutant protein, which does not remain in the B^{act ΔPrp2} complex, the G551N Prp2 mutant protein, although it does not support splicing, nevertheless binds tightly to the B^{act ΔPrp2} complex (55). For locating Prp2 within the B^{act ΔPrp2} complex, recombinant dominant-negative G551N Prp2 protein (kindly provided by Jana Schmitzovà) was added to the sample after elution from the amylose column. Purified B^{act ΔPrp2} complexes were incubated with 2-fold molar excess of the G551N Prp2 mutant protein. The same molar amount of recombinant wild-type Spp2 was added. After incubation the B^{act+Prp2} complex was loaded directly onto a glycerol gradient.

Glycerol-gradient sedimentation of the B^{act} complex

The B^{act} peak from the amylose column was loaded onto a glycerol gradient [10–30% glycerol (v/v) in G75 buffer containing 0.5 mM each of DTT and PMSF]. Native gradients were run using 4.4 ml polyallomer tubes in a TH660 rotor at 4° C for 17 hours at 21,000 rpm. When particles were centrifuged under cross-linking conditions, DTT and PMSF were omitted from the gradient, the 30% solution was supplemented with 0.1% EM-grade glutaraldehyde (EMS) and the 10% solution was supplemented with 1 mM

PMPI (Thermo Scientific). After centrifugation, gradients were harvested from bottom to top in 24 fractions of about 180 µl. Crosslinked fractions were immediately quenched with 50 mM each of aspartate and cysteine, pH 7. Before electron cryomicroscopy samples were subjected to a buffer exchange against G75 buffer containing 2 mM IPTG and 0.5 mM DTT, but without glycerol and NP-40.

Crosslinking of B^{act} complexes and crosslink identification by mass spectrometry

Approximately 10–20 pmol of purified B^{act} complexes were cross-linked with 150 µM BS3 for 30 min at 25 °C, pelleted by ultracentrifugation and analyzed essentially as described before (56), with the following modifications: precipitated material was dissolved in 4 M urea / 50 mM ammonium bicarbonate, reduced with DTT, alkylated with iodoacetamide, diluted to 1 M urea and digested with trypsin (1:20 w/w). Peptides were reverse-phase extracted and fractionated by gel filtration on a Superdex Peptide PC3.2/30 column (GE HealthCare). 50 µl fractions corresponding to an elution volume of 1.2–1.8 ml were analyzed on a Thermo Scientific Orbitrap Fusion Tribrid and on Sciex TripleTOF 5600+ (dataset 1), Thermo Scientific Q Exactive (dataset 2) or Q Exactive HF (dataset 3) mass spectrometers. Protein-protein crosslinks were identified by pLink1.22 or 1.23 search engine and filtered at FDR 1% (pfind.ict.ac.cn/software/pLink) according to the recommendations of the developers (57). For simplicity, the crosslink score is represented as a negative value of the common logarithm of the original pLink score, that is Score = $-\log_{10}$ ("pLink Score"). The crosslinks observed with at least 2 spectral counts are listed in Table S2. For model building, a maximum distance of 3 nm between the Cα-atoms of the crosslinked lysines was allowed. The actual distribution of Cα-Cα distances

between crosslinked residues that can be mapped in the model of the B^{act} complex is shown in Fig. S19.

EM and image processing

Purified spliceosomes were allowed to adsorb on a thin carbon film prior to rapid plunge freezing into liquid ethane at 100% humidity and 4 °C. Images were recorded at -193 °C in a Titan Krios electron microscope (FEI Company, The Netherlands) on a Falcon II direct electron detector at 74.000x magnification resulting in a pixel size of 2 Å on the specimen level. We extracted ~1 million particle images from the micrographs and applied several sorting steps at the 2D and 3D level. The first sorting was based on CTF parameters by applying multivariate statistical analysis and classification to power spectra as implemented in Imagic-5 (58). Only particles in classes revealing isotropic Thon rings were used for the subsequent rounds of sorting. 2D multivariate statistics and classification was then applied to the non-aligned particle images and subsequently to the aligned particles. In each round, particles contributing to bad classes were excluded from further processing. The remaining ~650.000 particles were then CTF corrected by CTFFIND (59) and applied to 3D classification in RELION (60). For the high-resolution structure determination, the ~122.000 particles contributing to the best 3D class were used for refinement revealing an 8Å resolution structure. Roughly 30% of the spliceosome density were not clearly defined at this level of resolution. As these densities largely disappear during the higher-resolution structure calculations, we excluded them with a mask in the final rounds of the refinement. A soft mask with a cut-off of 6 voxel was used for the refinement and for the determination of resolution. We obtained 5.8 Å resolution for the final map by using the Fourier-shell-correlation function calculated

from two independent data sets and a threshold of 0.143. The molecular components which were masked away are indicated in Figures S12, S13 and S17. A local resolution plot revealed that there are indeed areas of high resolution in the catalytic RNP core of the B^{act} complex that approach the maximum achievable resolution limit corresponding to the Nyquist frequency (4 Å). Some peripheral regions have somewhat lower resolution.

Model fitting and building

Available X-ray or homology models of proteins were initially fit into the EM density by CHIMERA (61). Individual models of substructures (e.g. domains or structural motifs) were further fitted as rigid bodies by COOT (62). After visual inspection, the models were adjusted manually in the density, the disordered regions were removed and regions that were reorganized or were not present in the initial models (e.g. loops and various elements of secondary structure) were built in COOT. The detailed processing of protein models incorporated into the B^{act} structure is described in Table S1. Initially, the U5 snRNA model of the *S. cerevisiae* tri-snRNP (13), the U2/U6 snRNA catalytic core and the branch-point helix of the *S. pombe* ILS spliceosome (10), as well as a 5' group II intron fragment (5'-GUUAU/gu-3')(23) were fitted into the 10 Å cryo-EM density by visual inspection in CHIMERA. All further adjustments were done manually by using the COOT program with the 5.8 Å cryo-EM map. The 5' stem-loop of U6 and the U2/U6 helix II were generated by rigid-body fitting of idealized double-stranded RNA helices. Sections of the RNA models that could not be placed unambiguously into a density, or that did not have an associated density because of their high flexibility, are shown in grey in Fig S1 (RNA–RNA interactions). The atomic model was refined by the real space

refinement routines as implemented in PHENIX, using base pairing restraints (63). The RNA model was then validated by the MolProbity server (64). A summary of the Molprobity scores is shown in Table S3. The Molprobity scores for all individual RNA nucleotides from the final model are provided in a separate HTML file. Final visualization was carried out with CHIMERA and PyMOL (<http://www.pymol.org>).

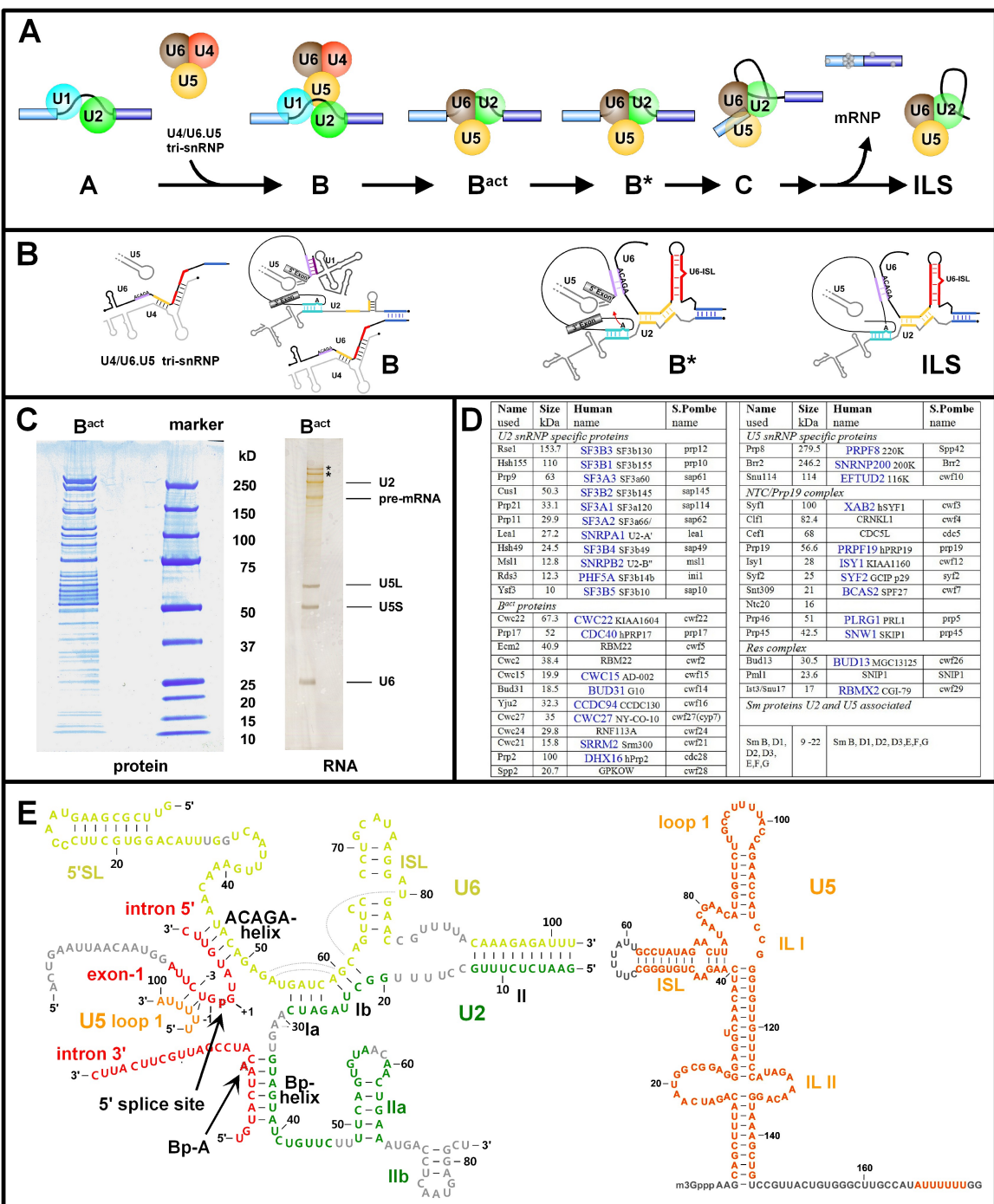


Fig. S1
Purification and characterization of B^{act} spliceosomes from the yeast *Saccharomyces cerevisiae*. (A) Assembly and remodeling steps of the spliceosome during activation and catalysis. (B) RNA–RNA rearrangements occurring during spliceosome

activation and the catalysis of splicing. **(C)** Proteins and RNA isolated from purified B^{act} complexes were visualized on an SDS-polyacrylamide gel by Coomassie blue staining (left) or by silver staining (right). **(D)** Proteins present in yeast B^{act} complexes and their molecular masses. Proteins were identified by mass spectrometry (17). Standard names for human proteins are shown in blue. **(E)** Schematic representation of the secondary structure of RNA in the B^{act} spliceosome. The complete secondary structure of the U5 snRNA is shown on the right. Only selected regions of the pre-mRNA and U2 snRNA are shown. Regions of the RNA that could not be placed unambiguously into the EM density or that did not have an associated density owing to their high flexibility are shown in grey. Tertiary interactions are indicated by stippled lines.

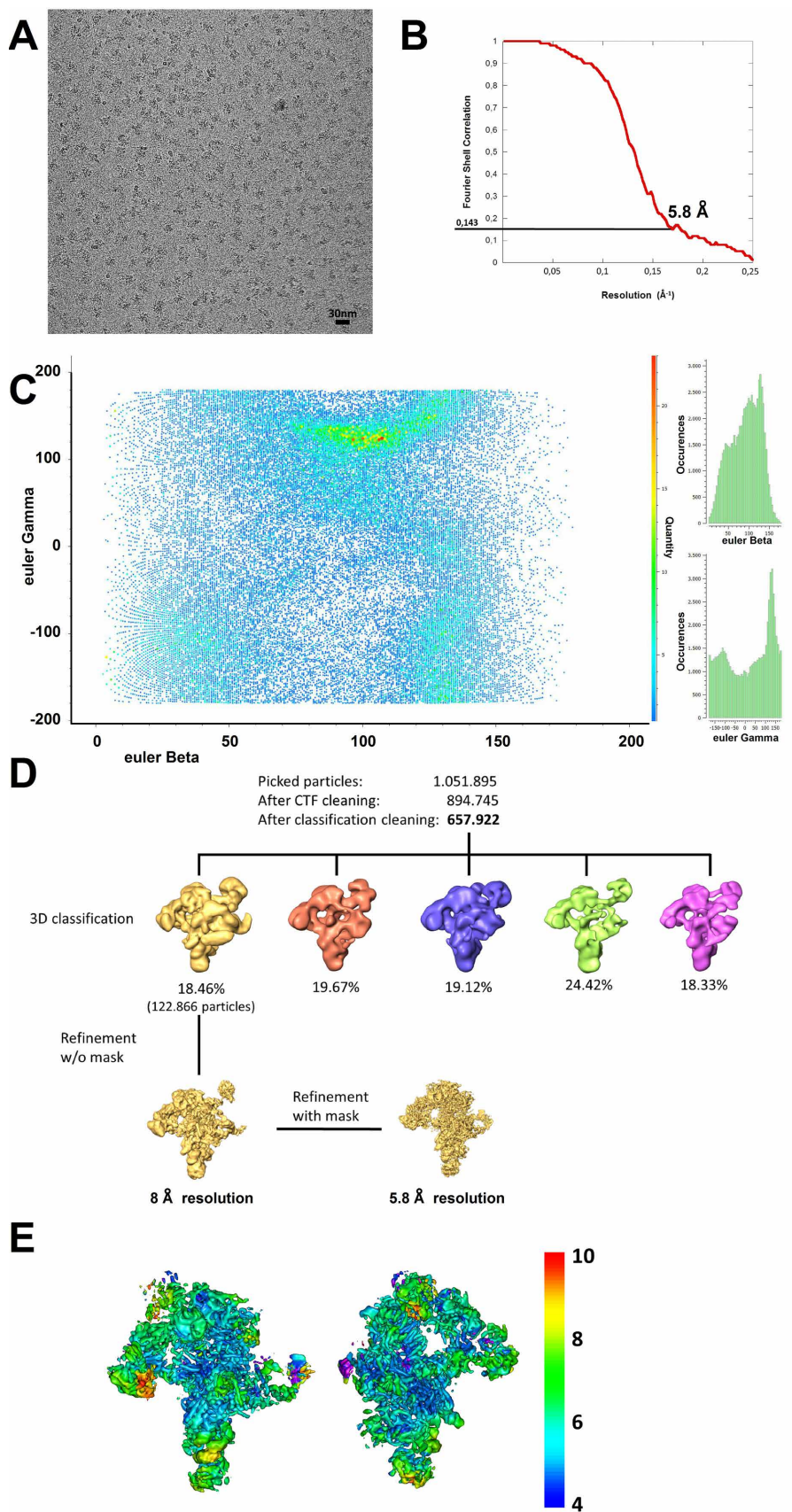


Fig. S2

Cryo-EM and image-processing of the yeast B^{act} complex. **(A)** Typical cryo-EM raw image of *S. cerevisiae* B^{act} spliceosomes recorded with a Titan Krios (FEI Company) electron microscope at a nominal magnification of 74,000x with a Falcon II direct electron detector resulting in a pixel size of 2 Å/pixel. **(B)** Fourier-shell correlation function of two independently refined half data sets indicates a global resolution of 5.8 Å for the masked B^{act} spliceosome comprising ca. 70% of the density of the whole spliceosome. **(C)** Euler angle distribution of all particle images that contributed to the final 3D map. The coordinates describe the beta and gamma angles. Size and color of the plotted dots indicate the number of particles at any given Euler angle. Although one angular orientation of B^{act} dominated, an almost complete angular coverage was obtained. **(D)** Computational sorting scheme. Roughly 1 million particle images were selected from the micrographs. In a first sorting step ~10% of particle images were discarded based on the quality of Thon rings in local power spectra. Another 15% particles were excluded according to multiple rounds of 2D classifications. The remaining 657,922 particles were separated into 5 classes by 3D classification in RELION (60). Images contributing to the best defined spliceosome structure (~18.5%) were then refined to a structure at 8 Å resolution without masking. The final structure at 5.8 Å resolution was obtained by applying a soft mask during the final steps of the refinement process. **(E)** Local resolution plot reveals a resolution distribution from about 4-10 Å with some less well defined parts at the periphery of the complex. Higher resolution regions (in blue, close to 4 Å resolution) were obtained for the centrally-located catalytic core of the spliceosome.

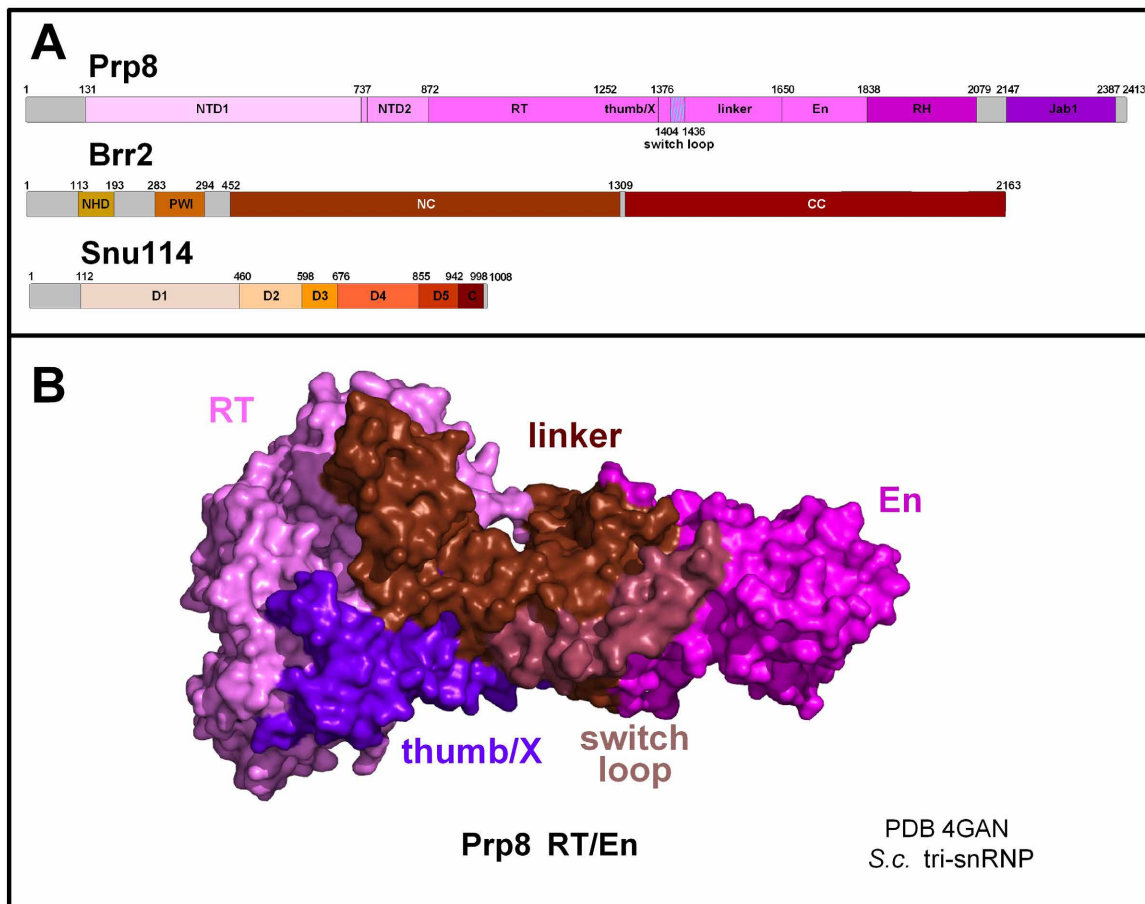


Fig. S3

Structural organization of Prp8, Brr2 and Snu114. (A) Organization of Prp8, Brr2 and Snu114 domains. Prp8, NTD1 and NTD2, N-terminal domains 1 and 2; RT, reverse-transcriptase-like; thumb/X, linker; En, endonuclease-like; RH, RNase H-like; Jab1, Jab1/MPN-like. Brr2, NHD, N-terminal helical domain; PWI, N-terminal, non-canonical PWI domain; NC/CC N-terminal/C-terminal helicase cassette. Snu114, D1–D5 homologous to EF-G/EF-2. (B) Three-dimensional organization of the *S. cerevisiae* tri-snRNP, according to (11). The location of the switch loop is also indicated.

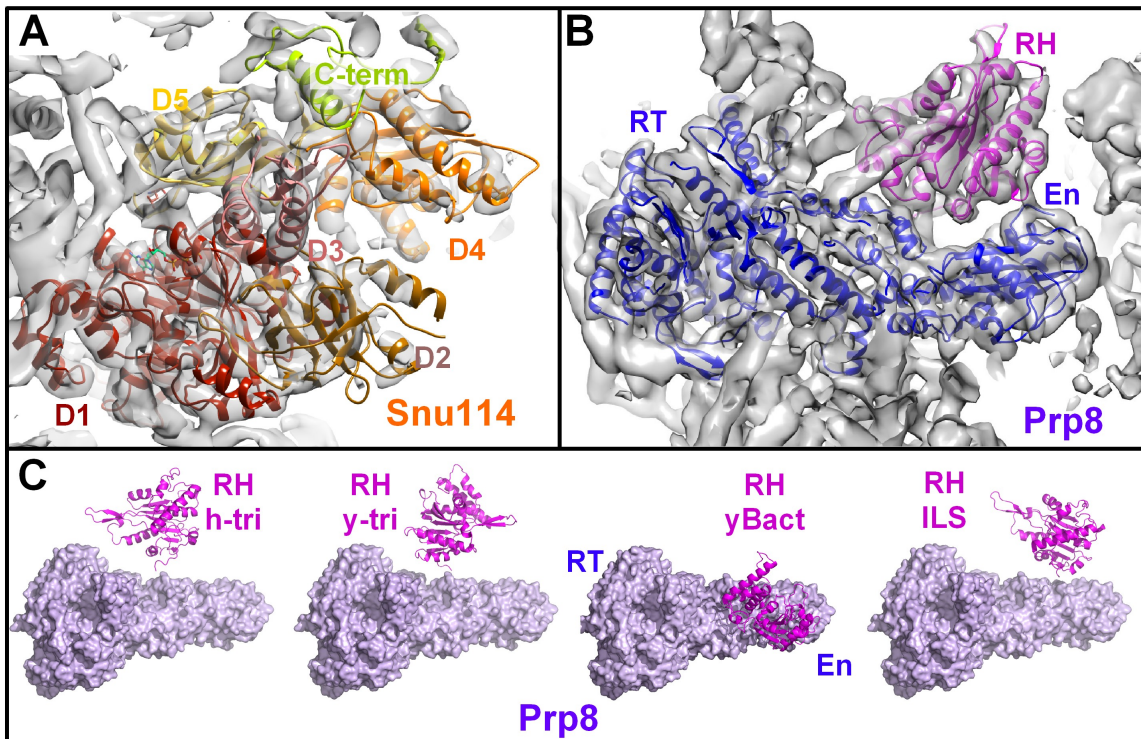


Fig. S4

Structure and location of Snu114 and Prp8 in the yeast B^{act} complex. (A) Density fit of Snu114 domains D1–D5. (B) Density fit of Prp8: RT, reverse-transcriptase-like; En, endonuclease-like; RH, RNase H-like domains; (C) Variation in the position of Prp8's RH domain (magenta ribbon model) relative to the Prp8 En domain in human (h) and yeast (y) tri-snRNPs, and in the *S. cerevisiae* B^{act} complex and *S. pombe* intron-lariat spliceosome (ILS). The structure of the Prp8 (from *S. cerevisiae* B^{act}) RT, thumb/X linker and En domains are shown as a space filling model in grey. In B^{act} the RH domain is closely associated with the “back side” of the En domain, whereby the RH RNA-binding β sheet faces the En domain. The palm edge of the RH domain interacts with the En domain of Prp8 in a region where in the ILS (and tri-snRNPs) the tip of a major β -hairpin-loop (switch loop) is instead located (see also Fig. 2 and text). The density for the

β -hairpin-loop of the RH domain is not well defined in the B^{act} structure, consistent with the possibility that it adopts a more open conformation.

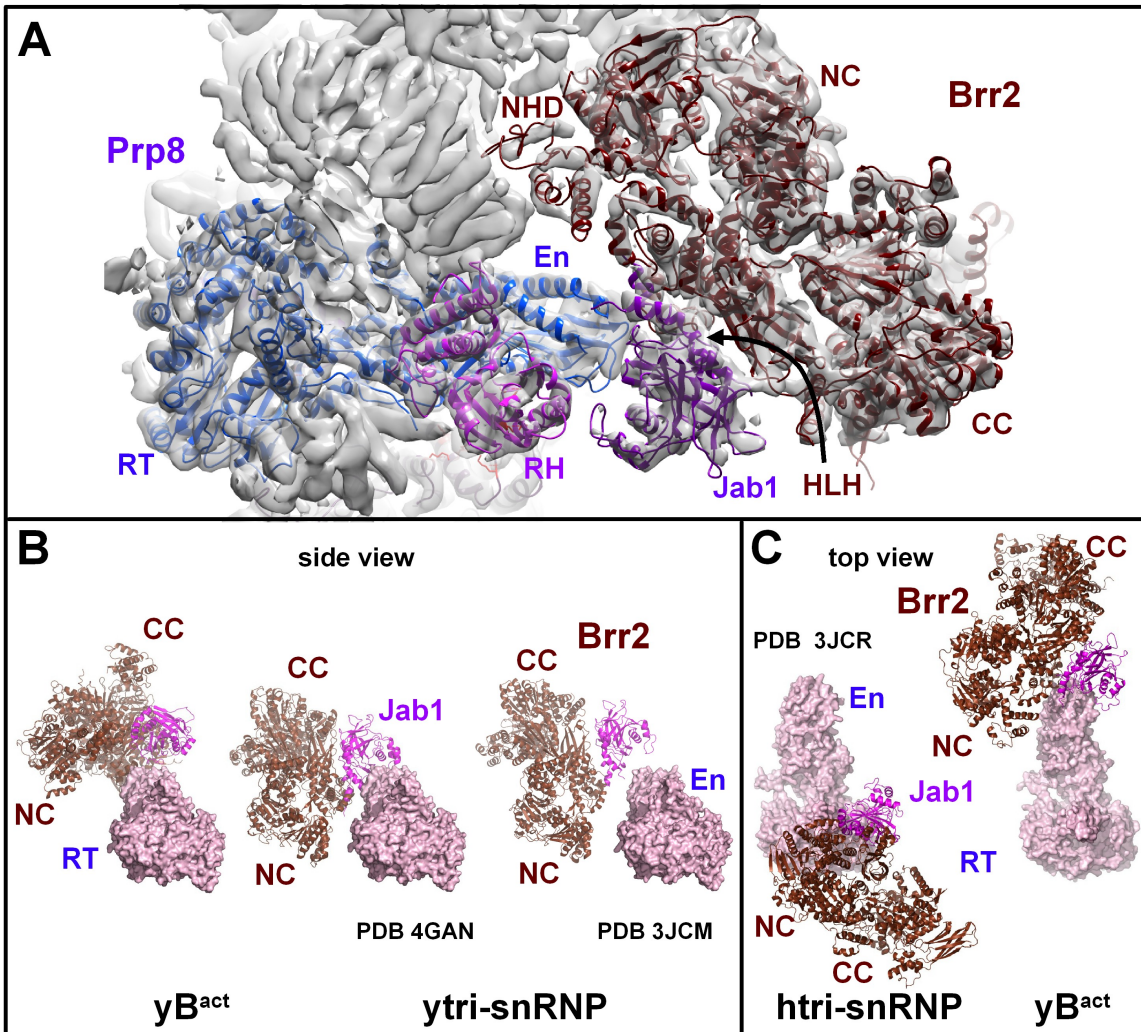


Fig. S5

Structure and location of the RNA helicase Brr2 and Prp8 Jab1 domain. (A) Expanded view of the shallow slope of B^{act} (Fig. 1A) showing the fit of Brr2's helicase region in complex with Prp8's Jab1 domain. The tip of Prp8's En domain interacts with Brr2 through the HLH domain of the NC cassette. **(B)** Brr2 is located at the same end of Prp8's RT/En domain in B^{act} and the yeast tri-snRNP (13-15); however, in the two models Brr2 has a different orientation (side views). **(C)** Top view illustrating that Brr2 is located at radically different positions in the human tri-snRNP (16) and yeast B^{act} complex. It is found at opposite ends of Prp8's RT/En domain in the two models.

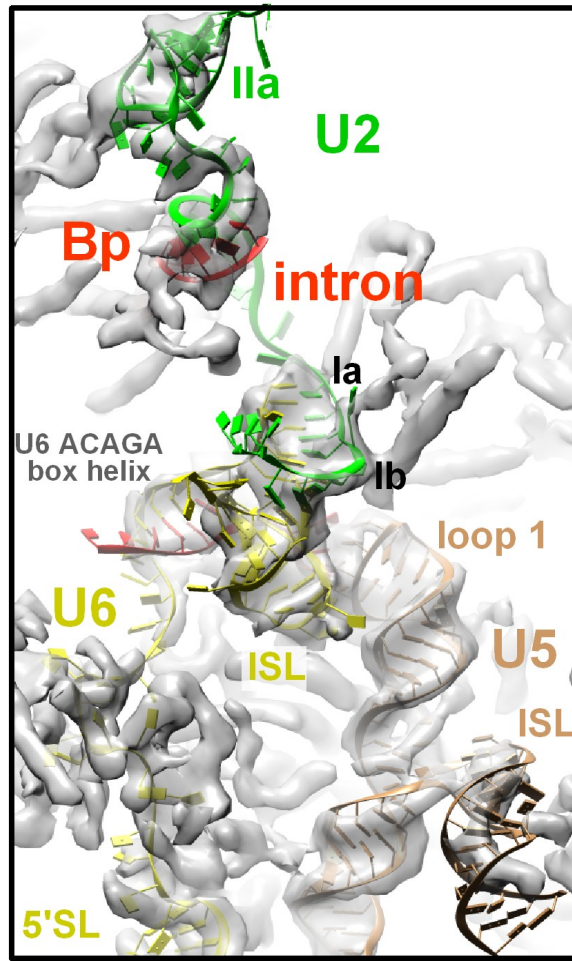


Fig. S6

A close-up view of the central RNA network in the B^{act} spliceosome. Shown is a slice through the spliceosome showing only the high density elements of the cryo-EM map, comprising U5 RNA, U2/U6 catalytic RNA network, the BS/U2 RNA helix, the U6 ACAGA box helix, the U2 RNA helix IIa and corresponding linker regions.

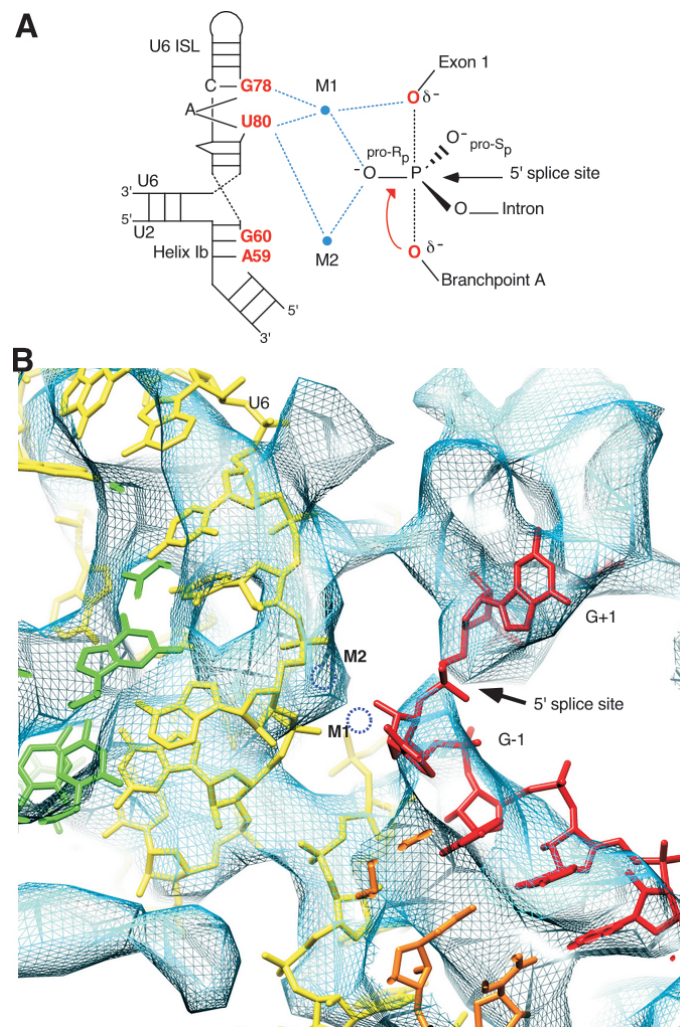


Fig. S7

Putative location of the two catalytic metal ions in the B^{act} complex. (A) Constellation of the catalytic metals for step one of pre-mRNA splicing. The diagram is adapted from (24). The scissile phosphate of the pre-mRNA is shown as a pentacoordinate transition state and the blue dashed lines depict the coordinations of oxygens directly involved in the reaction (red). M2 is further coordinated by A59 and G60. (B) Model of the catalytic RNA-RNA network in the experimental EM map, where U2 snRNA is shown in green, U6 snRNA in yellow, and the pre-mRNA in red. The putative position of the catalytic metal ions are shown as stippled blue circles (see also text).

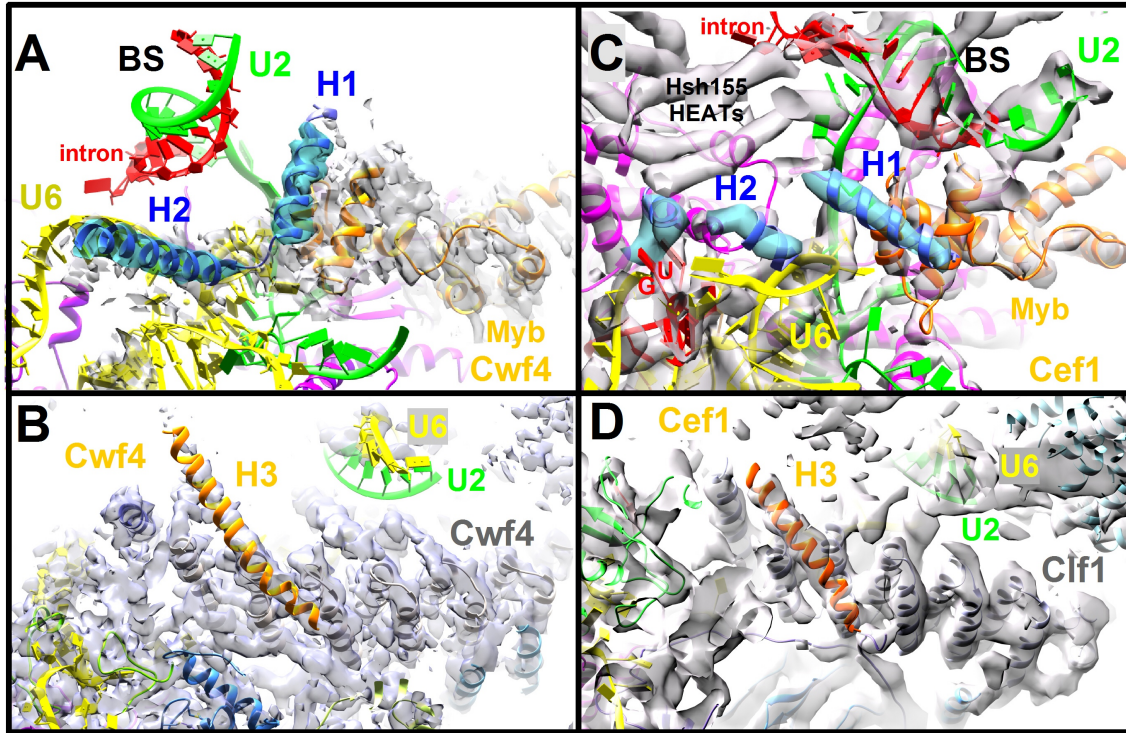


Fig. S8

Differential organization of the N-terminal region of Cef1 (Cdc5) in B^{act} and ILS complexes. Slices through the *S. pombe* ILS structure showing density elements of the Cryo-EM map (10), comprising the N-terminal region of the *S. pombe* Cdc5 protein (*S. cerevisiae* Cef1) including its Myb domains and the more C-terminally located α -helices H1 and H2 (A) and H3 (B). (C, D) Slices through the *S. cerevisiae* B^{act} structure showing density elements of the Cryo-EM map comprising the Cef1 Myb domains and the potentially rearranged α -helical elements corresponding to the Cdc5 helices H1 and H2, respectively, and, (D), the Cef1 α -helix H3 (corresponding to the *S. pombe* H3 α -helix). For better orientation, the positions of certain U2 and U6 RNA elements in the ILS and B^{act} structures are also indicated in panels A to D. In the *S. cerevisiae* B^{act} complex, the Cef1 Myb domains and α -helix H3 have nearly the same structure and position as in the ILS (see corresponding densities with orange helices shown in panels A, B and C, D,

respectively), consistent with protein crosslinks (Table S1). Densities for the *S. pombe* H1 and H2 α -helices are clearly missing at corresponding positions in B^{act} (compare blue densities in panels A and C, respectively). One possibility is that both Cdc5 α -helices H1 and H2 are restructured in B^{act} such that H1 is rotated by 110° and H2 corresponds to the kinked α -helical element in B^{act} , with its C-terminal part being situated in the density element close to the 5'ss, while the N-terminal part of the kinked helix remains close to the U6 snRNA turn. As an alternative explanation, the regions of Cef1 corresponding to the Cdc5 α -helices H1 and H2 are flexible in the B^{act} structure (and therefore not visible in our EM map) and the density elements close to the 5'ss and the U6 turn, as well as the density element associated with the Myb domains in the B^{act} structure may therefore comprise parts of one or more other proteins. Even if this were true, it does not, however, invalidate our major conclusion that the 5'ss is shielded via its close interaction with a protein element that hinders access of the BS adenine to the 5'ss. Moreover, our data indicate that the N-terminal region of Cef1(Cdc5) restructures from the B^{act} to ILS transition.

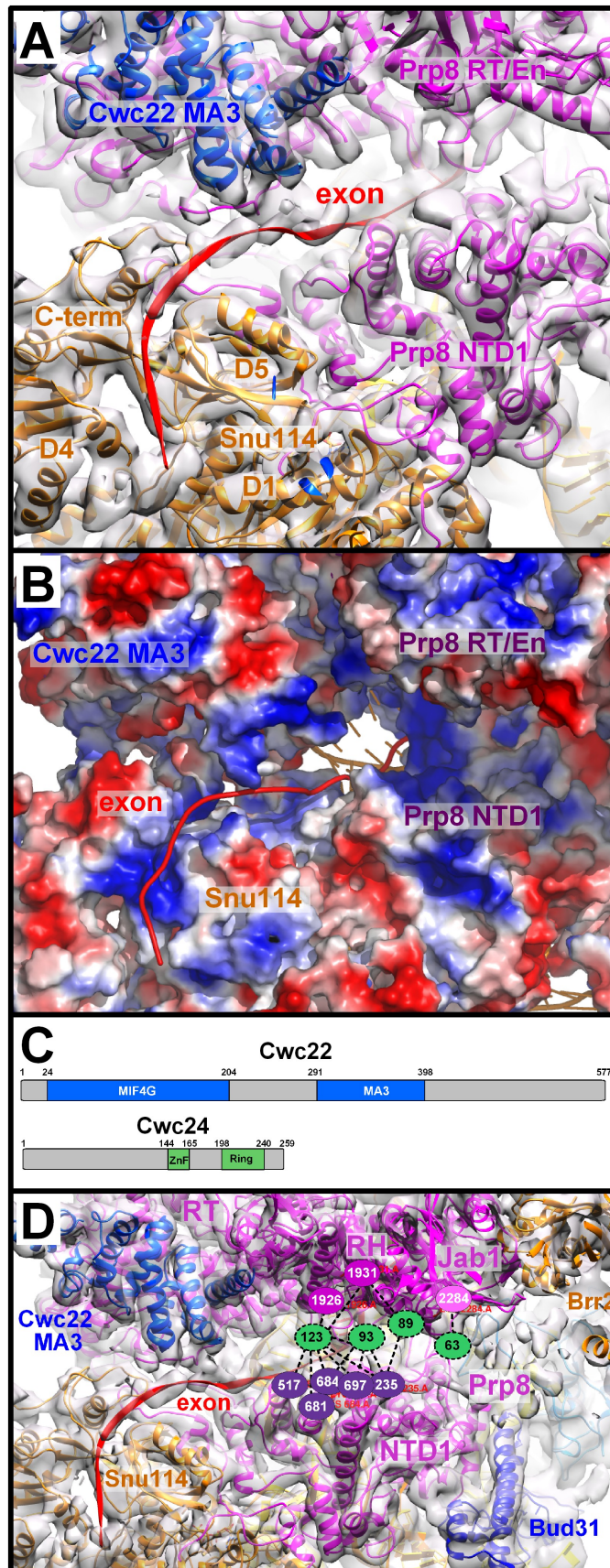


Fig. S9

Crosslinking of Cwc24 to Prp8 domains close to the 5' exon binding channel. (A)

Path of the 5' exon binding channel in B^{act} (as in Fig. 4A). **(B)** Electrostatic surface potential of the 5' exon binding channel. The RNA follows the basic patches (blue), whereas acidic patches (red) are avoided. **(C)** Domain structure of Cwc22 and Cwc24. **(D)** Crosslinks of Cwc24 to Prp8's NTD1, RH and Jab1 domains. The crosslinks indicate that the N-terminal region of Cwc24 is located centrally in the cleft between Prp8's RH and NTD1 domains, close to the 5' exon binding channel. Numbers indicate the positions of crosslinked lysine residues (connected by stippled lines) in each protein. Numbers in ovals without borders are residues in the modeled part of the protein, whereas those in ovals with stippled borders are residues within non modeled regions. The latter are arbitrarily placed close (less than 30 Å) to their crosslinking partners observed in our model.

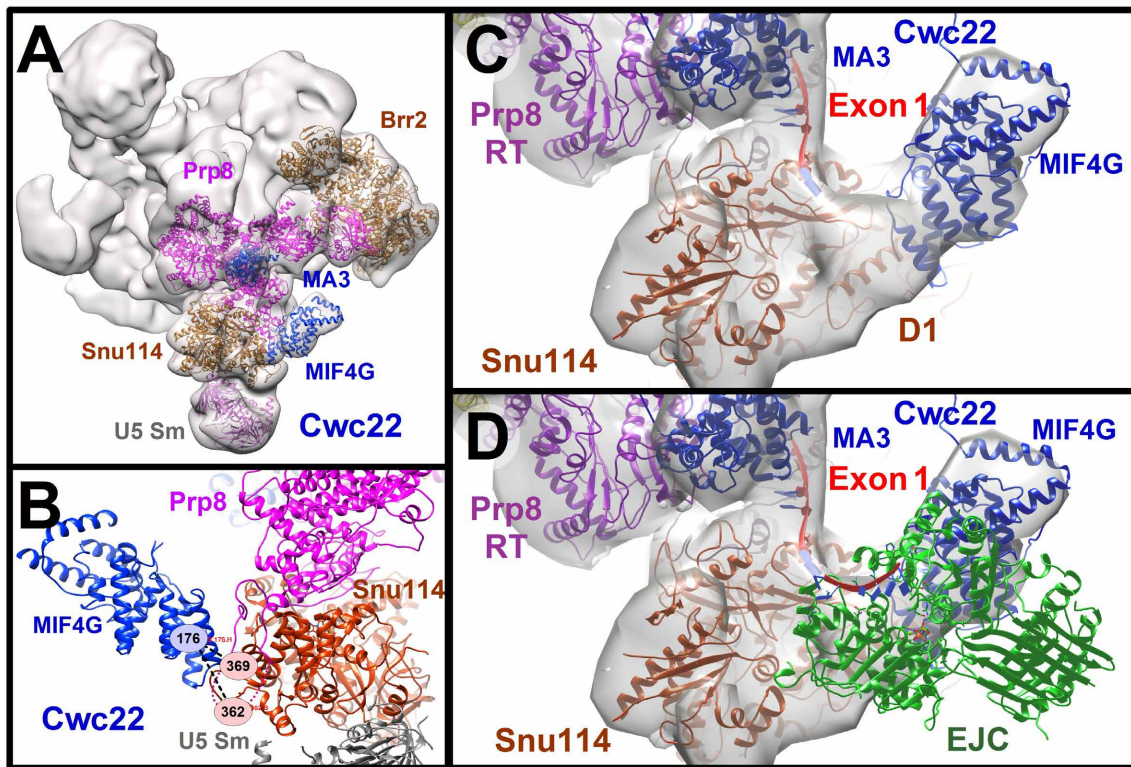


Fig. S10

Position of the Cwc22-MIF4G domain and possible location of the exon junction complex in subsequently formed spliceosomes. **(A)** Back view of the low resolution B^{act} model with the placement of U5 proteins and Cwc22's MA3 and MIF4G domains. **(B)** Crosslinks between the Cwc22's MIF4G domain and Snu114. Lysine residues 362 and 369 are located in the region of Snu114's D1 domain, which is encircled by the lasso-like protrusion of Prp8's NTD1 domain (10). **(C)** Close-up view of the fit of Cwc22's MIF4G domain into the density element close to Snu114's D1 domain, as observed in the low resolution B^{act} model. **(D)** Putative location of the EJC in the spliceosome. The crystal structure used to place Cwc22 contains an EIF4G molecule with its two RecA domains (PDB 4c9b; see Table S2). To determine the putative location of an EJC in the spliceosome, the RecA2 domain of EIF4G from that structure was

superimposed with the RecA2 domain of the EIF4G contained in the EJC structure (PDB codes 2joq and 2jos). The small piece of RNA contained in the EJC structure (red arrow) would be close to the exon channel and has the correct polarity. We note that this is a model for the location of the EJC in spliceosomes from those organisms having an EJC, and that yeast *S. cerevisiae* does not belong to this group. In addition, the EJC is stably recruited to the spliceosome after the first step of splicing as shown for the human spliceosome (65).

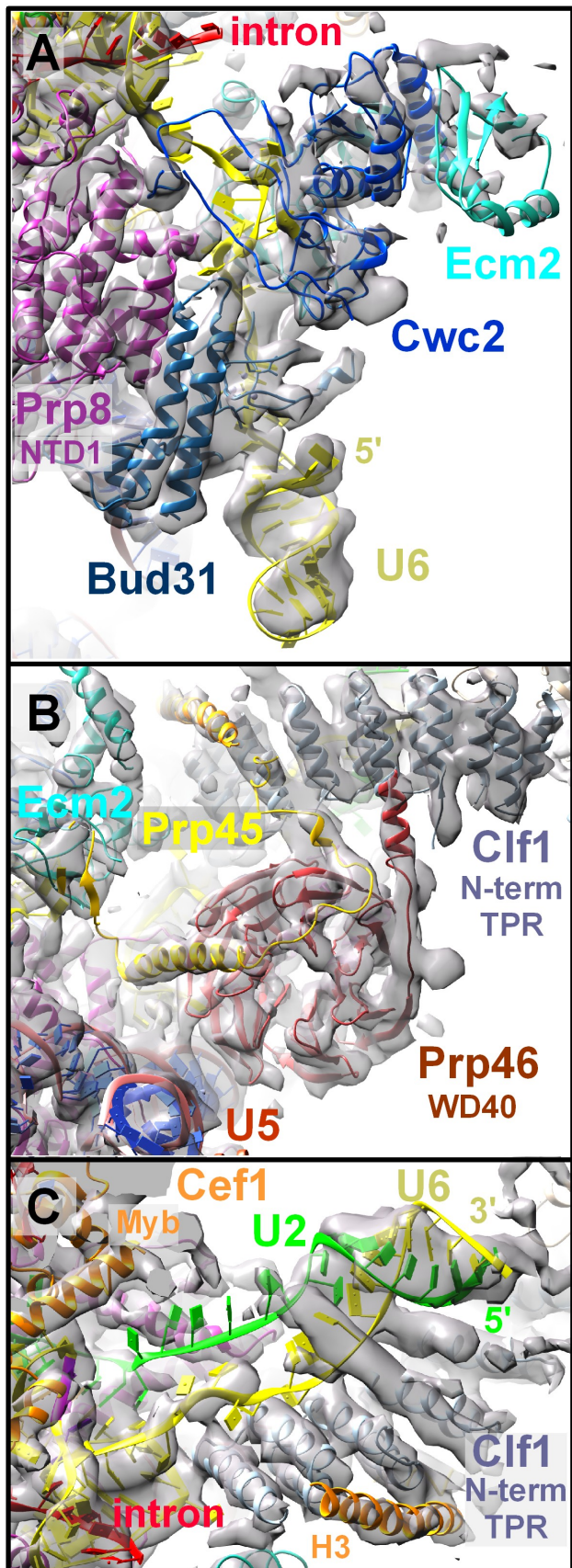


Fig. S11

Structure and location of the 5'- and 3'-terminal parts of U6 snRNA and the proteins with which they interact. (A) Fit of Cwc2, Ecm2 and Bud31 in the EM density map. All three proteins are in close contact with the 5'-terminal stem-loop (SL) of U6 snRNA. (B) The N-terminal TPR repeats of Clf1 and the WD40 domain of Prp46 fit into a pocket formed by the ISL loop of U6 snRNA and stem I of the U5 snRNA in B^{act} as also found in the *S. pombe* ILS. (C) Cef1 (Cdc5) α -helix 3 (H3) is located next to the N-terminal TPRs of Clf1 in an almost identical position as in the *S. pombe* ILS, consistent protein crosslinking (Table S2 and Fig. S12B).

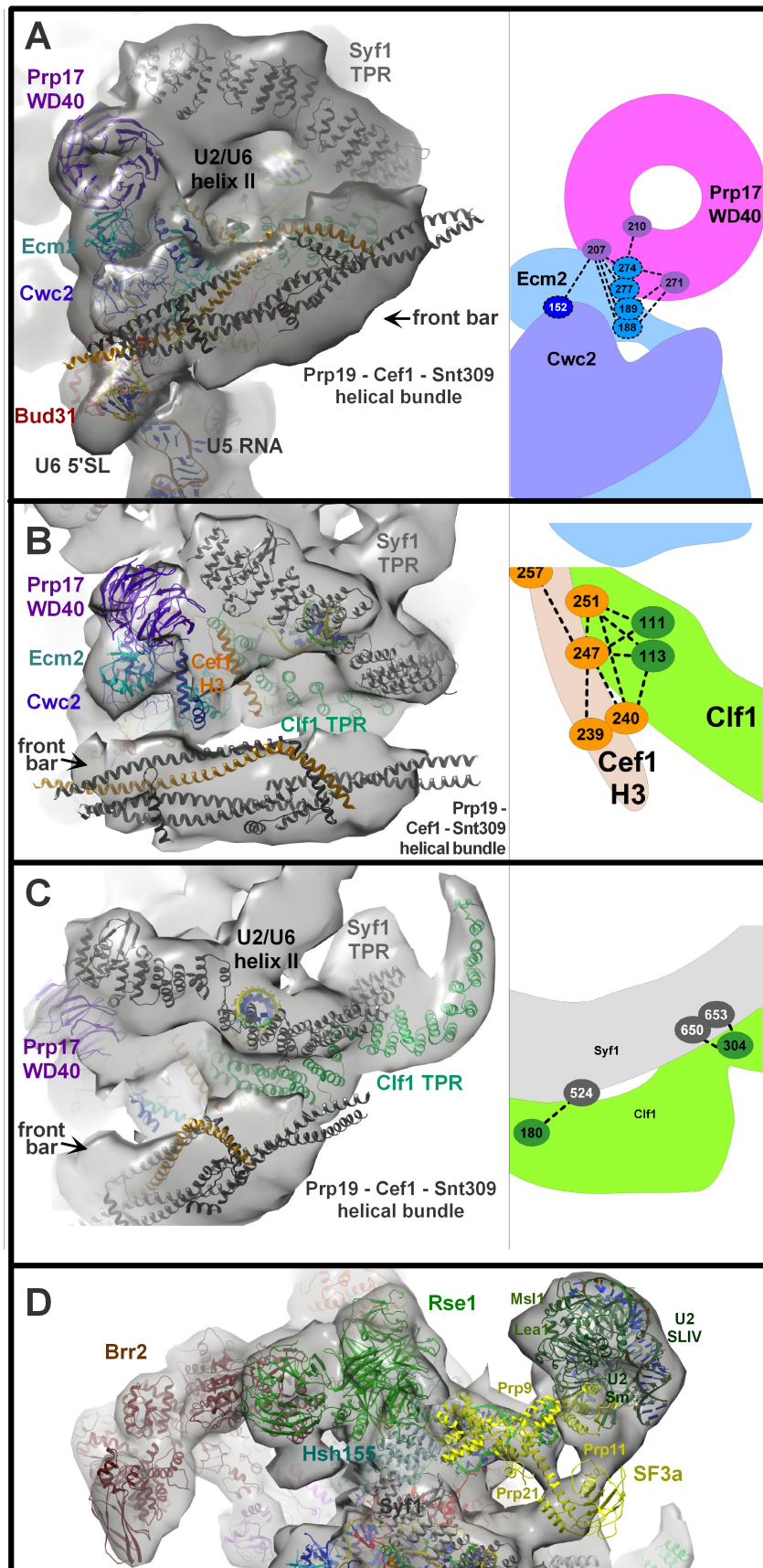


Fig. S12

Location and crosslinks of Prp17-WD40 domain, NTC proteins and U2 components

in the B^{act} complex. (A) Front view of the low resolution B^{act} model and location of the Prp17-WD40 domain above Ecm2. In the 3D reconstruction of the B^{act} complex generated without masking, the course of the N-terminal TPR repeats of Syf1, connected with structural elements of Cwc2 and Prp17-WD40, can be identified clearly. Right: intermolecular crosslinks between the Prp17-WD40 domain and Ecm2 and Cwc2. The numbers indicate the positions of crosslinked lysine residues in the three proteins. (B) Top view of the low resolution B^{act} model and location of the Clf1 TPR repeats and Cef1 (Cdc5) helix3 (H3) (see Table S1). A density element lying perpendicular to the central part of the main body in the front view is sized suitably to accommodate the helical-bundle domain with the Prp19 core (Prp19-Cef1-Snt309 bar). Right: intermolecular crosslinks between the Clf1 TPRs and Cef1 H3. (C) Front view of the B^{act} complex showing the long, curved TPR repeats of Syf1 and Clf1, which cross one another and together form a basket-like structural element as shown in the upper part of the *S. pombe* ILS (10). Much of the mass of the *S. pombe* proteins can be fit as rigid bodies into the corresponding density regions in the B^{act} spliceosome. Some local adaptations were necessary, but the curvature of the repeats and also the cross-over points are organised in a similar way in the B^{act} complex and the *S. pombe* ILS. As the density of the TPR repeats of Clf1 and Syf1 in the 5.8 Å B^{act} structure breaks off abruptly, this only becomes clear when one also takes into account the non-masked spliceosome model and intermolecular crosslinks that are found between Clf1 and the Syf1 TPRs, as shown on the right. (D) Top view of the low resolution B^{act} model and density elements in B^{act} attributed to the U2 Sm core RNP and part of the SF3a protein complex. Within the

density region that was identified at high resolution by masking, the last reliably fit element is stem-loop IIa of the U2 snRNA. In B^{act} , this element is connected to a very large density region that is structurally less stable and was masked out to obtain the high resolution structure. The non-masked 3D reconstruction shows that this region has a very large globular structure, bridged to the U2-SF3b complex and the NTC region containing Syf1 and Clf1. Its position with respect to the U2 stem-loop IIa and the SF3b proteins – and also its very large size – indicate that it contains the large 3'-terminal components of U2 snRNP: the U2 Sm ring with the proteins Lea1 und Msl1 associated with stem-loop IV (SLIV). A main connection is likely provided between the 3' terminal U2 snRNP domain and the top domain of B^{act} through the SF3a protein complex. The low resolution in this region prevents exact localization, despite the availability of the crystal structure of the SF3a core complex (66).

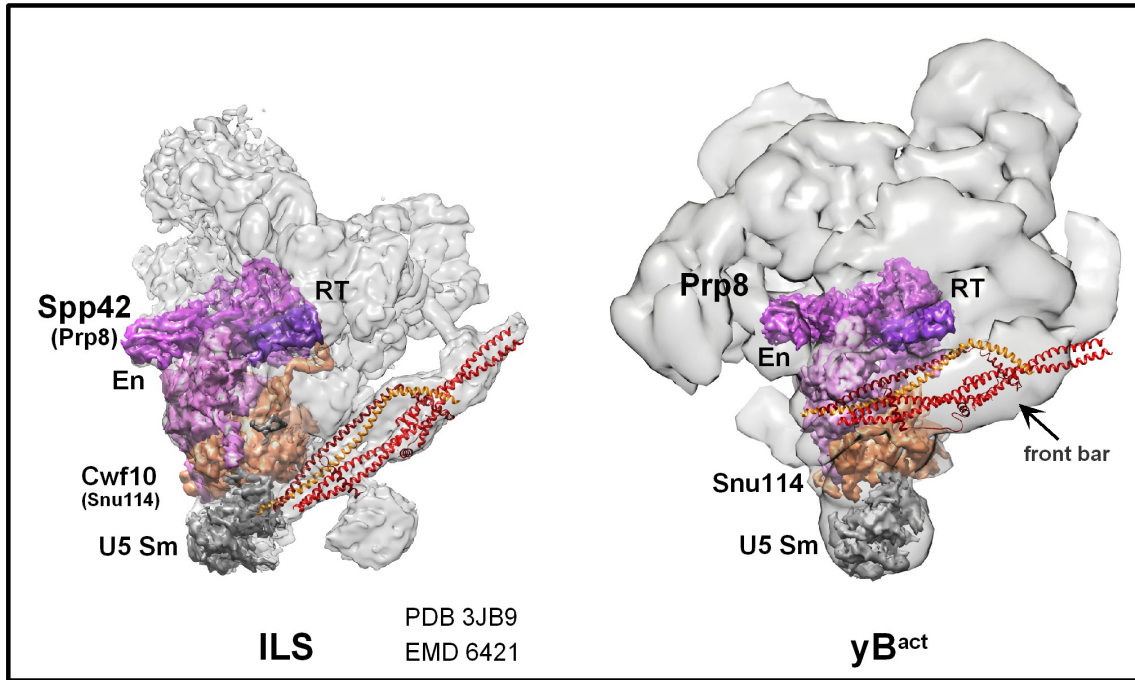


Fig. S13

Prp19's helical bundle is differentially orientated in B^{act} versus the ILS. EM density maps of the *S. pombe* ILS (EMD 6421) and *S. cerevisiae* B^{act} complexes (front view of the low resolution B^{act} model) with the U5 snRNP proteins Prp8 (purple), Snu114 (orange) and Sm core (grey) indicated. The positions of the U5 snRNP proteins and their structural organisation share many similarities in both spliceosomal complexes. In the *S. pombe* spliceosome the coiled-coil elements of the four copies of Prp19 (red), together with Snt309 (dark purple) and the C-terminal region of Cef1 (Cdc5; dark orange), form a helical bundle that runs, as a self-contained arm II domain, parallel to the main body of the *S. pombe* spliceosome and is only bound to it by thin structural elements (10). There is no density at this corresponding position in the B^{act} complex that would correspond to that in the *S. pombe* spliceosome – either in the 5.8 Å model or in the non-masked low resolution B^{act} model shown here. Rather, in the latter model there is a density element that lies orthogonal to the central part of the main body in the front view (called front bar

in Fig. 1A) and is suitably sized to accommodate the helical-bundle domain with the Prp19 core. The non-masked model of B^{act} was aligned by using the U5 proteins with the structure of the *S. pombe* ILS, and the position of the Prp19 helical bundle was deduced.

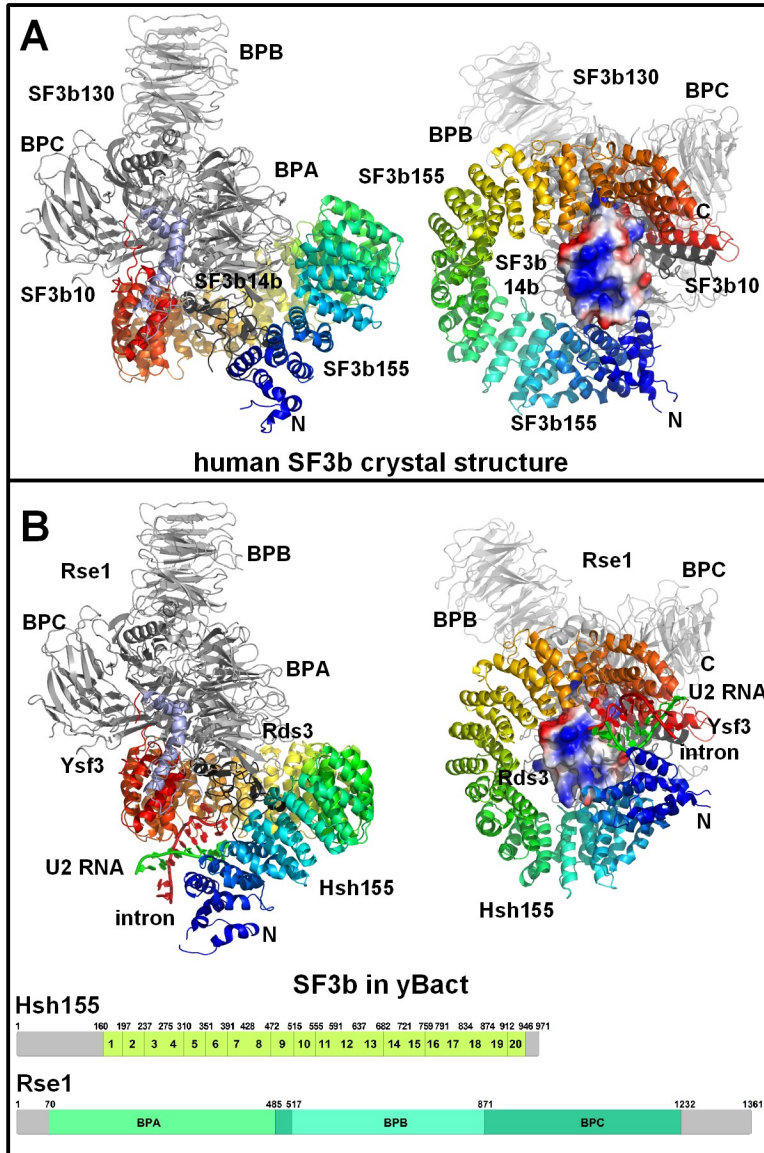


Fig. S14

Structure of the yeast SF3b core complex in the B^{act} spliceosome and in the crystal structure of a protease-resistant human SF3b core complex. Ribbon representation of SF3b proteins in (A) the crystal structure of the human SF3b core complex comprised of SF3B155's entire C-terminal HEAT repeat domain, SF3b130 (yeast Rse1) and the small proteins SF3b14 (yeast Rds3) and SF3b10 (yeast Ysf3) (37) and (B) in the B^{act} complex. Left: side views, right: bottom views. SF3b14 (yeast Rds3) is shown in blue in a space

filling model in the middle of the structure. Superposition of the HEAT domains from the two orthologs shows that the N-terminal H1–H5 and C-terminal H16–H20 regions are restructured versus the central H6–H15 region. In this way, HEAT repeats H1 and H19 come to lie almost on top of each other and with the distance between them shortened from 24 Å (in the crystal structure) to 18 Å (in B^{act}). Given that the isolated yeast SF3b complex has a similar structure, this suggests that the Hsh155 HEAT repeats are restructured after incorporation of SF3b into the spliceosome. SF3b130's (yeast Rse1) three β propeller (WD40) clusters (BPA+ BPB +BPC) are also indicated. An RNA density element consisting of the U2/BS RNA helix is located in the opening between the terminal HEAT repeats of Hsh155 in the B^{act} structure (see below).

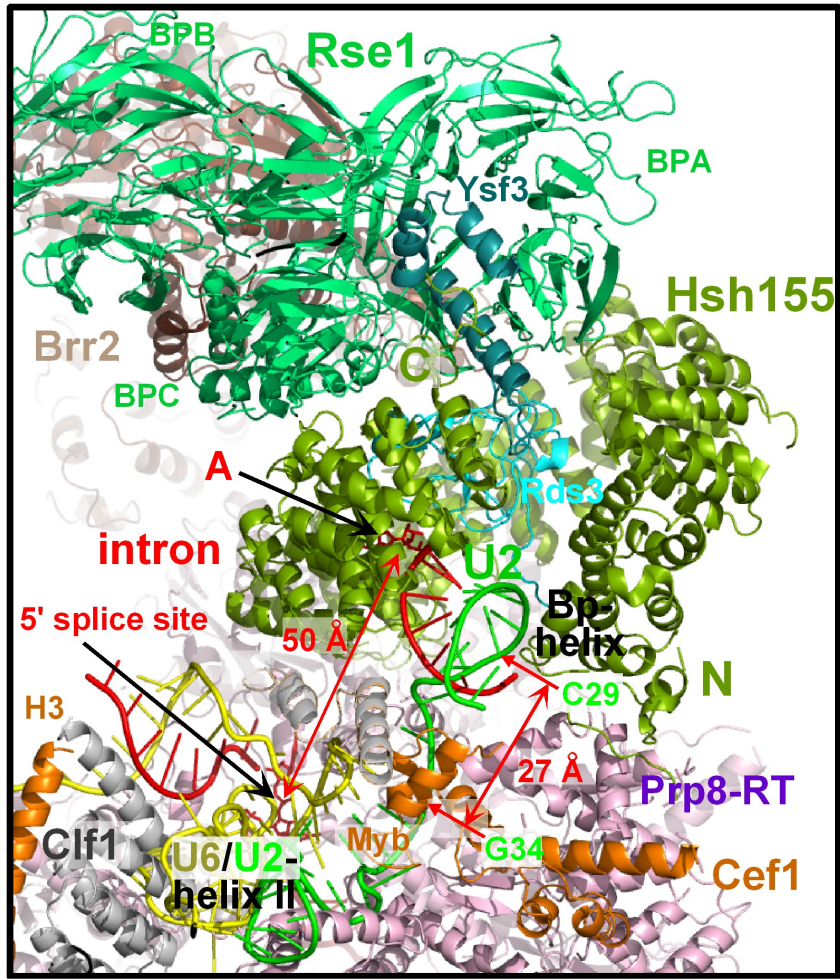


Fig. S15

Location of the U2/BS RNA helix, Hsh155 and the 5' splice site. The U2/BS RNA helix is located between the terminal HEAT repeats of Hsh155 and the BS adenosine is spatially separated from the scissile bond of the 5'ss by 50 Å. The 5' terminal nucleotides of U2 of the U2/BS helix (U2-C29) is spatially separated from the 3' terminal U2 nucleotides of U2/U6 helix Ia (U2-G34) by 27Å.

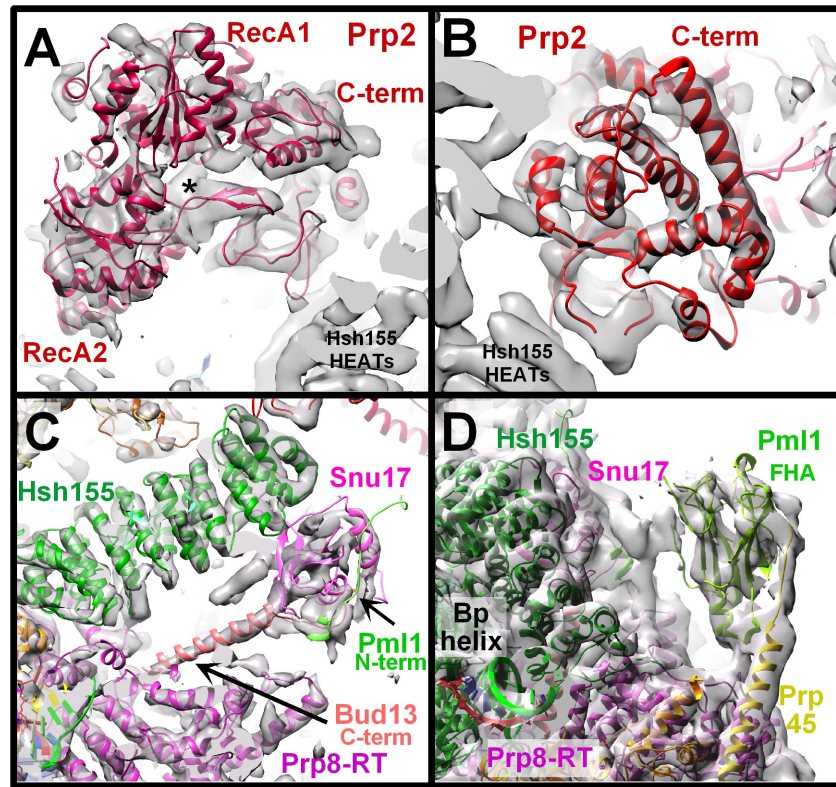


Fig. S16

Location of the Prp2 RNA helicase and the RES proteins. (A) Close-up view of the fit of the Prp2 RecA domains, into the Prp2 density associated with Hsh155's HEAT domain (see also Fig. 6A) in the B^{act} model. The asterisk indicates unassigned density likely to be occupied by parts of Spp2. (B) Close-up view of the fit of Prp2's C-terminal domain, including its OB-fold domain, into the corresponding Prp2 density of the B^{act} model. (C) Expanded view of the B^{act} steep slope (see Fig. 1A), showing the fit of Hsh155's HEAT repeats, Snu17's RRM and the C-terminal region of Bud13 into the corresponding densities. The Bud13 C-terminal helix occupies a density tube that continues further down to Prp8-RT/En. Two crosslinks of Snu17 to HEAT repeats 7 and 8 of Hsh155 support its location and the orientation of this central part of the RES

complex (Table S1). **(D)** Pml1's N-terminal FHA (forkhead-associated) domain forms a bridge between Snu17 and the C terminus of the Prp8-RT-associated Prp45 helix.

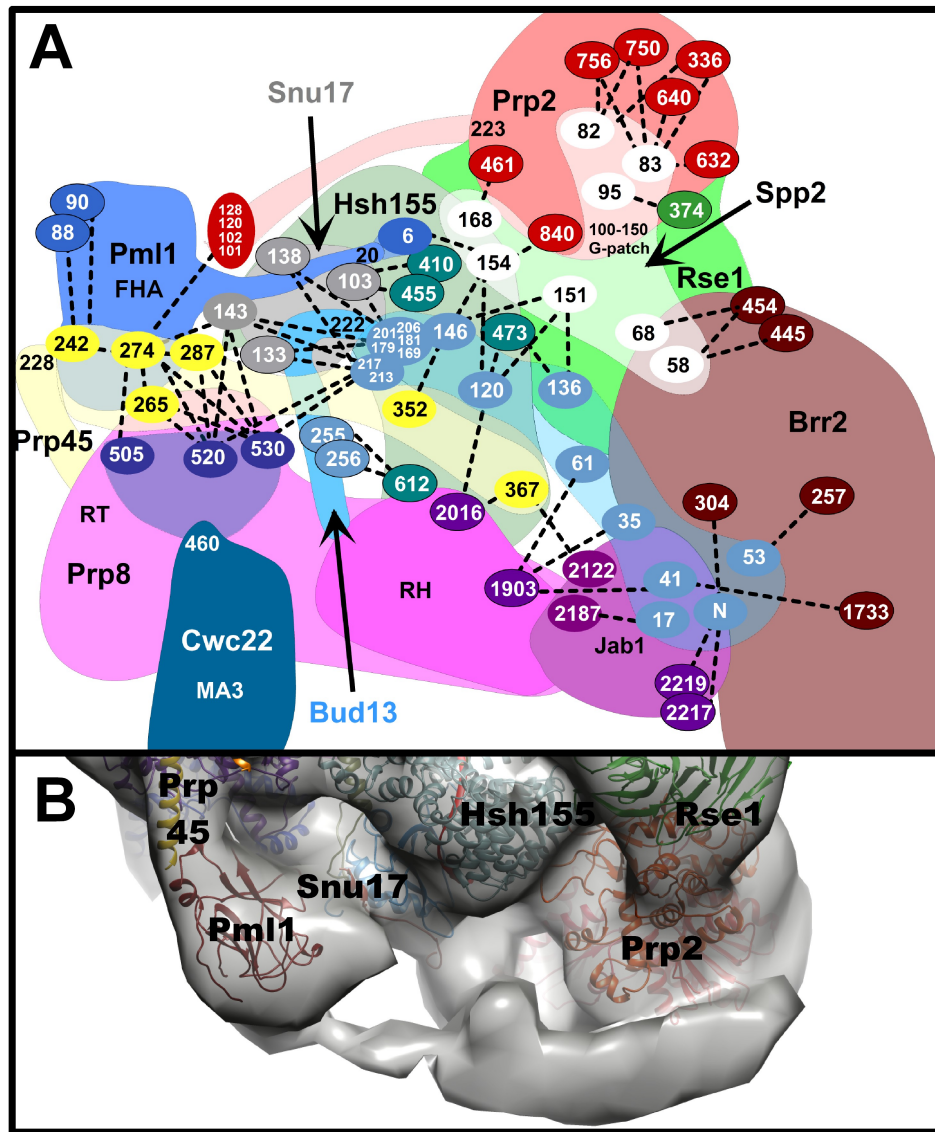


Fig. S17

Intermolecular crosslinks support the juxtaposition of Spp2 with Prp2 and the RES complex, and suggest the position of the C-terminal parts of Cwc22 and Prp45. (A)

Schematic diagram of the back of the front view of the B^{act} complex (see Figure 1A). Intermolecular crosslinks between the protein domains are shown. Numbers indicate the positions of crosslinked lysine residues (connected by stippled lines) in each protein. Numbers in ovals with black borders indicate the residues in the modeled parts of the proteins, whereas those in ovals without borders are residues within non-modeled

regions. The latter are arbitrarily placed close (less than 30 Å) to their crosslinking partners observed in our model. Numbers without ovals represent the terminal residues of protein regions modeled in the high resolution B^{act} structure. Red ovals represent Prp2 residues, white – Spp2, green – Rse1, turquoise – Hsh155, brown – Brr2, violet – Prp8, purple – Cwc22, yellow – Prp45, blue – Pml1, light blue – Bud13 and grey – Snu17. Tentative localization of the non-modeled regions of a given protein is indicated by semi-transparent coloring. Although projected onto the plane of the paper, the positions in space of the crosslinked lysines correspond to their positions in the 3D structures of their respective protein domains. The maximum observed length for any crosslink was less than 30 Å. **(B)** Top view shows unassigned regions of the unmasked EM density likely to be occupied by flexible parts of RES, Spp2, Prp2, Hsh155, Cwc22 and Prp45 proteins not resolved in 5.8 Å EM map. Prp45 appears to play a role in stabilizing the various protein-protein interactions.

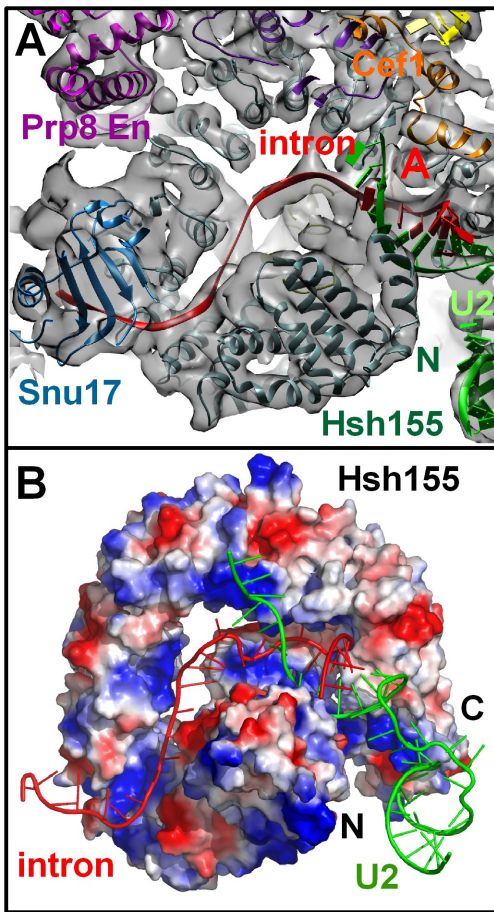


Fig. S18

Path of the intron's 3' end across the Hsh155 HEAT domain in the yeast \mathbf{B}^{act} complex. **(A)** Path of the intron across the Hsh155 HEAT repeat spiral. Clear densities are present for the intron just after the branch site and Hsh155 HEAT repeat H6 on the opposite site. The density for the central nucleotides of the BS-3'SS region of actin pre-mRNA (UCCGAUU) is not well resolved and thus the placement is ambiguous. **(B)** The electrostatic surface potential of the Hsh155 HEAT domain with the path of the intron's 3' end (red). The RNA lies in a basic channel (blue), well-separated from the red acidic patches. Upon exiting the ring, the RNA passes through a clamp-like structure (bottom left).

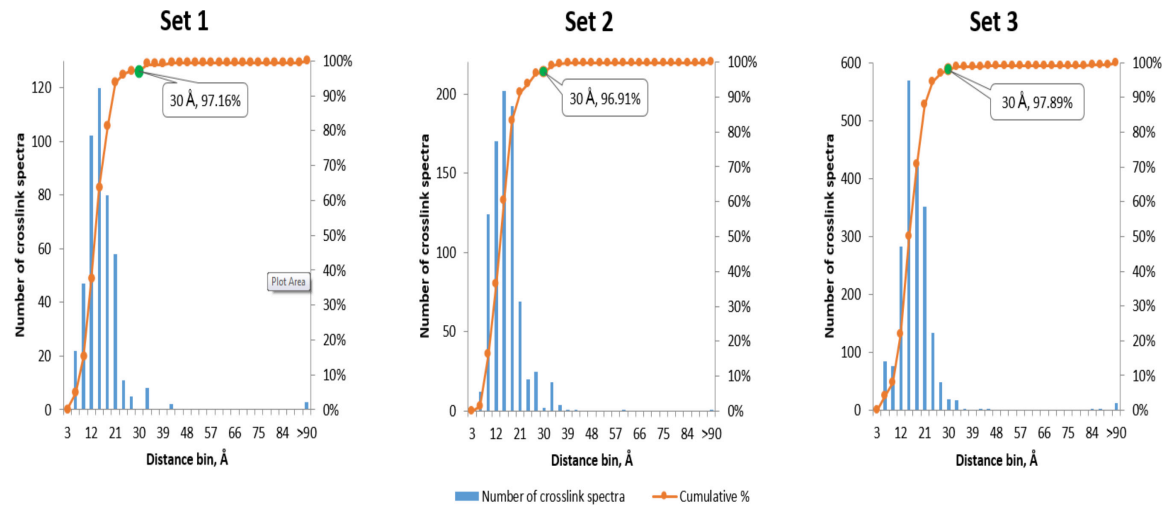


Fig. S19

Distribution of the Ca-C α distances between BS3-crosslinked residues. The Euclidian distances were measured in the 5.8 Å model of the yeast B^{act} complex using PyMOL (<http://www.pymol.org>). More than 95% of all crosslink-assigned spectra correspond to crosslink distances of 30 Å or less.

Movie S1

Hsh155 – SF3b HEAT domain transformation

Movie S2

yB^{act} rotation

Table S1.

Protein and model building information for all modeled yeast B^{act} proteins. Protein names, their molecular weight and detailed information about the model building process are provided.

Table S2.

BS3-crosslinks of proteins in the yeast B^{act} complex. Statistics (Spectral Counts and Score_{max}) of the CX-MS data for the proteins of the purified yeast B^{act}. “Inter” and “Intra” indicate inter-protein and intra-protein crosslinks, respectively. Numbers in the Residue 1 and 2 columns indicate the position of the crosslinked lysine or N-terminal methionine residue. Euclidian C α -C α distances between crosslinked residues are given in Ångström (column "Å"). The Table includes crosslinks of all proteins of the B^{act} complex, even if they were not observed/modeled into the EM density.

Table S3.

MolProbity validation of the final RNA model of the yeast B^{act} complex. For the clash score, a percentile is given with the 100th percentile being the best structure among structures of comparable resolution (N=1784, all resolutions).

Table S1: Positioning of proteins in the cryo-EM structure model of *S. cerevisiae* B^{act}

Protein	Domain	Positioning
Prp8 279.5 kDa 2413 aa	NTD1 131-737	The <i>S. cerevisiae</i> NTD1 structure (PDB 5GAN), determined as part of the cryo-EM investigation of the <i>S. cerevisiae</i> (S.c.) tri-snRNP (13) was used for rigid-body fitting followed by refinement with the COOT program (62). The position and structure of NTD1 in B ^{act} are similar to those observed in the human (16) and S.c. tri-snRNP (13-15) and the ILS (10).
	NTD2 738-872	The model of the orthologous <i>S. pombe</i> (S.p.) structure (PDB 3JB9) determined by cryo-EM of the S.p. ILS complex (10) was used for rigid-body fitting followed by refinement with COOT. The linker between NTD1 and NTD2 was reconstructed with COOT. The position and structure of NTD2 in B ^{act} are equivalent to those in the ILS (10).
	RT/En 873-1838	The RT/En structure (PDB 5GAN) determined by cryo-EM of the S.c. tri-snRNP (13) was used for rigid-body fitting followed by refinement with COOT. Several loops (1039–1043, 1201–1213, 1375–1385, 1402–1427, 1614–1623) were manually adjusted or rebuilt. RT/En position and structure in B ^{act} are similar, but not identical, to those in the ILS (10).
	RH 1839- 2078	The RH structure (PDB 5GAN) determined by cryo-EM of the S.c. tri-snRNP (13) was used for rigid-body fitting followed by refinement with COOT. The loops 1831–1839 and 1858–1874 were adjusted or rebuilt manually. The position of RH in B ^{act} is different from those observed in the human (16) and S.c. tri-snRNP (13, 15) and the ILS (10).
	Jab1 2148- 2398	The Jab1-Brr2 complex of the S.c. structure (PDB 5DCA) determined by X-ray analysis of the co-crystal with Brr2 (19) was used for rigid-body fitting followed by refinement with COOT.
Snu114 114.0 kDa 1008 aa	D1 111–460	The Snu114 structure (PDB 5GAN) determined by cryo-EM of the S.c. tri-snRNP (13) was used for rigid-body fitting followed by refinement with COOT. The Snu114 position and structure in B ^{act} are equivalent to those of the human (16) and S.c. tri-snRNP (13, 15) and the ILS (10).
	D2 461–598	
	D3 599–676	
	D4 677–852	
	D5 853–941	
	C-term 942–998	
Brr2 246.1 kDa 2163 aa	NC-CC 453-2163	For rigid-body fitting of the two helicase cassettes, the structure of the Jab1-Brr2 complex of S.c. (PDB 5DCA) was used (19) followed by refinement with COOT. The position of Brr2 in B ^{act} is very different from the corresponding position in the human tri-snRNP (16), and Brr2 is differently bound and oriented compared with the S.c. tri-snRNP (13, 15).
	PWI 284-294	For rigid-body fitting of the PWI domain, the Jab1-Brr2 co-crystal (67) (PDB 5DCA) was used. The domain was fitted into a density on top of the NC cassette close to the Prp8-Jab1 domain, and this was followed by refinement with COOT. The position of PWI in the B ^{act} complex is different from, but close to, the position found in the Brr2-Jab1 crystal structure and in the human tri-snRNP (16).
	NHD 115-191	To identify the position of the small NHD domain, its position in the human tri-snRNP (PDB 3JCR) relative to the easily locatable Brr2 NC-CC cassettes was used. The density for the NHD domain is well-defined and fits well with the protein's 3D structure; it places the NHD in B ^{act} in a location and orientation relative to NC-CC that are similar to the corresponding location and orientation found in the human tri-snRNP. The S.c. structure of NHD

		(PDB 5DCA) determined by X-ray analysis of a co-crystal with Brr2 (19) and modified according the conformation in the human tri-snRNP was used for fitting.
U5-Sm	Sm domains of SmB, SmD1, SmD2, SmD3, SmE, SmF, SmG	For rigid-body fitting of the U5-Sm, its structure determined by cryo-EM of the S.c. tri-snRNP (PDB 5GAN) (13) was used. The U5-Sm position in B ^{act} is equivalent to that of the human (16) and S.c. tri-snRNP (13, 15) and the ILS (10).
Cwc2 38.4 kDa 339 aa		For rigid body fitting the orthologous S.p. structure (PDB 3JB9) determined by cryo-EM of the ILS complex (10) was used, followed by refinement with COOT. The Cwc2 position is equivalent to the one in the ILS (10).
Ecm2 40.9 kDa 364 aa	8–284	For rigid-body fitting the orthologous model of the S.p. structure (PDB 3JB9) as determined by cryo-EM of the ILS complex (10) was used; this was followed by refinement with COOT. The position of Ecm2 is equivalent to its position in the ILS (10). For refinement COOT was used.
Bud31 18.4 kDa 157 aa	17–154	For rigid-body fitting of Bud31, the S.c. structure (2MY1) determined by crystallography (68) was used; this was followed by refinement with COOT. The position of Bud31 in B ^{act} is equivalent to its position in the ILS (10).
Prp17 52 kDa 455 aa	WD40 150–455	A structural model of the WD40 domain was produced by using the Robetta server. It was placed in such a way into a poorly resolved density of the non-masked low-resolution structure, just above Cwc2 und Ecm2, so that the observed crosslinks with Cwc2 and Ecm2 would be possible. Although exact positioning was not possible, the principal orientation is determined by the crosslinks (see Fig. S12). In the S.p. ILS structure (10) the only part of Prp17 identified was a helical N-terminal region not conserved in the S.c. sequence.
Prp45(69) 42.5 kDa 379 aa	31–235	An orthologous model of the S.p. structure (PDB 3JB9) as determined by cryo-EM of the ILS complex (10) was used for rigid-body fitting followed by refinement with COOT. Well-fitting densities for the helical and β-sheet regions were found in the B ^{act} structure at positions equivalent to those found in the ILS. The fitted structure ends C-terminally, with a helix tightly attached to the RT end of the Prp8-RT/En domain. The remaining C terminus, which is not present in the ILS model (10), on the basis of evidence from crosslinks (see Fig. S17), runs around the back side of the B ^{act} complex, passing the RES-complex proteins, and reaches the vicinity of the RH and Jab1 domains of Prp8. A short stretch (229–236) was modeled into a thin thread of density running along the Pml1-FHA domain.
Prp46(69) 50.7 kDa 451 aa	WD40 107–446	For rigid-body fitting, an orthologous model of the S.p. structure (PDB 3JB9) as determined by cryo-EM of the ILS complex (10) was used, followed by refinement with COOT. The position of Prp46-WD40 is equivalent to its position in the ILS.
Cef1 67.7 kDa 590 aa	tandem Myb 12–110	For rigid-body fitting an orthologous model of the S.p. structure (PDB 3JB9) as determined by cryo-EM of the ILS complex (10) was used; this was followed by refinement with COOT. The position of Cef1-Myb is equivalent to its position in the ILS.

	H1 143–160 H2 164–185	Densities as observed for the <i>S. pombe</i> H1 and H2 α -helices are clearly missing in B^{act} and may be restructured instead into a H1 helix rotated by 110° and a kinked α -helix (Fig. S8). The C-terminal part of the latter would be situated in a density close to the 5'ss, the N-terminal part instead would remain close to the U6 snRNA turn. However, it cannot be excluded that the parts of Cef1 corresponding to the <i>S. pombe</i> H1 and H2 helices are not visible in the EM map due to high flexibility. Although the conclusion that the 5'ss is clearly shielded by protein elements can be drawn, an unambiguous assignment to a specific protein is not possible.
	H3 230–259	In the ILS upstream of H2 a straight, 34-aa-long helix of unknown sequence is positioned on the loop side of the N-terminal Clf1/Syf3 TPRs. In the B^{act} complex a density rod at a similar position, but of shorter length, is also present above the Clf1/Syf3 N-terminal TPRs. Modeling by the Robetta server revealed a long helix downstream of H2. The Clf1/Syf3 internal crosslinks support the presence of a helix between amino acids 230 and 259 (Fig. S12) and the helix model of this stretch fits perfectly into the density rod. Crosslinks to the Clf1 TPR support not only the helix placement but also its orientation with the N terminus to the outside and its C terminus pointing to the catalytic center, as observed in the ILS model. Refinement was performed with COOT.
	C-helix 500–590	An orthologous model of the <i>S.p.</i> structure (PDB 3JB9) as determined by cryo-EM of the ILS complex (10) was used to model the helical bundle that the C-terminal helix of Cef1/Cdc5 forms with helices of Prp19 and Snt309. The helical bundle fits into the elongated density bar of the front view. This density is present only in the non-masked lower-resolution structure, and an exact placement is not possible.
Prp19 56.5 kDa 503 aa	HD 76–140	An orthologous model of the <i>S.p.</i> structure (PDB 3JB9) as determined by cryo-EM of the ILS complex (10) was used to model the helical bundle that four copies of the Prp19 helical domain (HD) form with helices of Cef1/Cdc5 and Snt309. The helical bundle was placed as described above (Cef1/Cdc5, C helix).
Snt309 20.7 kDa 175 aa	1–175	An orthologous model of the <i>S.p.</i> structure (PDB 3JB9) as determined by cryo-EM of the ILS complex (10) was used to model the helical bundle that Snt309 forms with helices of Cef1/Cdc5 and Prp19. The helical bundle was placed as described above (Cef1/Cdc5, C helix).
Syf1 100.2 kDa 859 aa	TPR 393–654	For modeling the TPR domain of <i>S.c.</i> protein Syf1, the sequence of the human orthologue Xab2 was used to produce a first model with the Robetta server. Xab2 was used because in the <i>S.c.</i> sequence an <i>S.c.</i> -specific insert (170–216) prevents TPR continuity. The Xab2 model was then bent to fit into the non-masked B^{act} density that resembles the Cwf3/Syf1 density of the <i>S.p.</i> ILS. From the Xab2 structure the <i>S.c.</i> orthologue model was then built. The ILS model of the Cwf3/Syf1 protein covers only a short stretch of sequence (homologous to the <i>S.c.</i> Syf1 sequence position 498–734). From this stretch an orthologous model was created and used to replace the corresponding stretch in the model built with Xab2. A short region (393–654) of Syf1 passes through a density of the masked high-resolution B^{act} structure. Here, the TPRs show excellent fit with TPR-typical densities. Refinement was performed with COOT.
Clf1/Syf3 82.4 kDa 687 aa	TPR 39–272	In the <i>S.p.</i> ILS model (10) only for the N-terminal Cwf4/Clf1 TPRs was the sequence (homologous to the <i>S.c.</i> Clf1 sequence 36–291) provided. An orthologous <i>S.c.</i> model was generated and could be fitted with only slight adjustments into TPR-typical densities of the high-resolution B^{act} structure. In the B^{act} , the positioning of the N-terminal TPR close to the catalytic center corresponds to the position in the ILS model. For the remaining C-terminal TPRs no high-resolution density is present in the masked structure; density is

		only found in the lower-resolution structure obtained without application of a mask. For these C-terminal Clf1 TPRs, a model produced by the Robetta server was used; the model was fitted by bending it into the density corresponding to a similar density region in the ILS structure. Crosslinks between Syf1 and Clf1 TPRs (Fig. S12) verify this ILS-based arrangement of the Syf1 and Clf1 TPRs. COOT refinement was applied in areas with sufficient resolution.
Cwc22 67.3 kDa 577 aa	MIF4G 11–263	Using the structure of this domain in the human Cwc22 orthologue (PDB 4C9B), determined by X-ray analysis of the co-crystal with eIF4AIII (33), an orthologous model was produced and fitted into a prominent density of the non-masked, low-resolution B ^{act} structure. This density protrudes obliquely out of the central main body and has exactly the shape of the MIF4G domain. One strong crosslink (K369 to K176 of Snu144) and a minor one (K362 to K176 of Snu114) verify the position and orientation of the MIF4G domain. The MIF4G is bound to the D1 domain of Snu114, where a lasso-like loop of the Prp8-NTD1 domain encircles a little protrusion of the D1 domain. The sequence region 425–430 of the NTD1 lasso seems to contribute to the Cwc22-MIF4G binding site. Refinement was performed with COOT.
	MA3 280–533	A model of the region containing the MA3 domain was produced by the Robetta server and fitted with slight adjustments perfectly into a well-resolved density above the MIF4G domain. It is attached to the linker domain of Prp8-RT/En, with its N-terminal helix in contact with Prp8-RH and its C terminus close to the RES complex region. The extreme C-terminal region of Cwc22 could not be placed into a B ^{act} density, but a network of crosslinks places it in the RES complex region (see Fig. S17).
Cwc24 29.7 kDa 259 aa	63–123	Submission of the Cwc24 sequence to the Robetta server resulted in the separation of the small Cwc24 protein into several domains. N-terminal amino acids 93, 89 and 123 of Cwc24 form a network of crosslinks to the NTD1 and RH domains of Prp8 (see Fig. S9). Amino acid 63 crosslinks to the Jab1 domain of Prp8. In the high-resolution structure of B ^{act} we cannot discern a clear density, which could accommodate this region of the Cwc24 protein.
Hsh155 110.0 kDa 971 aa	HEAT repeats 126–960	The structures of the four <i>S.c.</i> SF3b proteins were modeled according to the crystal structure of the human protease-treated SF3b complex consisting of SF3b155/Hsh155, SF3b130/Rse1, SF3b14b/Rds3 and SF3b10/Ysf3. In the <i>S.c.</i> B ^{act} structure well-resolved and well-defined densities are immediately visible for the Hsh155 HEAT repeats forming a spiral of parallel density rods and the Rse1 WD40 domains visible as three similar, protruding ring densities. The entire homology modeled <i>S.c.</i> SF3b complex docks easily into the B ^{act} density, but some significant adaptations are necessary. While the central (8–15) HEAT repeats can be docked as a rigid body, the N- and C-terminal repeats have to be moved upward and downward, respectively, and both need to be tilted inwards, thus narrowing the diameter of the spiral. As Rse1 is mainly connected to the C-terminal HEAT repeats it is positioned more sideward compared to the crystal structure. The small Ysf3 protein is part of the Hsh155-Rse1 binding region and its density is well recognizable in the B ^{act} structure. In the crystal structure the Rds3 protein has a central position within the Hsh155 spiral. In the equivalent position a well-defined density in the B ^{act} structure perfectly fits Rds3. All four protein structures were refined by using COOT.
U2-Sm	Sm domains of SmB, SmD1,	In the high-resolution structure of B ^{act} no other density element apart from the one at the bottom housing U5-Sm has the shape typical of the heptamic Sm ring. In the non-masked lower-resolution B ^{act} structure, however, such a density can be observed in the upper right corner of the front view; this density contributes to a large extent to the steep slope. In this density the U2-

	SmD2, SmD3, SmE, SmF, SmG	Sm ring with the two bound U2-specific proteins Lea1 and Ms11 and the SLIV of U2RNA can be placed as the complex structure determined within the S.p. ILS (PDB 3JB9) by cryo-EM (10).
Lea1 27.2 kDa 238 aa	1–185	
Ms11 12.8 kDa 111 aa	24–111	
Prp9 63.0 kDa 530 aa	1–378	The structure of a large part of the S.c. SF3a complex was solved by crystallography (66). For this large, roughly Y-shaped structure (PDB 4DGW), no matching density is present in the high-resolution structure of the B ^{act} complex. In the non-masked lower-resolution B ^{act} structure a suitably sized forked density is present that connects the branch-point helix and the region containing U2-SLII of the high-resolution part with the density of the less well-resolved structure into which the U2-Sm complex fits. Since the resolution of the forked density does not allow unambiguous positioning of the arms, the positioning of SF3a is at present arbitrary.
Snu17/Ist3 17.1 kDa 148 aa	RRM 26–135	Snu17 is the central RES complex component and binds to the other two RES complex proteins, Pml1 and Bud13 (70). The structure of the RRM domain of Snu17 in complex with a short N-terminal sequence of Pml1 (20–43) and a C-terminal sequence (213–246) of Bud13 (PDB 2MKC) has been solved by NMR (71). Additionally, the Snu17 structure was also determined within a complex with a longer piece of the Bud13 C terminus (PDB 4UQT) (10) that also includes a short helix (240–256) at the C terminus. Merged, the two structures fit well into a density on the back of B ^{act} . This density is connected to the lower loops of Hsh155 HEAT repeats 7–9 and is framed by Prp8-RT/En, Prp8-RH and Cwc22-MA3. The Bud 13 C-terminal helix occupies a density tube that continues further down to Prp8-RT/En. Two crosslinks of Snu17 to HEAT repeats 7 and 8 (K103 to Hsh155 K410 and K455) support this location and orientation of this central part of the RES complex.
Pml1 23.6 kDa 204 aa	FHA 28–42 51–204	The structure of a large part (51–204) of the S.c. protein Pml1 (PDB 2JKD, PDB 3ELV) containing the FHA domain was determined by crystallography (72, 73). A well-fitting density is located close to the side of Snu17 where the bound Pml1 N terminus exits. In its position within the B ^{act} complex, Pml1 forms a bridge between Snu17 and the C terminus of the Prp8-RT-associated Prp45 helix. Refinement was performed with COOT.
Bud13/Cwc26 30.5 kDa 266 aa	235–266	For Bud13 only the structure of a short piece of the C terminus (222–256) is known from the Snu17-Bud13 complex NMR structure (see above, Snu17/Ist3). A network of crosslinks indicates that the large N-terminal part extends from Snu17 up to the Brr2-Jab1 region of the B ^{act} complex. The C-terminal helix was further modeled into the density extension (see above, Snu17/Ist3).
Prp2 99.8 kDa 876 aa	RecA1 186–397	The Prp2 RecA domains and the C-terminal domain were modeled with Prp43 as a template (PDB 2XAU) (74). The modeled C-terminal domain fits perfectly into a density region connecting the OB-fold of that domain to Hsh155 HEAT repeats 7 and 8. The RecA domains fit into two densities that are attached on the outside of the C-terminal domain which establishes contact with the main body of B ^{act} . Both RecA domains have no contact to any other high-resolution B ^{act} density. The RecA domain densities are in close proximity to the mask applied for producing the high-resolution B ^{act} structure and are less well defined than the C-terminal domain is.
	RecA2 401–575	
	C-term/OB-fold	

	587–864	Refinement was performed with COOT.
Spp2 20.6 kDa 185 aa		The structure of Spp2 has not yet been determined. Not surprisingly, evidence from a network of crosslinks places Spp2 in the B ^{act} complex close to Prp2 (see Fig. S17). The N-terminal Spp2 region resides in the vicinity of Brr2, while the C-terminal region is located closer to the RES complex. The central domain seems to be the main Prp2-binding region. The known Prp2-binding sequence, the G-patch domain, links the central domain to the C-terminal domain. No crosslinks are at present available to allow positioning of the G-patch sequence region.

Table S2: BS3-crosslinks of proteins in the yeast B^{act} complex

Type	Protein 1	Protein 2	Residue 1	Residue 2	Å	Spectral count			Score _{max}			Total spectral count	Best Score _{max}	
						Set 1	Set 2	Set 3	Set 1	Set 2	Set 3			
Inter	Brr2	Bud13/Cwc26	71	115				3			3,40	3	3,40	
			74	115				2			7,06	2	7,06	
			91	53				1			3,42	1	3,42	
			304	2		5		4	14,17		11,82	9	14,17	
				15				2			5,65	2	5,65	
				35				1			3,46	1	3,46	
				414				1			2,20	1	2,20	
				417				1			7,12	1	7,12	
				61				1			1,81	1	1,81	
				1733		41	4	1			3,26	5	3,26	
	Cwc24		748	256		1			0,20			1	0,20	
			2109	29			2	2		7,16	7,35	4	7,35	
	Cwc27		1504	213		1		1	0,94			2,00	2	2,00
			1529	225		1	3	1	0,47	5,11	7,64	5	7,64	
	Ecm2		82	356				1			2,03	1	2,03	
	Hsh155		82	35				1			1,49	1	1,49	
	Prp17		1414	153		1			0,97			1	0,97	
	Prp2		2	211				1			6,22	1	6,22	
			28	211				2			7,29	2	7,29	
			1437	45				1			5,60	1	5,60	
			1623	2				1			2,31	1	2,31	
			2070	2				3			8,79	3	8,79	
			2109	2				10			10,91	10	10,91	
			2116	2				1			7,51	1	7,51	
			2121	2				35			16,89	35	16,89	
	Prp8		2	1903				2			9,54	2	9,54	
			25	1903		1			1,15			1	1,15	
			31	1903		1			0,32			1	0,32	
			50	2016				1			7,68	1	7,68	
			74	2016				3			8,59	3	8,59	
			91	2154				1			8,47	1	8,47	
			2284					1			1,15	1	1,15	
			304	2167				1			6,73	1	6,73	
			2187					1			6,89	1	6,89	
			2213					2			5,60	2	5,60	
			1055	2108				2			5,65	2	5,65	
			2149		17,5			1			5,78	1	5,78	
	Prp9		2154		16,4		3	6		5,43	5,02	9	5,43	
	Rse1		152	519			1			0,14		1	0,14	
			304	556				2			6,29	2	6,29	
			414	556				7			8,66	7	8,66	
			417	556				1			3,42	1	3,42	
			758	1269				1			1,69	1	1,69	
			795	1269				1			4,89	1	4,89	
			967	556				1			6,22	1	6,22	
	SmD2		1904	59			1			2,76		1	2,76	
	Snt309		748	94			1			0,55		1	0,55	
	Snu114		2	955				1			5,16	1	5,16	
			7	955				1			4,08	1	4,08	
	Spp2		74	133				1			6,69	1	6,69	
			85	133				1			3,56	1	3,56	
			91	58				3			15,52	3	15,52	
				133		1		5	0,62		16,93	6	16,93	
			168	38				1			4,12	1	4,12	
			445	38				1			5,97	1	5,97	
				58		1			3,83			1	3,83	
			454	38				5			3,46	5	3,46	
			68		2			1	1,65		1,27	3	1,65	
			769	38				4			10,34	4	10,34	
				46				1			4,44	1	4,44	
	Bud13/Cwc26	Syf1	259	362		1			0,58			1	0,58	
	Bud13/Cwc26	Brr2	2	304		5		4	14,17			11,82	9	14,17
			15	304				2			5,65	2	5,65	
			35	304				1			3,46	1	3,46	
			41	1733			4	1		3,26	2,82	5	3,26	
			53	91				1			3,42	1	3,42	
			417					1			7,12	1	7,12	
			61	417				1			1,81	1	1,81	
			64	414				1			2,20	1	2,20	
			115	71				3			3,40	3	3,40	
				74				2			7,06	2	7,06	
	Clf1		115	458				1			4,06	1	4,06	
	Cus1		255	40		1			0,79			1	0,79	
	Cwc22		201	520				1			3,45	1	3,45	
			213	520				2			6,91	2	6,91	
				530		2		1	3,05		1,61	3	3,05	
	Cwc24		217	520			1			1,88		1	1,88	
			115	4		1			3,23			1	3,23	
			213	100		1			1,03			1	1,03	

Type	Protein 1	Protein 2	Residue 1	Residue 2	Å	Spectral count			Score _{max}			Total spectral count	Best Score _{max}
						Set 1	Set 2	Set 3	Set 1	Set 2	Set 3		
Hsh155			120	473	20,0 16,7		3	1	2,42	2,23	4	2,42	
			511	511			2	4	4,13	9,36	2	4,13	
			130	473				1	13,86	1	9,36		13,86
			511	511				1	2,03	1	2,03		
			136	473				1	8,53	20	8,53		
			255	612		1	4	15	4,45	7,00	20		
			256	612		2	2	5	0,53	5,10	7	5,10	
			115	567				1		0,09	1	0,09	
			181	2				1		6,85	1	6,85	
			136	367		1		1		5,55	1	5,55	
Prp2			146	352	33,4		1	1	2,53	2,42	2	2,53	
			2	2217			1	1	0,63		1	0,63	
			2219				1	1	5,15	1,47	2	5,15	
			15	2187				2		11,00	2	11,00	
			17	2187		2			3,68		2	3,68	
			35	1903		3			1,92		3	1,92	
			41	1903		2			2,22		2	2,22	
			53	2016				1		8,14	1	8,14	
			61	2016				1		2,19	1	2,19	
			68	2187				2		4,23	2	4,23	
Rse1			120	2016	1				0,68		1	0,68	
			181	1926				2		4,40	2	4,40	
			255	1589				2		7,71	2	7,71	
			115	1269				1		5,69	1	5,69	
			169	133			2	1	4,84	2,06	3	4,84	
			138			4	7	4	3,39	6,93	15	8,23	
			179	138			4	6	4,88	14,63	10	14,63	
			143			1	2	4	2,73	1,41	7	9,46	
			180	138				2		6,88	2	6,88	
			181	133			1	3	3,77	5,55	4	5,55	
Snu17/Ist3			138		12	17	48	10,00	6,95	77	10,00		
			143			2	2	0,52	1,85	4	1,85		
			201	138		1	4	4,09	3,27	9,39	21	9,39	
			143				6		5,09	6	5,09		
			206	138		3	4	11,35		7,72	7	11,35	
			143			1		0,97			1	0,97	
			213	133		3	5	3	6,15	6,66	11	6,66	
			138			5	6	5	8,35	6,20	16	9,39	
			143			1		0,90			1	0,90	
			244	10	2				4,43		2	4,43	
Spp2			115	151			8			10,72	8	10,72	
			120	151		13	17	12,61		9,30	30	12,61	
			154			3		1,97			3	1,97	
			136	151		3		1	7,57	13,17	10	13,17	
			154					1		5,35	1	5,35	
			182				2		4,89	2	4,89		
			146	151		2	1	0,69		2,77	3	2,77	
			154			1	2	1,81		9,42	3	9,42	
			151	181				1		2,59	1	2,59	
			10	495						1,53	1	1,53	
Bud31			35	78	39,1			2		4,58	2	4,58	
			40	230				1		9,34	1	9,34	
			240	113		11,1	6	9	6,06	8,32	19	11,14	
			247	111		14,5	2	1	7,51	2,12	6	8,45	
				113		11,5	2	1	2,42	0,29		3	2,42
			251	111		14,5			1,16		1	1,16	
				113		13,6	2	2	10,44	4,75		4	10,44
			318	507				1		2,52	1	2,52	
			294	42				1		1,49	1	1,49	
			359	205		1			0,18		1	0,18	
Cef1			305	94	21			2		3,90	2	3,90	
			305	94									
			305	94									
			305	94									
			305	94									
			305	94									
			305	94									
			305	94									
			305	94									
			305	94									
Isy1			22	36	21		1		1,92		1	1,92	
			444	108		5		13	4,63	6,83	18	6,83	
			454	130		2	2	2	3,58	9,32	6	9,32	
			496			1			2,63		1	2,63	
			496	107		3	3	16	8,53	2,42	22	8,53	
			496	108		3	5	14	1,87	8,46			
			500	108		21	23	220	14,32	7,01	22	7,01	
			558	108			1		2,63	5,71			
			263	732			1		7,46		1	7,46	
			166	98		1			5,68		1	5,68	
Prp2			294	1910	3		1		0,62		1	0,62	
			496	2192					0,46		1	0,46	
			187	76					0,95		1	0,95	
			321	85					0,46		1	0,46	
			187	26						1,36	1	1,36	
			293	770		3	4	2	3,68	4,58	9	4,58	
			294	770				1	1,22		1	1,22	
			296	770				1	0,78		1	0,78	
			312	770		1			2,91		1	2,91	
			239	173		3	1		4,95	0,55	4	4,95	
SmD3			240	159	5		1		7,61	11,75	21	3,73	
			173			6	10			9,07		11,75	

Type	Protein 1	Protein 2	Residue 1	Residue 2	Å	Spectral count			Score _{max}			Total spectral count	Best Score _{max}	
						Set 1	Set 2	Set 3	Set 1	Set 2	Set 3			
Clf1	Bud13/Cwc26	247	159				1	4	6	3,71	6,44	10	6,44	
		173	173			2	1	2	4,91	1,42	8,77	5	8,77	
		251	173			1			0,55			1	0,55	
		259	173											
		458	115									1	4,06	
		Cef1	111	247	14,5	2	1	3	7,51	2,12	8,45	6	8,45	
			251	14,5						1,16		1	1,16	
			113	240	11,1	6	9	4	6,06	8,32	11,14	19	11,14	
				247	11,5	2	1		2,42	0,29		3	2,42	
	Cus1		251	13,6		2	2		10,44	4,75		4	10,44	
			507	318				1			2,52	1	2,52	
			24	202		1						1	4,36	
				289		2						2	2,29	
			Cwc2	24	236		1			4,19			1	4,19
			Cwc21	25	62								0,91	
			Ecm2	24	164								4,54	
				59	116		1	2				3	2,98	
				668	230							1	2,55	
Cus1	Isy1	529	104			1				3,23			1	3,23
		Ntc20	451	121			2	2				4	6,69	
		Prp2	425	10				1					2,46	
		Prp46	273	67			1	3		4,33	12,55	4	12,55	
				87				3					9,49	
				88		1		1					10,44	
		Rds3	640	42		1	1	3	3,50	0,50	5,76	5	5,76	
		SmG	668	1		1			0,08			1	0,08	
		Snt309	670	94				1					4,05	
	Syf2	Snu114	670	627				1					1	0,28
		Spp2	458	151				1					2,99	
		Syf1	180	524		3	5	3	5,16	2,04	5,79	11	5,79	
				531		2		1	2,81		2,27	3	2,81	
				289	653			1			8,83	1	8,83	
				304	650	8	3	5	16,67	5,17	6,87	16	16,67	
					653	12	10	54	17,65	11,96	13,33	76	17,65	
					173		4	6		2,24	4,57	10	4,57	
				113	159	7	7	5	4,73	2,95	7,19	19	7,19	
SmB	Hsh49		173			4		2	10,42		7,42	6	10,42	
			180	121				8			9,41	8	9,41	
		Bud13/Cwc26	40	255		1				0,79		1	0,79	
		Clf1	202	24		1				4,36		1	4,36	
			289	24		2				2,29			2,29	
		Cwc2	436	10				1					5,61	
		Ecm2	429	203				1					6,37	
		Hsh155	102	237		1	1	1	3,85	0,69	2,42	3	3,85	
				325		4		1	2,40	3,50		5	3,50	
	Prp11		223	722				4					2,31	
			226	722				5					5,11	
			236	722		13	42		8,32	7,90		55	8,32	
		Hsh49	102	204				1					2,65	
		Isy1	41	59		1			0,03			1	0,03	
			48	59				1					3,17	
			317	157				1					1,98	
		Msl1	102	2				2					6,19	
			128	2		1		1	8,56			2	8,56	
SmD1	Rse1	Prp11	223	28				4					5,60	
			48					2					0,99	
			60					2					3,26	
			192					1					2,44	
			226	11				3					4,34	
	Prp19		28					2					5,53	
			36			4				2,17		4	2,17	
			48					4					5,15	
			60			1	2		3,83	3,98		3	3,98	
			192				1			5,00		1	5,00	
SmD1	Prp21	Prp19	357	272		2				1,11		2	1,11	
		Prp2	102	2				1			6,10	1	6,10	
		Prp21				1				0,13		1	0,13	
		Prp9	128	466		1	2	2	3,23	1,24	2,61	5	3,23	
				468		1		1	0,38		5,52	2	5,52	
	Rse1		492					1					3,31	
		Rse1	245	1342		2	11	19	1,01	7,20	11,47	32	11,47	
			246	1342		5	19	8	6,41	12,16	11,56	32	12,16	
			347	1149		1	2		4,32	4,68		3	4,68	
			79	186				1					3,62	
SmD1	SmB		83	138				2					4,68	
			145					1					2,97	
			186					1					4,86	
			86	138				1					1,97	
			95	138		1	2		0,44		8,99	3	8,99	
	SmD1	102	138					4					8,02	
			186					1					7,29	
			128	117		1		1	1,46			2	4,59	
			83	128				1					4,47	
												1	4,47	

Type	Protein 1	Protein 2	Residue 1	Residue 2	Å	Spectral count			Score _{max}			Total spectral count	Best Score _{max}
						Set 1	Set 2	Set 3	Set 1	Set 2	Set 3		
SmD3			102	128				3			8,62	3	8,62
			79	2				17			9,62	17	9,62
			83	2				4			9,14	4	9,14
				86				2			6,19	2	6,19
				86	2			2			4,62	2	4,62
				85				1			1,90	1	1,90
			102	2				1			3,26	1	3,26
SmE			39	6		4	2	10	2,02	2,30	4,35	16	4,35
			48	6		1	1	16	0,86	0,64	5,50	18	5,50
			53	6				1			1,87	1	1,87
			58	6				1			2,86	1	2,86
				79	6		2					2	3,36
SmF			58	20							2,80		2,80
			2	8		2						2	1,18
			16	24							2,89	5	8,83
			79	2			2	13			3,68	15	9,91
SmG				8								1	3,97
			83	2							3,09	1	3,09
				8							2,50	2	2,50
			Syf1	317	146	4	5	3	15,41	11,09	10,86	12	15,41
				329	146						1,31	1	1,31
			Ysf3	102	12						3,31	1	3,31
				15		1		1	0,22		1,15	2	1,15
Cwc15	Cwc24		41	228		1			0,36			1	0,36
	Ecm2		16	27		1			1,20			1	1,20
	Prp45		41	71		1			4,39		6,62	2	6,62
			43	71								1	1,32
	Prp8		151	1242			1	1		1,32		1	5,95
			172	1205			1			0,70		1	0,70
				1310		3			3,49			3	3,49
	Rse1		43	557							3,38	2	3,38
	Snu114		140	60		1			5,78			1	5,78
			145	59		1			3,47			1	3,47
				60		1	2	1	0,63	4,30	5,72	4	5,72
			150	59		4	1	2	4,12	0,67	3,96	2	3,96
Cwc2				60					2,10			5	4,12
				72		1						1	2,10
			151	59					1		1,79	1	1,79
				60		2	4	3	9,75	7,80	8,57	9	9,75
				72				4			13,68	4	13,68
				81				14			12,86	14	12,86
	Syf2		102	9		1			0,13			1	0,13
	Clf1		236	24		1			4,19			1	4,19
	Cus1		10	436							5,61	1	5,61
	Cwc24		152	93					1		6,93	1	6,93
Cwc24	Ecm2		2	230		1	2	11	1,27	4,41	6,91	14	6,91
				233		1	6	11	4,08	2,53		7	4,08
			152	188			2	4		5,56	11,32	6	11,32
				189		29	26	132	14,18	8,62	14,79	187	14,79
			236	116				2			5,12	2	5,12
				119	26,3			6			6,76	6	6,76
				157		3	3	4	4,36	1,44	6,79	10	6,79
				164		2	2	5	8,28	3,07	10,52	9	10,52
				167		1	1	12	15,55	3,07	12,74	14	15,55
			173	30,7		4	2	1	2,40	2,32	5,14	7	5,14
Isy1			247	18,7		2		2	2,21		6,84	4	6,84
				152	7	1			3,83			1	3,83
				27				1			2,53	1	2,53
				40		1			3,32			1	3,32
				42								2	2,56
Prp17			152	207		4	2	1	9,51	5,81	1,66	7	9,51
	Prp19		286	107				2			3,09	2	3,09
				108		3	3	31	4,55	1,57	11,28	37	11,28
				320	108	4	4	7	7,67	6,27	8,30	15	8,30
Cwc21	Prp46		286	56		1			0,65			1	0,65
	SmG		310	8								2	1,04
	Syf1		310	524								2	4,43
				531					1		1,35	1	1,35
			320	424		4	1	3	5,37	5,03	3,68	8	5,37
	Clf1		62	25			4	1		0,30	0,91	5	0,91
	Cwc27		98	234			3			0,96		3	0,96
	Prp19		98	404					1		2,36	1	2,36
	Prp2		48	756							10,75	1	10,75
	Prp8		12	351							9,11	1	9,11
Cwc22				1205		3		2	3,97		4,62	5	4,62
	Snu114		12	955		6	2	6	9,33	5,91	12,44	14	12,44
	Bud13/Cwc26		520	201				1			3,45	1	3,45
				213							6,91	2	6,91
				217		1					1,88	1	1,88
				530	213	2		1	3,05		1,61	3	3,05
	Bud31		495	10							1,53	1	1,53
	Cwc24		294	123				1			4,16	1	4,16

Type	Protein 1	Protein 2	Residue 1	Residue 2	Å	Spectral count			Score _{max}			Total spectral count	Best Score _{max}	
						Set 1	Set 2	Set 3	Set 1	Set 2	Set 3			
Cwc24	Cwc27		176	295	10,3	5		1	1,56			5	1,56	
	Ntc20		203	1				1		0,36		1	0,36	
	Prp11		548	28				1		1,68		1	1,68	
	Prp2		520	137				1		2,20		1	2,20	
	Prp45		505	130		1			2,06			1	2,06	
			274			5	1	1	6,23	3,75	4,11	7	6,23	
			520	265		1	1	7	5,13	4,37	11,97	9	11,97	
			274			18	11	17	11,78	9,46	14,67	46	14,67	
			287			4	1	7	2,44	0,74	3,90	12	3,90	
			530	265		4	4	3	6,04	6,92	7,54	11	7,54	
			274			16	7	14	8,37	3,25	7,13	37	8,37	
			287			4	8	14	5,49	4,49	7,60	26	7,60	
	Prp8		294	1435				2			13,19	2	13,19	
			505	121		4			2,82			4	2,82	
	Snu114		176	369		5			4,02			5	4,02	
	Snu17/lst3		520	138				1		4,91		1	4,91	
			530	143		1			2,93			1	2,93	
	Syf1		548	311			1			26,34		1	26,34	
	Ysf3		203	15		147,7			0,49			1	0,49	
	Brr2		29	2109			2	2	7,16	7,35		4	7,35	
			256	748		1			0,20			1	0,20	
	Bud13/Cwc26		4	115			1		3,23			1	3,23	
			100	213			1		1,03			1	1,03	
	Cwc15		228	41		1			0,36			1	0,36	
	Cwc2		93	152						6,93		1	6,93	
	Cwc22		123	294						4,16		1	4,16	
	Cwc27		63	171						6,12		2	6,12	
	Prp2		232	870						1,61		1	1,61	
			256	40						1,78		2	1,78	
	Prp8		63	2284		3			2,13			3	2,13	
			93	235		2	2	3	3,33	0,89	10,67	7	10,67	
			517			1			1,40			1	1,40	
			684			4	8	6	10,33	7,89	8,80	18	10,33	
			697			3	1		3,79	1,77		4	3,79	
			1926					8		6,65		8	6,65	
			1931					1		5,32		1	5,32	
			98	235		13,5	1			0,69		1	0,69	
			1926	28,4				5		5,07		5	5,07	
			1931	28,7		123	2		0,39	4,69		3	4,69	
			235		13,5	3	3		1,02	0,42		6	1,02	
			517			2	3		3,45	3,27		5	3,45	
			681			1			0,84			1	0,84	
			684			2	1	1	1,46	5,97	6,15	4	6,15	
			697			5	2	2	14,16	8,26	6,08	9	14,16	
			1435					3		10,51		3	10,51	
			1926			3	1	8	5,55	3,54	7,20	12	7,20	
			1931			2		4	3,57		10,66	6	10,66	
	Rse1		182	1342				3		3,96		3	3,96	
	Spp2		4	151		1			0,05			1	0,05	
	Brr2		213	1504		1		1	0,94		2,00	2	2,00	
			225	1529		1	3	1	0,47	5,11	7,64	5	7,64	
	Bud31		78	35				2			4,58	2	4,58	
	Cwc21		234	98			3			0,96		3	0,96	
	Cwc22		295	176		5			1,56			5	1,56	
	Cwc24		171	63				2			6,12	2	6,12	
	Prp8		123	1713				6			11,34	6	11,34	
	SmD1		216	140		1			2,77			1	2,77	
	Brr2		356	82				1			2,03	1	2,03	
	Bud31		230	40	39,1			1			9,34	1	9,34	
	Cif1		116	59			1	2		0,56	2,98	3	2,98	
			164	24				2			4,54	2	4,54	
			230	668				1			2,55	1	2,55	
	Cus1		203	429				1			6,37	1	6,37	
	Cwc15		27	16		1			1,20			1	1,20	
	Cwc2		116	236				2			5,12	2	5,12	
			119	236	26,3			6			6,76	6	6,76	
			157	236		3	3	4	4,36	1,44	6,79	10	6,79	
			164	236		2	2	5	8,28	3,07	10,52	9	10,52	
			167	236		1	1	12	15,55	3,07	12,74	14	15,55	
			173	236		30,7	4	2	1	2,40	2,32	5,14	7	5,14
			188	152				2	4	5,56	11,32	6	11,32	
			189	152		29	26	132	14,18	8,62	14,79	187	14,79	
			230	2	18,7	1	2	11	1,27	4,41	6,91	14	6,91	
			233	2		1	6		4,08	2,53		7	4,08	
			247	236		2		2	2,21		6,84	4	6,84	
	Prp17		188	207		4	2	1	3,14	2,72	4,89	7	4,89	
			271			1			4,58			1	4,58	
			189	207		1	2	2	0,21	1,97	7,29	5	7,29	
			271			9	4	2	14,24	9,54	6,86	15	14,24	
			203	207				2			3,11	2	3,11	
			274	207		2		2	2,15		9,05	4	9,05	
			210			1			0,00			1	0,00	
			271				4			1,03		4	1,03	

Type	Protein 1	Protein 2	Residue 1	Residue 2	Å	Spectral count			Score _{max}			Total spectral count	Best Score _{max}	
						Set 1	Set 2	Set 3	Set 1	Set 2	Set 3			
Hsh155			315			1		1	2,93		1,87	2	2,93	
			277	207		1			0,15			1	0,15	
	Snu114		188	111			1			0,82		1	0,82	
			353	746		1			0,46			1	0,46	
	Snu17/Ist3		188	123			1		0,08			1	0,08	
	Syf2		138	148		1			0,08			1	0,08	
	Brr2		35	82				1			1,49	1	1,49	
	Bud13/Cwc26		473	120			3	1		2,42	2,23	4	2,42	
				130				4			9,36	4	9,36	
				136				1			2,03	1	2,03	
Cus1			511	120			2	1			4,13	2	4,13	
			130								13,86	1	13,86	
			612	255	20,0	1	4	15	4,45	7,00	8,53	20	8,53	
				256	16,7		2	5		0,53	5,10	7	5,10	
			237	102		1	1	1		3,85	0,69	3	3,85	
			325	102			4	1			2,40	5	3,50	
			722	223				4				2,31	4	2,31
				226				5				5,11	5	5,11
				236			13	42			8,32	55	8,32	
	Prp11		722	11				1				2,24	1	2,24
Rds3	Prp2		237	2				1				5,79	1	5,79
	Prp8		35	906		7	6	27	2,85	4,13	5,79	40	5,79	
				1007			1	5			1,53	6	5,55	
			51	920				2				8,77	2	8,77
			104	1007				1				12,88	1	12,88
			137	956	15,3	12	5	10	9,03	2,25	12,45	27	12,45	
			142	956	21,0	1	4	7	6,97	7,13	7,47	12	7,47	
			151	956				2				8,87	2	8,87
			612	1588	30,5			1				6,21	1	6,21
				1589	31,6		6				6,78	6	6,78	
Rse1	Rse1		696	1588	9,7		2	1			3,56	3	6,15	
			276	29	43,7			3				5,61	3	5,61
			455	53	20,3	3						3	10,29	
			500	53	13,5	4						4	8,27	
			511	53	19,2	2						5	8,47	
				56	19,3			3				3	9,22	
			511	221	22,6		2	1			0,52	3	2,40	
				1269				4				4	6,95	
			595	1269				5				5	15,04	
			632	1269				2				2	4,56	
Hsh49			713	1269				4				7,49	4	7,49
				1342				1				5,21	1	5,21
	SmB		223	76		1					0,73	1	0,73	
			325	186			2				3,04	2	3,04	
	SmD1		158	128				2				6,46	2	6,46
				129				1				3,09	1	3,09
	Snu17/Ist3		736	128		1					3,09	1	3,09	
			66	96		5	2	5	3,20	1,92	3,46	12	3,46	
			104	96			2				4,99	2	4,99	
			410	103		14					15,45	14	15,45	
Isy1	Ysf3		455	103	17,8	6					12,69	6	12,69	
			500	10		2					14,08	2	14,08	
			932	4			2				0,68	2	0,68	
				12	12,7		3				3,56	3	3,56	
	Cus1		204	102				1				2,65	1	2,65
	Isy1		82	87				1				1,16	1	1,16
	Msl1		130	2		1		1				2,53	2	2,53
	Prp11		42	48				4				2,59	5	2,59
			101	103				2				2,47	2	2,47
	Prp21						2				1,53	2	1,53	
Hsh49	Prp9		39	462		1		1	1,39			1,59	2	1,59
			101	429				1				2,02	1	2,02
			147	371				1				2,10	1	2,10
			204	468		2	4	6	12,40	3,63	4,81	12	12,40	
				475			1	1			0,18	2	2,54	
			208	468		2	5	6	3,70	4,70	5,83	13	5,83	
				475			3	5			0,70	8	3,61	
				492		1		13	0,15			7,01	14	7,01
	Rse1		39	1176		4	2	8	5,21	0,44	3,10	14	5,21	
	Cef1		42	294				1				1,49	1	1,49
Cwc2	Clf1		104	529		1					3,23	1	3,23	
	Cus1		59	41		1					0,03	1	0,03	
				48				1				3,17	1	3,17
			157	317				1				1,98	1	1,98
			27	152		1						2,53	1	2,53
			40	152		1						1	3,32	
			42	152			1	1				1,48	2	2,56
	Hsh49		87	82				1				1,16	1	1,16
	Prp11		27	103				1				4,44	1	4,44
				126				2				5,64	2	5,64
Isy1				192				1				2,82	1	2,82
				56	192			1				1,53	1	1,53

Type	Protein 1	Protein 2	Residue 1	Residue 2	Å	Spectral count			Score _{max}			Total spectral count	Best Score _{max}
						Set 1	Set 2	Set 3	Set 1	Set 2	Set 3		
Lea1	Prp21					1			4,84			1	4,84
	SmB	106	100			1			1,19			1	1,19
	SmG	104	8							2,89		1	2,89
	Syf1	7	259					2		5,83		2	5,83
		328				1	3	6	10,49	5,14	9,35	10	10,49
		424				1	2	5	1,18	5,11	7,02	8	7,02
		27	328			1			2,03			1	2,03
		40	328			2	3	7	2,37	2,44	4,75	12	4,75
		139	146			2			5,57			2	5,57
		143	146			2	4	1	5,24	4,45	4,06	7	5,24
		157	220				1	4	0,70	9,62		5	9,62
			249					1		3,79		1	3,79
			161	220		3	7	9	2,63	2,37	4,94	19	4,94
			171	220		9	6	1	4,61	5,04	2,46	16	5,04
	Syf2	7	26			1	4	3	1,75	2,47	4,26	8	4,26
		27	26				1	4		1,36	4,12	5	4,12
Msl1		42	173			1	2		5,98	1,83		3	5,98
	Yju2/Cwc16	103	63				1			0,27		1	0,27
	Cef1	205	359			1					0,18	1	0,18
	Msl1	215	2					1			3,65	1	3,65
	Prp21						1				0,27	1	0,27
	Prp9	2	140								7,02	1	7,02
		194	115								1,75	1	1,75
		215	107								1,72	1	1,72
			115			3	5	8	3,15	2,06	11,71	16	11,71
			121			1		2	3,07		3,26	3	3,26
			216	115							1,38	1	1,38
			232	121							1,81	1	1,81
	SmB	125	76				3	11		1,57	8,77	14	8,77
	Syf1	232	32			1	1			2,40	1,79	2	2,40
	Cus1	2	102					2			6,19	2	6,19
Ntc20			128			1		1	8,56		5,86	2	8,56
	Hsh49	2	130				1	1		2,16	2,53	2	2,53
	Lea1	2	215					1			3,65	1	3,65
	Prp9	2	115			1		6	12,81		10,88	7	12,81
			121					4			4,11	4	4,11
			124					8			5,13	8	5,13
	Rse1	2	1001			1			1,63			1	1,63
	SmB	2	105			2			1,64			2	1,64
			114					1			1,59	1	1,59
			124					1			1,92	1	1,92
			138					2			4,30	2	4,30
			186				1			0,03		1	0,03
	SmD3	2	85					1			4,79	1	4,79
	Cef1	94	305					2			3,90	2	3,90
Pml1	Clf1	121	451				2	2		3,86	6,69	4	6,69
	Cwc22	1	203					1			0,36	1	0,36
	Syf1	27	498			6		2	4,07		8,58	8	8,58
			558			2	2	2	1,41	1,40	5,11	6	5,11
	Prp2	6	820			1			0,39			1	0,39
	Prp45	88	242			1		1	0,50		5,76	2	5,76
		90	242			2	8	1	2,44	5,39	2,84	11	5,39
	Syf1	153	372					1			1,13	1	1,13
	Cef1	36	22			1				1,92		1	1,92
	Cus1	11	226					3			4,34	3	4,34
		28	223					4			5,60	4	5,60
			226					2			5,53	2	5,53
		36	226				4			2,17		4	2,17
		48	223					2			0,99	2	0,99
Prp11			226					4			5,15	4	5,15
		60	223					2			3,26	2	3,26
		192	223				1	2		3,83	3,98	3	3,98
			226					1			2,44	1	2,44
	Cwc22	28	548					1			5,00	1	5,00
	Hsh155	11	722					1			1,68	1	1,68
	Hsh49	48	42			1		4	0,96		2,24	1	2,24
		103	101					2			2,59	5	2,59
	Isy1	103	27					1			2,47	2	2,47
		126	27					2			4,44	1	4,44
		192	27					1			5,64	2	5,64
			56					1			2,82	1	2,82
	Prp2	121	43					1			1,53	1	1,53
	Prp21						11	26	47	4,49	8,14	84	8,50
Prp8	Prp8	11	956						1		11,80	1	11,80
	Prp9	11	58						3		7,10	1	7,10
			371						1		6,61	3	6,61
		173	58						9		12,95	1	12,95
			61						1		11,12	9	11,12
		175	61								2,35	1	2,35
	SmB	103	138					3			1,26	3	1,26
			145						1		2,54	1	2,54
		126	186						1		1,21	1	1,21
											2,38	1	2,38

Type	Protein 1	Protein 2	Residue 1	Residue 2	Å	Spectral count			Score _{max}			Total spectral count	Best Score _{max}
						Set 1	Set 2	Set 3	Set 1	Set 2	Set 3		
Prp17	Syf1		192	424		1		4	2,48	5,17	7,93	5	7,93
	Syf2		192	26		2	3	5	3,34	6,42	10	6,42	
	Brr2		153	1414		1			0,97			1	0,97
	Cwc2		207	152		4	2	1	9,51	5,81	1,66	7	9,51
	Ecm2		207	188		4	2	1	3,14	2,72	4,89	7	4,89
			189			1	2	2	0,21	1,97	7,29	5	7,29
			203					2			3,11	2	3,11
			274			2		2	2,15		9,05	4	9,05
			277			1			0,15			1	0,15
			210	274		1			0,00			1	0,00
Prp19	271		188			1			4,58			1	4,58
			189			9	4	2	14,24	9,54	6,86	15	14,24
			274				4		1,03			4	1,03
			315	274		1		1	2,93		1,87	2	2,93
			27	170				1			2,99	1	2,99
			404	670		1			0,48			1	0,48
			Cef1	107	496	3	3	16	8,53	2,42	8,46	22	8,53
			108	444		5		13	4,63		6,83	18	6,83
			496			3	5	14	1,87	7,01	5,71	22	7,01
			500			21	23	220	14,32	14,03	16,95	264	16,95
Prp19			558					1			7,46	1	7,46
			130	454		2	2	2	3,58	9,32	5,03	6	9,32
			135	454			1			2,63		1	2,63
			Cus1	272	357			2			1,11	2	1,11
			Cwc2	107	286						3,09	2	3,09
			108	286		3	3	31	4,55	1,57	11,28	37	11,28
				320		4	4	7	7,67	6,27	8,30	15	8,30
			Cwc21	404	98						2,36	1	2,36
			Prp17	170	27						2,99	1	2,99
			Prp21			1						1	0,08
Prp8			Prp8	107	1372	2			0,08			2	1,22
				1378		1			1,22			1	1,38
				108	1209			1	1,38		0,41	1	0,41
			SmB	378	55	1			3,42			1	3,42
				60		2	3	1	4,83	2,16	0,94	6	4,83
			SmG	130	24	1			0,98			1	0,98
			Snt309	107	25	12	3	8	10,81	8,62	13,48	23	13,48
				32		2		12	4,50		13,91	14	13,91
				46		1	4		1,70	10,80		5	10,80
				48		6	3	11	6,46	1,19	8,82	20	8,82
Prp2				67		7	4	10	14,65	3,43	9,05	21	14,65
				72			1		0,21			1	0,21
				108	25	15	9	9	14,90	10,62	17,25	33	17,25
				46		9	6	9	9,75	5,41	5,51	24	9,75
				48				1		12,06		1	12,06
				120	25	4	2	4	5,76	4,11	7,08	10	7,08
				130	26	1	1	1	0,24	2,43	6,54	3	6,54
				135	11	1			1,31			1	1,31
				139	26	2	2		4,21	3,59		4	4,21
	Brr2		2	1623			1				2,31	1	2,31
Prp2				2070			3				8,79	3	8,79
				2109			10				10,91	10	10,91
				2116			1				7,51	1	7,51
				2121			35				16,89	35	16,89
				45	1437		1				5,60	1	5,60
				211	2		1				6,22	1	6,22
			Bud13/Cwc26	2	181			2			7,29	2	7,29
				567	115		1				6,85	1	6,85
			Cef1	732	263		1				0,09	1	0,09
			Clf1	10	425			1			5,68	1	5,68
Prp8			Cus1	2	102			1			2,46	1	2,46
			Cwc21	756	48			1			6,10	1	6,10
			Cwc22	137	520			1			10,75	1	10,75
			Cwc24	40	256			2			2,20	1	2,20
				870	232			1			1,78	2	1,78
			Hsh155	2	237			1			1,61	1	1,61
			Pml1	820	6	1		1			5,79	1	5,79
			Prp11	43	121			1			8,50	1	8,50
			Prp45	2	274			1			5,90	1	5,90
				60	274			1			6,27	1	6,27
Prp8				101	274	1	2	1,35			9,86	3	9,86
				102	265		1				10,38	1	10,38
				113	274	2	2	3,95			11,12	4	11,12
				274			1				3,13	1	3,13
				274			2				6,24	2	6,24
				120	274	2	2	0,95			7,59	4	7,59
				128	274	1		0,80				1	0,80
				130	274		1				2,15	1	2,15
				133	274		5				6,22	5	6,22
				40	672		1				1,38	1	1,38
Prp8				467	1903	84,6	2				3,45	2	3,45
				560	1903	82,5	2				3,48	2	3,48

Type	Protein 1	Protein 2	Residue 1	Residue 2	Å	Spectral count			Score _{max}			Total spectral count	Best Score _{max}
						Set 1	Set 2	Set 3	Set 1	Set 2	Set 3		
Prp9			756	519	155,0			1			5,49	1	5,49
			820	817		1			2,95			1	2,95
	Prp9		83	235			1			0,94		1	0,94
	Rds3		10	42				3			3,45	3	3,45
	SmD1		756	128				1			2,24	1	2,24
	SmE		14	1		1						1	0,82
	Snu114		40	115				1			2,34	1	2,34
			632	955	149,8			2			7,04	2	7,04
			756	749	208,0			1			1,75	1	1,75
				955	160,1			5			5,61	5	5,61
Spp2			763	955	147,7			1			5,73	1	5,73
			851	955	135,7			3			6,41	3	6,41
	Spp2		336	82		2		5	1,67		7,16	7	7,16
			83			1		4	2,28		2,76	5	2,76
			461	168		4		6	3,34		5,84	10	5,84
			181					1			2,80	1	2,80
			632	82				1			3,53	1	3,53
			83			2		2	7,68		7,77	4	7,77
			640	83		1			4,92			1	4,92
			750	82		1		1	1,21		3,93	2	3,93
Prp21			756	82		1			1,91			1	1,91
				83		1		2	3,40		2,90	3	3,40
				95				1			5,34	1	5,34
			840	154		1			2,83			1	2,83
	Yju2/Cwc16		732	29		2			0,44			2	0,44
	Cus1		261	53			1			0,13		1	0,13
	Hsh49		175	147			2			1,53		2	1,53
	Isy1		189	7		1			4,84			1	4,84
	Lea1		175	194			1			0,27		1	0,27
	Prp11		68	175				1			2,66	1	2,66
Prp19			177	175			4			3,18		4	3,18
			183	121			7	1		5,85		8	6,15
			199	126			1	4		1,72		5	3,13
			205	192				1			5,64	1	5,64
			234	139		3	6	4	1,71	8,14	11,74	13	11,74
			240	11				3			8,58	3	8,58
			130					1			2,15	1	2,15
			139			4	4	12	4,49	5,55	11,80	20	11,80
			247	11				1			5,42	1	5,42
			192					1			2,90	1	2,90
Prp45			254	11				3			2,84	3	2,84
			28					1			2,39	1	2,39
			126			1			0,70			1	0,70
			192			2	2	7	1,31	1,07	6,91	11	6,91
			194					1			2,16	1	2,16
			256	28				1			2,85	1	2,85
			36					1			2,56	1	2,56
			192			1	1	2	0,02	2,23	4,18	4	4,18
			261	28				1			2,39	1	2,39
			192				1	1		1,00	2,27	2	2,27
Prp8			177	18		1			0,08			1	0,08
	Prp45		175	237		1			0,00			1	0,00
	Prp8		247	777				1			2,63	1	2,63
	Prp9		20	47			3			1,48		3	1,48
			58			5	2		4,61		5,46	7	5,46
			29	58				1			3,99	1	3,99
			41	58							5,63	1	5,63
			68	47			19	13		2,14	2,37	32	2,37
			58			5	12	81	4,47		10,51	98	10,51
			61			3	2		2,58		5,34	5	5,34
Prp19			105	107		7	2	7	2,65	1,77	6,82	16	6,82
			115			6	13	14	10,69	3,91	4,70	33	10,69
			116	107				1			7,28	1	7,28
			121			1	1		0,68	1,32		2	1,32
			143	107		3	7	13	18,44	12,85	6,21	23	18,44
			175	371		1	7	4	0,98	7,82	10,71	12	10,71
			68	194				1			1,62	1	1,62
			175	124			1			1,50		1	1,50
			240	424				2			4,63	2	4,63
			247	424				1			4,45	1	4,45
Prp45			254	424		3		5	3,40			8	6,01
			256	424		1		4	1,06		4,15	5	4,15
			247	26				1			4,02	1	4,02
			254	26			1			3,40		1	3,40
	Bud13/Cwc26		352	146		1		1	2,53		2,42	2	2,53
			367	136				1			5,55	1	5,55
	Cwc15		71	41		1		1	4,39		6,62	2	6,62
			43				1			1,32		1	1,32
	Cwc22		130	505		1			2,06			1	2,06
			265	520		1	1	7	5,13	4,37	11,97	9	11,97
				530		4	4	3	6,04	6,92	7,54	11	7,54
				274	505	5	1	1	6,23	3,75	4,11	7	6,23
				520		18	11	17	11,78	9,46	14,67	46	14,67

Type	Protein 1	Protein 2	Residue 1	Residue 2	Å	Spectral count			Score _{max}			Total spectral count	Best Score _{max}	
						Set 1	Set 2	Set 3	Set 1	Set 2	Set 3			
Pml1			530			16	7	14	8,37	3,25	7,13	37	8,37	
			287	520		4	1	7	2,44	0,74	3,90	12	3,90	
			530			4	8	14	5,49	4,49	7,60	26	7,60	
			242	88		1		1	0,50		5,76	2	5,76	
			90			2	8	1	2,44	5,39	2,84	11	5,39	
	Prp2		265	102				1			10,38	1	10,38	
			113					1			3,13	1	3,13	
Prp21			274	2				1			5,90	1	5,90	
			60					1			6,27	1	6,27	
			101			1		2	1,35		9,86	3	9,86	
			102			2		2	3,95		11,12	4	11,12	
			113					2			6,24	2	6,24	
			120			2		2	0,95		7,59	4	7,59	
			128			1			0,80			1	0,80	
			130					1			2,15	1	2,15	
			133					5			6,22	5	6,22	
			60	319	15,4	1			0,00			1	0,00	
Prp46			81	249	15,0	2	1	5	12,63	4,95	10,91	8	12,63	
	Prp8		129	159	9,6	1		1	1,05		3,50	2	3,50	
			242	858		1			0,83			1	0,83	
			274	810		1			2,89			1	2,89	
			352	2097				1			1,69		1,69	
			367	1910				3			2,91	1	2,91	
			2016			2		9	5,39		10,16	11	10,16	
SmB			2122					6			6,52	3	6,52	
			373	2016				4			11,41	6	11,41	
			60	138				4			6,17	4	6,17	
			186					2			5,94	4	5,94	
			71	131			2			5,37		2	5,37	
			132			1					1,55		1,55	
			138			2	4	5	1,09		9,06	11	9,06	
Snu17/Ist3			145					1			7,76	1	7,76	
			287	143				1			2,17	1	2,17	
	Yju2/Cwc16		36	142				1			1,02	1	1,02	
			145			15	10	27	13,10	3,00	5,38	52	13,10	
			151			4	5	10	12,24	4,37	18,80	19	18,80	
			71	1				2			0,22	2	0,22	
			129	1		1						1	0,59	
Prp46			Clf1	67	273			1			4,33	12,55	4	12,55
			87	273				3			9,49	3	9,49	
			88	273		1		1	5,98		10,44	2	10,44	
	Prp8		Cwc2	56	286			1			0,65		1	0,65
			249	81	15,0	1		1	1,05		3,50	2	3,50	
			319	60	15,4	2	1	5	12,63	4,95	10,91	8	12,63	
			SmB	319	138			1			3,70	1	3,70	
Snu114			186					1			4,93	1	4,93	
			173	81				2			1,64	2	1,64	
	Brr2		Syf2	56	145			1			2,52	1	2,52	
			67	145				1			3,17	1	3,17	
			87	145		1		3	7,44		6,64	4	7,44	
			88	145		2			3,30			2	3,30	
			1903	2				2			9,54	2	9,54	
Bud13/Cwc26			25			1			1,15			1	1,15	
			31			1			0,32			1	0,32	
			2016	50				1			7,68	1	7,68	
			74					3			8,59	3	8,59	
			2108	1055				2			5,65	2	5,65	
			2149	1055	17,5			1			5,78	1	5,78	
			2154	91				1			8,47	1	8,47	
			1055	1055	16,4		3	6		5,43	5,02	9	5,43	
			2167	304				1			6,73	1	6,73	
			2187	304				1			6,89	1	6,89	
Cef1			2213	304				2			5,60	2	5,60	
			2284	91				1			1,15	1	1,15	
	Cwc15		1589	255	33,4			2			7,71	2	7,71	
			1903	35		3			1,92			3	1,92	
			41			2			2,22			2	2,22	
			1926	181			2				4,40	2	4,40	
			2016	53			1				8,14	1	8,14	
			61					1			2,19	1	2,19	
			120			1					0,68	1	0,68	
Cef1			2187	15		2		2	3,68		11,00	2	11,00	
			17			2					4,23	2	4,23	
			68					2				1	0,63	
			2217	2		1			0,63			1	0,63	
			2219	2		1		1	5,15		1,47	2	5,15	
Cwc15			98	166		1			0,62			1	0,62	
			1910	294		3			1,20		1,46	4	2,80	
			2192	496		1			0,46			1	0,46	
			1205	172			1			0,70		1	0,70	
Prp2			1242	151				1			5,95	1	5,95	
			1310	172		3			3,49			3	3,49	

Type	Protein 1	Protein 2	Residue 1	Residue 2	Å	Spectral count			Score _{max}			Total spectral count	Best Score _{max}
						Set 1	Set 2	Set 3	Set 1	Set 2	Set 3		
Cwc21		351	12					1		9,11		1	9,11
		1205	12			3		2	3,97		4,62	5	4,62
	Cwc22	121	505			4			2,82			4	2,82
		1435	294	10,3				2		13,19		2	13,19
	Cwc24	235	93			2	2	3	3,33	0,89	10,67	7	10,67
		98	13,5			1			0,69			1	0,69
		123				3	3		1,02	0,42		6	1,02
		517	93			1			1,40			1	1,40
		123				2	3		3,45	3,27		5	3,45
		681	123			1			0,84			1	0,84
Cwc26		684	93			4	8	6	10,33	7,89	8,80	18	10,33
		123				2	1	1	1,46	5,97	6,15	4	6,15
		697	93			3	1		3,79	1,77		4	3,79
		123				5	2	2	14,16	8,26	6,08	9	14,16
		1435	123					3		10,51		3	10,51
		1926	93					8		6,65		8	6,65
		98	28,4					5		5,07		5	5,07
		123				3	1	8	5,55	3,54	7,20	12	7,20
		1931	93				1	1		0,39	4,69	1	5,32
		98	28,7				2	2			10,66	3	4,69
Cwc27		123				2		4	3,57			6	10,66
		2284	63			3			2,13			3	2,13
		1713	123					6		11,34		6	11,34
	Hsh155	906	35			7	6	27	2,85	4,13	5,79	40	5,79
		920	51					2		8,77		2	8,77
		956	137	15,3		12	5	10	9,03	2,25	12,45	27	12,45
		142	21,0			1	4	7	6,97	7,13	7,47	12	7,47
		151						2		8,87		2	8,87
		1007	35				1	5		1,53	5,55	6	5,55
		104						1		12,88		1	12,88
Prp11		1588	612	30,5				1		6,21		1	6,21
		696	9,7			2	1			3,56	6,15	3	6,15
		1589	612	31,6			6			6,78		6	6,78
		956	11					1		7,10		1	7,10
		670	404			1			0,48			1	0,48
	Prp19	1209	108					1		0,41		1	0,41
		1372	107			2			1,22			2	1,22
		1378	107			1			1,38			1	1,38
	Prp2	519	756	155,0				1		5,49		1	5,49
		672	40					1		1,38		1	1,38
Prp21		817	820			1			2,95			1	2,95
		1903	467	84,6				2		3,45		2	3,45
		560	82,5					2		3,48		2	3,48
	Prp45	159	129	9,6		1			1		2,63	1	2,63
		810	274			1				0,83		1	0,83
		858	242			1				1,69		1	1,69
		1910	367					3		2,89		1	2,89
		2016	367			2		9	5,39		6,52	3	6,52
		373						4		10,16		11	10,16
		2097	352					1		6,17		4	6,17
Rse1		2122	367					6		2,91		1	2,91
		2080	1269					1		11,41		6	11,41
		2097	1269					1		8,87		1	8,87
	SmB	90	138					1		7,64		1	7,64
		98	138				2	1		3,21		1	3,21
		186						1		10,12		1	10,12
		103	138					1		8,45		1	8,45
		159	186					1		3,66		3	4,22
		166	186					3		6,58		1	6,58
		586	186					2		9,02		1	9,02
SmD1		743	145					1		6,94		3	6,94
		810	186				1	3		6,62		2	6,62
		194						1		2,20		1	2,20
		98	140					1		5,94		4	5,94
		846	13			1			0,11		3,15	1	3,15
		490	72					1		0,43		1	0,43
	Snt309	325	173	13,1		8	23	13	8,22	8,13	7,04	44	8,22
	Snu114	333	173	18,4		4	9	4	7,21	8,32	5,39	17	8,32
		334	173	17,8		1	3			6,62	8,38	4	8,38
		810	59				1	1		1,49	3,17	2	3,17
Prp9		60					4	1		6,13	4,46	5	6,13
		1209	669	19,6				1		0,95		1	0,95
		1299	955	24,0			1			0,87		1	0,87
	Spp2	835	14			1			0,32			1	0,32
	Syf1	300	2				1			0,08		1	0,08
	Brr2	519	152				1			0,14		1	0,14
	Cus1	466	128			1	2	2	3,23	1,24	2,61	5	3,23
		468	128				1	1		0,38	5,52	2	5,52
		492	128					1		3,31		1	3,31
	Hsh49	371	147					1		2,10		1	2,10
		429	101					1		2,02		1	2,02

Type	Protein 1	Protein 2	Residue 1	Residue 2	Å	Spectral count			Score _{max}			Total spectral count	Best Score _{max}
						Set 1	Set 2	Set 3	Set 1	Set 2	Set 3		
Lea1	462	39				1	2	1	1,39	3,63	4,81	2	1,59
	468	204				2	5	6	12,40	4,70	5,83	12	12,40
	208					2		6	3,70			13	5,83
	475	204					1	1		0,18	2,54	2	2,54
	208						3	5		0,70	3,61	8	3,61
	492	208				1		13	0,15		7,01	14	7,01
	107	215						1			1,72	1	1,72
	115	194						1			1,75	1	1,75
	215					3		8	3,15	2,06	11,71	16	11,71
	216							1			1,38	1	1,38
Msl1	121	215				1		2	3,07			3,26	3
	232							1			1,81	1	1,81
	140	2						1			7,02	1	7,02
	115	2				1		6	12,81		10,88	7	12,81
	121	2						4			4,11	4	4,11
Prp11	124	2						8			5,13	8	5,13
	58	11						3			6,61	3	6,61
	173							9			11,12	9	11,12
	61	173						1			2,35	1	2,35
Prp2	175					3				1,26		3	1,26
	371	11						1			12,95	1	12,95
	235	83				1				0,94		1	0,94
Rse1	Prp21					23	72	139	18,44	12,85	10,71	234	18,44
	Rse1	462	1176			1	5	3	0,71	6,80	8,97	9	8,97
	492	1001						3			6,37	3	6,37
SmB	1184							4			5,39	4	5,39
	235	65				1		2	1,09			2,35	3
	68							1			4,54	1	4,54
	238	65						1			2,58	1	2,58
	68							2			5,17	2	5,17
	371	138						3			7,73	3	7,73
	186							4			12,93	4	12,93
	466	117						1			2,87	1	2,87
	468	117				2				1,78		2	1,78
	360	128				1		1			2,35	1	2,35
Rds3	371	128					5			0,66	4,46	6	4,46
	129						1				2,25	1	2,25
	140						4				4,98	4	4,98
	Yju2/Cwc16	371	68				1				2,32	1	2,32
	Cif1	42	640			1	1	3	3,50	0,50	5,76	5	5,76
	Hsh155	29	276	43,7				3			5,61	3	5,61
	53	455	20,3	3					10,29			3	10,29
	500	13,5	4						8,27			4	8,27
	511	19,2	2					3	0,77		8,47	5	8,47
	56	511	19,3					3			9,22	3	9,22
Rse1	Prp2	42	10					3			3,45	3	3,45
	Ysf3	13	9	16,6			1					1	0,14
	Brr2	556	304					2			6,29	2	6,29
		414						7			8,66	7	8,66
		417						1			3,42	1	3,42
Bud13/Cwc26		967	83,3					1			6,22	1	6,22
		1269	758					1			1,69	1	1,69
		795						1			4,89	1	4,89
		1269	115					1			5,69	1	5,69
	Cus1	1149	347			1	2		4,32	4,68		3	
		1342	245			2	11	19	1,01	7,20	11,47	32	11,47
		246				5	19	8	6,41	12,16	11,56	32	12,16
	Cwc15	557	43					2			3,38	2	3,38
	Cwc24	1342	182					3			3,96	3	3,96
	Hsh155	221	511	22,6			2	1		0,52	2,40	3	2,40
Hsh49		1269	511					4			6,95	4	6,95
		595						5			15,04	5	15,04
		632						2			4,56	2	4,56
		713						4			7,49	4	7,49
		1342	713					1			5,21	1	5,21
		1176	39			4	2	8	5,21	0,44	3,10	14	5,21
		1001	2			1			1,63			1	1,63
		1269	2080					1			8,87	1	8,87
		2097						1			7,64	1	7,64
	Prp9	1001	492					3			6,37	3	6,37
Snt309		1176	462			1	5	3	0,71	6,80	8,97	9	8,97
		1184	492					4			5,39	4	5,39
		1057	48			1		4			1,68	1	1,68
		374	38					6			12,26	6	12,26
		83						1			4,28	1	4,28
		145	83									1	2,97
		186	79					1			3,62	1	3,62
SmB	Cef1	76	187			1			0,95			1	0,95
	Cus1	117	128			1		1	1,46		4,59	2	4,59
		138	83					2			4,68	2	4,68
		86						1			1,97	1	1,97
		95				1	2			0,44	8,99	3	8,99
Spp2		102						4			8,02	4	8,02
		145	83					1			2,97	1	2,97
		186	79					1			3,62	1	3,62

Type	Protein 1	Protein 2	Residue 1	Residue 2	Å	Spectral count			Score _{max}			Total spectral count	Best Score _{max}	
						Set 1	Set 2	Set 3	Set 1	Set 2	Set 3			
Hsh155			83					1		4,86	1	4,86		
			102					1		7,29	1	7,29		
			76	223		1			0,73			1	0,73	
			186	325			2			3,04		2	3,04	
	Isy1		100	106		1			1,19			1	1,19	
	Lea1		76	125			3	11		1,57	8,77	14	8,77	
	Msl1		105	2		2			1,64			2	1,64	
			114	2				1		1,59	1	1,59		
			124	2				1		1,92	1	1,92		
			138	2				2		4,30	2	4,30		
Prp11			186	2			1			0,03		1	0,03	
			138	103				1		2,54	1	2,54		
			145	103				1		1,21	1	1,21		
			186	126				1		2,38	1	2,38		
Prp19			55	378		1				3,42		1	3,42	
			60	378		2	3	1	4,83	2,16	0,94	6	4,83	
	Prp21						1	1		1,50	1,62	2	1,62	
Prp45			131	71			2			1,55		2	1,55	
			132	71		1						1	1,09	
			138	60				4				4	5,94	
				71		2	4	5	7,44	5,86	9,06	11	9,06	
			145	71				1			7,76	1	7,76	
			186	60				2			5,37	2	5,37	
	Prp46		138	319				1			3,70	1	3,70	
			186	319				1			4,93	1	4,93	
Prp8			138	90				1			3,21	1	3,21	
				98				1			8,45	1	8,45	
				103				1			6,58	1	6,58	
			145	743				1			2,20	1	2,20	
			186	90				1			10,12	1	10,12	
				98		2	1			4,22	3,66	3	4,22	
				159				1			9,02	1	9,02	
				166				3			6,94	3	6,94	
				586				2			6,62	2	6,62	
				810		1	3			2,09	5,94	4	5,94	
Prp9			194	810				1			3,15	1	3,15	
			65	235		1		2	1,09		2,35	3	2,35	
				238				1			2,58	1	2,58	
			68	235				1			4,54	1	4,54	
				238				2			5,17	2	5,17	
			117	466				1			2,87	1	2,87	
				468		2				1,78		2	1,78	
			138	371				3			7,73	3	7,73	
			186	371				4			12,93	4	12,93	
	SmD1		138	128				2			3,71	2	3,71	
SmD2			186	129				1			2,24	1	2,24	
			65	82				10			3,89	10	3,89	
	SmD3		19	79		15,3			1			2,33	1	2,33
			39	2				1			4,88	1	4,88	
			105	2				2			6,85	2	6,85	
				79		2	1			0,30	1,36	2	1,36	
				85		2	5	3	2,36	7,58	7,24	10	7,58	
				86			5	8		3,30	4,46	13	4,46	
	Snu114		76	60			1				1,86	1	1,86	
			105	99				2			7,28	2	7,28	
SmD1				159		4	5			4,15	3,67	9	4,15	
				186	617			1			4,88	1	4,88	
	Syf2		117	14				1			2,79	1	2,79	
	Yju2/Cwc16		105	2				1			1,39	1	1,39	
	Cus1		128	83				1			4,47	1	4,47	
				102				3			8,62	3	8,62	
	Cwc27		140	216		1				2,77		1	2,77	
	Hsh155		128	158				2			6,46	2	6,46	
				736		1				3,09		1	3,09	
				129	158			1			3,09	1	3,09	
Prp2			128	756				1			2,24	1	2,24	
	Prp8		140	98				1			3,18	1	3,18	
	Prp9		128	360				1			2,35	1	2,35	
				371		1	5			0,66	4,46	6	4,46	
SmB			129	371				1			2,25	1	2,25	
			140	371				4			4,98	4	4,98	
			128	138				2			3,71	2	3,71	
			129	186				1			2,24	1	2,24	
			54	82		1	9			0,29	4,32	10	4,32	
SmD2			111	59				3			5,09	3	5,09	
			128	27				4			4,84	4	4,84	
			128	2				1			2,95	1	2,95	
	Snu114		128	356		1	1	1	3,03	0,60	1,77	3	3,03	
			397	1	3			3			5,66	7	9,82	
Yju2/Cwc16			129	397				1			4,30	1	4,30	
			140	356		2					3,66	5,35	7	5,35
				397		4	3				2,94	1	2,94	
			128	74				1						

Type	Protein 1	Protein 2	Residue 1	Residue 2	Å	Spectral count			Score _{max}			Total spectral count	Best Score _{max}	
						Set 1	Set 2	Set 3	Set 1	Set 2	Set 3			
SmD2	Brr2		140	74				1			1,97	1	1,97	
	SmB		59	1904			1			2,76		1	2,76	
	SmD1		82	65				10			3,89	10	3,89	
			27	128				4			4,84	4	4,84	
			59	111				3			5,09	3	5,09	
			82	54			1	9		0,29	4,32	10	4,32	
SmD3	Spp2		80	3			1			0,21		1	0,21	
	Cef1		85	321		1						1	0,46	
	Cus1		2	79				17			9,62	17	9,62	
			83					4			9,14	4	9,14	
			86					2			4,62	2	4,62	
			102					1			3,26	1	3,26	
Msl1			85	86				1			1,90	1	1,90	
	SmB		86	83				2			6,19	2	6,19	
			85	2				1			4,79	1	4,79	
			2	39				1			4,88	1	4,88	
			105					2			6,85	2	6,85	
			79	19		15,3		1			2,33	1	2,33	
SmD1			85	105		2	1	1		0,30	1,36	2	1,36	
	SmG		86	105			5	3	2,36	7,58	7,24	10	7,58	
			86	105			5	8		3,30	4,46	13	4,46	
	Snu114		2	128			8				4,92	1	2,95	
			32	9				2			5,84	2	5,84	
			32	558				1			16,46	121	16,46	
SmE			85	159		10	15	96		6,72	9,09			
	Cus1		86	159		1	4	11		4,04	4,51	16	6,97	
			79	19			4	2		2,02	2,30	16	4,35	
			48			1	1	16		0,86	0,64	18	5,50	
			53					1			5,50	1	1,87	
			58					1			2,86	1	2,86	
SmF			79				2			3,36		2	3,36	
	Prp2		1	14			1			0,82		1	0,82	
	SmG		6	8		2	7	30	15,35	6,68	11,58	39	15,35	
			13					2			2,85	2	2,85	
			14				1	1		0,94	0,01	3	1,72	
	Cus1		20	58			2			2,80		2	2,80	
SmG			1	668		1				0,08		1	0,08	
	Clf1		2	79			2	13		3,68	9,91	15	9,91	
			83					1			3,09	1	3,09	
			8	2		2				1,18		2	1,18	
			79			1				3,97		1	3,97	
			83				1	1			1,39	2	2,50	
Cwc2			24	16			2	3			2,89			
	Isy1		8	310			2				2,89	1	2,89	
	Prp19		8	104				1				1	0,98	
	Prp8		24	130		1				0,98				
	SmD3		13	846		1				0,11		1	0,11	
	SmE		9	32			8	8	15,35	4,92		8	4,92	
Snt309			8	6		2	7	30		6,68	11,58	39	15,35	
	Brr2		13	6				2			2,85	2	2,85	
			13	6			1	1		0,94	0,01	3	1,72	
			14	6				1			0,55	1	0,55	
	Prp19		94	748			1	1				1,36	1	1,36
	Cef1		26	187				1				4,05	1	4,05
Snu114			94	670				1					1	
	Clf1		25	135		1				1,31		1	1,31	
	Prp19		107			12	3	8	10,81	8,62	13,48	23	13,48	
			108			15	9	9	14,90	10,62	17,25	33	17,25	
			120			4	2	4	5,76	4,11	7,08	10	7,08	
			26	130		1	1	1	0,24	2,43	6,54	3	6,54	
Prp8			139			2	2		4,21	3,59		4	4,21	
			32	107		2		12	4,50		13,91	14	13,91	
			46	107		1	4		1,70	10,80		5	10,80	
			108			9	6	9	9,75	5,41	5,51	24	9,75	
			48	107		6	3	11	6,46	1,19	8,82	20	8,82	
			108					1			12,06	1	12,06	
Rse1			67	107		7	4	10	14,65	3,43	9,05	21	14,65	
			72	107		1				0,21		1	0,21	
			72	490				1			0,43	1	0,43	
			48	1057		1				1,68		1	1,68	
	Brr2		955	2				1				5,16	1	5,16
			7					1				4,08	1	4,08
Cwc15			627	670				1				0,28	1	0,28
			59	145		1				3,47		1	3,47	
			150					2				3,96	2	3,96
			151					1				2,82	1	2,82
			60	140		1			5,78			1	5,78	
			145			1	2	1	0,63	4,30	5,72	4	5,72	
Cwc15			150			4	1		4,12	0,67		5	4,12	
			151			2	4	3	9,75	7,80	8,57	9	9,75	
			72	150		1			2,10			1	2,10	
			151					4			13,68	4	13,68	
			81	150				1			1,79	1	1,79	
			151					14			12,86	14	12,86	

Type	Protein 1	Protein 2	Residue 1	Residue 2	Å	Spectral count			Score _{max}			Total spectral count	Best Score _{max}				
						Set 1	Set 2	Set 3	Set 1	Set 2	Set 3						
Prp2	Cwc21		955	12	13,8	6	2	6	9,33	5,91	12,44	14	12,44				
	Cwc22		369	176		5	1	1	4,02	0,82	2,34	5	4,02				
	Ecm2		111	188		1			0,46			1	0,82				
			746	353								1	0,46				
			115	40		208,0	2	5	5,61	1,75	1	1	2,34				
			749	756								1	1,75				
			955	632								2	7,04				
												5	5,61				
Prp46			756	160,1		13,1	8	1	6,41	1,64	2	3	5,73				
			763	147,7								1	6,41				
			851	135,7								2	1,64				
			81	173								2	1,64				
Prp8			59	810		8	1	1	1,49	3,17	2	2	3,17				
			60	810								5	6,13				
			173	325								44	8,22				
			333	18,4		4	9	4	7,21	8,32	17	17	8,32				
			334	17,8								4	8,38				
			669	1209								1	0,95				
SmB			955	1299		24,0	1	1	0,87	1,86	1	1	0,87				
			60	76								1	1,86				
			99	105								2	7,28				
			159	105		13,1	4	5	4,15	3,67	9	9	4,15				
			617	186								1	4,88				
			356	128								3	3,03				
SmD1			140			2	1	1	3,03	0,60	1,77	2	1,44				
			397	128								7	9,82				
			140									1	4,30				
			159	85		13,6	10	15	16,46	6,72	9,09	121	16,46				
			86									16	6,97				
			558	32								2	5,84				
Snu17/Ist3	Bud13/Cwc26		10	244		16,1	2	2	4,43	2,06	3	2	4,43				
			133	169								3	4,84				
			181									4	5,55				
			213			13,8	3	3	6,15	6,66	6,20	11	6,66				
			169									15	8,23				
			179									10	14,63				
			180			12,17	4	2	4,88	14,63	6,88	2	6,88				
			181									7	10,00				
			201									21	9,39				
			206			14,3	1	4	11,35	7,72	7	7	11,35				
			213									16	9,39				
			179									7	9,46				
			181			17,8	2	2	2,73	1,41	9,46	4	1,85				
			201									6	5,09				
			206									1	0,97				
Spp2	Cwc22		138	520		17,8	1	1	4,91	4,91	1	1	4,91				
			143	530								1	2,93				
			123	188								1	0,08				
	Hsh155		10	500		17,8	2	5	14,08	3,46	12	2	14,08				
			96	66								2	4,99				
			104									4	4,99				
			103	410		17,8	14	2	15,45	12,69	14	6	15,45				
			455									3	12,69				
			143	287								1	2,17				
Prp45	Brr2		38	168		17,8	1	1	4,12	4,12	1	1	4,12				
			445									1	5,97				
			454									5	3,46				
			769			17,8	4	1	10,34	10,34	4	4	10,34				
			46	769								1	4,44				
			58	91								3	15,52				
			445			17,8	1	3	3,83	1,65	1	1	3,83				
			68	454								3	1,65				
			133	74								1	6,69				
Bud13/Cwc26			85			17,8	1	1	3,56	16,93	6	3	3,56				
			91									6	16,93				
			151	115								8	10,72				
			120			17,8	17	1	12,61	9,30	30	8	10,72				
			136									10	12,61				
			146									3	13,17				
			154	120		17,8	3	1	0,69	2,77	3	3	2,77				
			136									1	1,97				
			146									1	5,35				
Clf1			181	151		17,8	1	1	1,81	9,42	3	3	9,42				
			182	136								2	4,89				
			151	458								1	2,99				
			151	4		17,8	2	1	0,05	7,16	7	1	0,05				
			82	336								7	7,16				
			632									1	3,53				
			750			17,8	1	1	1,21	3,93	2	2	3,93				
			756									1	1,91				
Prp2			83	336								4	2,76				
			632			17,8	2	2	7,68	7,77	4	4	2,76				

Type	Protein 1	Protein 2	Residue 1	Residue 2	Å	Spectral count			Score _{max}			Total spectral count	Best Score _{max}
						Set 1	Set 2	Set 3	Set 1	Set 2	Set 3		
Syf1			640			1		2	4,92			1	4,92
			756			1		1	3,40	2,90		3	3,40
			95	756						5,34		1	5,34
			154	840		1			2,83			1	2,83
			168	461		4		6	3,34		5,84	10	5,84
			181	461				1		2,80		1	2,80
	Prp8		14	835		1			0,32			1	0,32
	Rse1		38	374				6		12,26		6	12,26
			83	374				1		4,28		1	4,28
			SmD2	3	80		1			0,21		1	0,21
Syf2	Brr2		362	259		1			0,58			1	0,58
	Cef1		770	293		3	4	2	3,68	4,58	3,13	9	4,58
				294			1			1,22		1	1,22
				296			1			0,78		1	0,78
				312		1			2,91			1	2,91
	Clf1		524	180		3	5	3	5,16	2,04	5,79	11	5,79
			531	180		2		1	2,81		2,27	3	2,81
			650	304		8	3	5	16,67	5,17	6,87	16	16,67
			653	289				1			8,83	1	8,83
				304		12	10	54	17,65	11,96	13,33	76	17,65
Yju2/Cwc16	Cus1		146	317		4	5	3	15,41	11,09	10,86	12	15,41
				329				1			1,31	1	1,31
	Cwc2		424	320		4	1	3	5,37	5,03	3,68	8	5,37
			524	310				2			4,43	2	4,43
			531	310				1			1,35	1	1,35
	Cwc22		311	548			1			26,34		1	26,34
	Isy1		146	139		2			5,57			2	5,57
			143			2	4	1	5,24	4,45	4,06	7	5,24
			220	157			1	4		0,70	9,62	5	9,62
			161			3	7	9	2,63	2,37	4,94	19	4,94
Syf2			171			9	6	1	4,61	5,04	2,46	16	5,04
			249	157				1			3,79	1	3,79
			259	7				2			5,83	2	5,83
			328	7		1	3	6	10,49	5,14	9,35	10	10,49
			27			1			2,03			1	2,03
			40			2	3	7	2,37	2,44	4,75	12	4,75
			424	7		1	2	5	1,18	5,11	7,02	8	7,02
	Lea1		32	232			1	1		2,40	1,79	2	2,40
	Ntc20		498	27		6		2			8,58	8	8,58
			558	27		2	2	2	1,41	1,40	5,11	6	5,11
Syf2	Pml1		372	153				1			1,13	1	1,13
	Prp11		424	192		1		4			7,93	5	7,93
	Prp21					4			12	3,40	6,01	16	6,01
	Prp8		2	300			1			0,08		1	0,08
	Syf2		362	11		3	4	8	7,31	2,06	5,86	15	7,31
			14			1		9	10,00		5,80	10	10,00
			413	23		1						1	9,20
			26			2	4	4	4,66	3,68	5,31	10	5,31
			424	26			1	1		1,10	3,29	2	3,29
			524	132				1			0,86	1	0,86
Yju2/Cwc16	531		121					3			9,05	3	9,05
			790	234		1			1,32			1	1,32
	Cef1		159	240				1			3,73	1	3,73
			247			1				1,07		1	1,07
			173	239		3	1		4,95	0,55		4	4,95
			240			5	6	10	7,61	11,75	9,07	21	11,75
			247				4	6		3,71	6,44	10	6,44
			251			2	1	2	4,91	1,42	8,77	5	8,77
			259			1			0,55			1	0,55
	Clf1		121	180				8			9,41	8	9,41
Syf2			159	113		7	7	5	4,73	2,95	7,19	19	7,19
			173	25			4	6		2,24	4,57	10	4,57
			113			4		2	10,42		7,42	6	10,42
	Cwc15		9	102		1			0,13			1	0,13
	Ecm2		148	138		1			0,08			1	0,08
	Isy1		26	7		1	4	3	1,75	2,47	4,26	8	4,26
			27			1		4		1,36	4,12	5	4,12
			173	42		1	2		5,98	1,83		3	5,98
	Prp11		26	192		2	3	5	3,34	5,17	6,42	10	6,42
	Prp21					1	1			3,40	4,02	2	4,02
Prp46	Prp45		1	71				2			0,22	2	0,22
			142	36				1			1,02	1	1,02
			145	36		15	10	27	13,10	3,00	5,38	52	13,10
			151	36		4	5	10	12,24	4,37	18,80	19	18,80
			145	56				1			2,52	1	2,52
			67					1			3,17	1	3,17
			87			1		3	7,44		6,64	4	7,44
			88			2			3,30			2	3,30
	SmB		14	117				1			2,79	1	2,79
	Syf1		11	362		3	4	8	7,31	2,06	5,86	15	7,31
			14	362		1		9	10,00		5,80	10	10,00
			23	413		1			9,20			1	9,20
			26	413		2	4	4	4,66	3,68	5,31	10	5,31

Type	Protein 1	Protein 2	Residue 1	Residue 2	Å	Spectral count			Score _{max}			Total spectral count	Best Score _{max}
						Set 1	Set 2	Set 3	Set 1	Set 2	Set 3		
Yju2/Cwc16	Yju2/Cwc16		424				1	1	1,10	3,29	2	3,29	
			121	531				3	9,05	3	9,05		
			132	524		1		1	0,86	1	0,86		
			11	22		1	1		1,04		1	1,04	
		Isy1	63	103					0,27		1	0,27	
		Prp2	29	732		2			0,44		2	0,44	
		Prp45	1	129		1			0,59		1	0,59	
		Prp9	68	371				1		2,32	1	2,32	
		SmB	2	105				1		1,39	1	1,39	
		SmD1	74	128				1		2,94	1	2,94	
Ysf3	Ysf3		140					1		1,97	1	1,97	
		Syf1	234	790		1			1,32		1	1,32	
		Syf2	22	11		1			1,04		1	1,04	
		Cus1	12	102				1		3,31	1	3,31	
			15	102		1			0,22		1,15	1,15	
		Cwc22	15	203	147,7	1			0,49		1	0,49	
		Hsh155	4	932			2			0,68		2	0,68
			12	932	12,7		3			3,56		3	3,56
		Rds3	9	13	16,6		1			0,14		1	0,14
Intra	Brr2	Brr2	1	2108			1		0,54		1	0,54	
			2	28		1		7	4,24		8	6,67	
				50				6			6	10,41	
				74				1			1	1,99	
				304				1			1	2,17	
				967				1			1	4,29	
				1437				2			2	2,83	
				1623				1			1	2,94	
				1634				4			4	9,97	
			7	25				1			1	3,75	
				50				2			2	4,06	
				967				1			1	1,41	
			9	91				1			1	2,74	
			11	720				1			1	0,99	
			25	7				1			1	3,75	
				50		3	2		1,47		5	3,50	
				59			1				1	2,26	
				454		1			0,74		1	0,74	
				1437			1			1,30		1,30	
				1623		1					1	1,37	
			28	2		1	7		4,24		8	6,67	
				50		4	9		3,74		13	4,89	
				71		1			1,55		1	1,55	
				74			2				2	5,74	
				82			1				1	5,97	
				91		1			0,39		1	0,39	
				454		1			2,58		1	2,58	
				967			1			10,20		10,20	
			50	2				6			6	10,41	
				7				2			2	4,06	
				25		3	2		1,47		5	3,50	
				28		4	9		3,74		13	4,89	
				59		2			1,55		1	1,55	
				71		4	57		5,07		63	14,40	
				74		2	8		10,06		10	3,53	
				74		2	13		3,53		15	9,88	
				82			4		7,80		4	7,03	
				85		1	4		0,48		5	6,86	
				91		1	4		5,34		5	8,41	
				967			1				1	1,11	
				1623			1				1	3,23	
				1634			1				1	4,28	
			59	25				1			1	2,26	
				50		2	4	57	5,07		63	14,40	
				74		4	9	11	6,95		24	14,69	
				82			1	7			8	9,87	
				85			3	1			8	2,87	
				91			1	7			8	19,64	
			71	28					1,55		1	1,55	
				50		2	8		3,53		10	3,53	
				82		7	6		6,25		13	6,25	
				85		6	3		5,97		9	5,97	
				90		3	1		4,12		4	4,12	
				91		4	4		5,55		8	9,23	
			74	2				1			1	1,99	
				28				2			2	5,74	
				50		2	13		7,80		15	9,88	
				59		4	11		14,69		24	14,69	
				85		1	6	20	4,46		27	8,15	
				90			2	3			5	4,30	
				91		5	9		13,71		14	15,07	
			82	28				1			1	5,97	
				50				4			4	7,03	
				59		1	7		0,59		8	9,87	
				71		7	6		6,25		13	6,25	

Type	Protein 1	Protein 2	Residue 1	Residue 2	Å	Spectral count			Score _{max}			Total spectral count	Best Score _{max}	
						Set 1	Set 2	Set 3	Set 1	Set 2	Set 3			
85	90					2	6	12	4,57	8,99	13,27	27	5,76	
	91							1		1,49	1	1,49		
	1051						1							
	50						1	4		0,48	6,86	5	6,86	
	59						3	1		1,78	2,87	4	2,87	
	71						6	3		5,97	4,96	9	5,97	
	74					1	6	20	4,46	5,70	8,15	27	8,15	
	91					11	17	30	8,76	9,01	11,41	58	11,41	
	454						2			0,25		2	0,25	
	90						3	1		4,12	2,51	4	4,12	
91	71						2			0,97	4,30	5	4,30	
	74						1	3						
	82						1	12		0,39	5,76	13	5,76	
	454					1	6	5	1,51	2,79	4,69	12	4,69	
	9							1			2,74	1	2,74	
	28									0,39		1	0,39	
	50						1	4		5,34	8,41	5	8,41	
	59						1	7		7,99	19,64	8	19,64	
	71						4	4		5,55	9,23	8	9,23	
	74						5	9		13,71	15,07	14	15,07	
91	82					2	6	19	4,57	8,99	13,27	27	13,27	
	85					11	17	30	8,76	9,01	11,41	58	11,41	
	431							1			5,50	1	5,50	
	445									5,94		2	5,94	
	1051					4		2	1,74		4,21	6	4,21	
	152	190	11,8								21,68	20	21,68	
	168	717	9,9	1		2		2	0,51	1,34	2,54	5	2,54	
	190	152	11,8								21,68	20	21,68	
	271	304					1	6		3,22	7,63	7	7,63	
	351							1			1,03	1	1,03	
304	276	304									7,89	1	7,89	
	380							1			14,08	1	14,08	
	967							1			4,52	1	4,52	
	2	52,2									2,17	1	2,17	
	271					1	6			3,22	7,63	7	7,63	
	276						1				7,89	1	7,89	
	339					5	7	3	6,02	8,77	9,54	15	9,54	
	414							2			1,99	2	1,99	
	417						2	7		3,17	12,29	9	12,29	
	967							1			1,95	1	1,95	
398	1372										12,26	1	12,26	
	1529							2			10,19	2	10,19	
	1634							1			2,70	1	2,70	
	339	304				5	7	3	6,02	8,77	9,54	15	9,54	
	351	271						1			1,03	1	1,03	
	398										1,86	1	1,86	
	417							1			1,71	1	1,71	
	364	1529									6,89	1	6,89	
	380	276									14,08	1	14,08	
	390	398				1				0,09		1	0,09	
414	417					2	2			5,20	1,46	4	5,20	
	967					1					1,86	1	1,86	
	304					3	7	10	9,40	3,59	6,31	20	9,40	
	417					2	1	13	2,60	0,39	8,45	16	8,45	
	967										3,17	12,29	9	12,29
	417	304						2			1,71	1	1,71	
	351										5,20	4	5,20	
	390						2	2			1,46			
	414					3	7	10	9,40	3,59	6,31	20	9,40	
	967					5	10	25	5,15	7,58	8,61	40	8,61	
431	431	91						1			5,50	1	5,50	
	445	91									5,94	2	5,94	
	457					21,5		2			1,49	2	1,49	
	454	25						1			0,74	1	0,74	
	28										2,58	1	2,58	
	85										0,25	2	0,25	
	90					1	6	5	1,51	2,79	4,69	12	4,69	
	457	445	21,5				2				1,49	2	1,49	
	546	549	8,3	24	54		12	14,56	9,53	11,58	90	14,56		
	549	546	8,3	24	54		12	14,56	9,53	11,58	90	14,56		
584	584	13,3	7	4	8			11,10	9,36	9,50	19	11,10		
	1904	21,4	7	8	51			18,55	7,94	9,46	66	18,55		
	564	611	9,9	9	8				8,38	11,63	17	11,63		
	1138	20,9	2	8	95			2,38	4,23	10,34	105	10,34		
	584	549	13,3	7	4			11,10	9,36	9,50	19	11,10		
	597	13,3	2	2	7			6,03	8,55	15,58	11	15,58		
	597	584	13,3	2	2			7	6,03	8,55	15,58	11	15,58	
	1589	19,0	5	6	69			11,85	11,53	25,58	80	25,58		
	1896	13,4	12	10	29			3,90	1,34	3,41	51	3,90		
	1904	20,8	3	13	15			2,55	3,42	4,62	31	4,62		
611	564	9,9			9		8		8,38	11,63	17	11,63		
	1138				4					10,10	4	10,10		

Type	Protein 1	Protein 2	Residue 1	Residue 2	Å	Spectral count			Score _{max}			Total spectral count	Best Score _{max}	
						Set 1	Set 2	Set 3	Set 1	Set 2	Set 3			
	659	967	22,4					1			2,35	1	2,35	
	717	168	9,9	1	2	2	0,51	1,34	2,54	5	2,54			
	720	4,9	1	7	9	5,58	0,65	3,77	17	5,58				
720	11				1				0,99	1	0,99			
	717	4,9	1	7	9	5,58	0,65	3,77	17	5,58				
	748	17,1	4	10					3,83	5,87	14	5,87		
748	720	17,1	4	10					3,83	5,87	14	5,87		
	758	15,6		2					7,77	2	7,77			
	760	18,2		1					3,01	1	3,01			
	769	25,3	1						1,75	1	1,75			
	795	15,6	17	68	128		10,40	6,59	7,71	213	10,40			
	1088	14,8		2					1,49	2	1,49			
758	748	15,6		2					7,77	2	7,77			
	778	16,5	8	28				7,79	11,55	36	11,55			
	782	16,8	12	1				2,09	1,53	13	2,09			
	795	9,2	11	21	5	7,32		4,12	3,85	37	7,32			
760	748	18,2	1					3,01		1	3,01			
769	748	25,3	1					1,75		1	1,75			
	778	13,2	2	1				3,98	1,63	3	3,98			
778	758	16,5	8	28				7,79	11,55	36	11,55			
	769	13,2	2	1				3,98	1,63	3	3,98			
	795	13,5	3	12	9	4,65		4,52	5,37	24	5,37			
782	758	16,8	12	1				2,09	1,53	13	2,09			
	795	10,5	7	6				13,60	9,20	13	13,60			
795	748	15,6	17	68	128		10,40	6,59	7,71	213	10,40			
	758	9,2	11	21	5	7,32		4,12	3,85	37	7,32			
	778	13,5	3	12	9	4,65		4,52	5,37	24	5,37			
	782	10,5	7	6				13,60	9,20	13	13,60			
967	2				1				4,29	1	4,29			
	7				1				1,41	1	1,41			
	28				1				10,20	1	10,20			
	50				1				1,11	1	1,11			
	276	52,2			1				4,52	1	4,52			
	304				1				1,95	1	1,95			
	398				1				3,64	1	3,64			
	414		2	1	13	2,60		0,39	8,45	16	8,45			
	417		5	10	25	5,15		7,58	8,61	40	8,61			
	659	22,4			1				2,35	1	2,35			
1042	1055	20,3		1				1,60		1	1,60			
1051	82				1				1,49	1	1,49			
	91		4		2	1,74			4,21	6	4,21			
	1055	5,8	1	5	13	2,44		2,76	6,40	19	6,40			
1055	1042	20,3		1				1,60		1	1,60			
	1051	5,8	1	5	13	2,44		2,76	6,40	19	6,40			
1088	748	14,8			2				1,49	2	1,49			
1138	564	20,9	2	8	95	2,38		4,23	10,34	105	10,34			
	611	22,4			4				10,10	4	10,10			
	1150	14,1	1	8	31	3,91		9,00	14,48	40	14,48			
1150	1138	14,1	1	8	31	3,91		9,00	14,48	40	14,48			
	1187	15,1	2					0,96		2	0,96			
	1634	57,5	1					1,42		1	1,42			
1158	1187	13,9	4		6			2,27	8,41	10	8,41			
1187	1150	15,1	2					0,96		2	0,96			
	1158	13,9	4		6			2,27	8,41	10	8,41			
1372	304				1				12,26	1	12,26			
1392	1504	12,8			1				1,78	1	1,78			
1437	2				2				2,83	2	2,83			
	25				1				1,30	1	1,30			
	2116	16,9			3				6,61	3	6,61			
	2121	16,5	7	14	74	14,39		7,39	13,36	95	14,39			
1441	2121	19,1			2				15,61	2	15,61			
1504	1392	12,8			1				1,78	1	1,78			
1529	304				2				10,19	2	10,19			
	364				1				6,89	1	6,89			
1589	597	19,0	5	6	69	11,85		11,53	25,58	80	25,58			
	1896	10,2	1	4	24	1,08		0,98	3,73	29	3,73			
	1904	19,2	8	11	72	16,27		6,25	10,71	91	16,27			
1600	1634	14,5			6				9,18	6	9,18			
1603	1634	14,4	3		6				1,02	4,62	9	4,62		
1623	2				1				2,94	1	2,94			
	25				1				1,37	1	1,37			
	50				1				3,23	1	3,23			
1634	2				4				9,97	4	9,97			
	50				1				4,28	1	4,28			
	304				1				2,70	1	2,70			
	1150	57,5	1					1,42		1	1,42			
	1600	14,5			6				9,18	6	9,18			
	1603	14,4	3		6				1,02	4,62	9	4,62		
1896	597	13,4	12	10	29	3,90		1,34	3,41	51	3,90			
	1589	10,2	1	4	24	1,08		0,98	3,73	29	3,73			
	1904	14,9	4		6				3,36	5,90	10	5,90		
1904	549	21,4	7	8	51	18,55		1,42	9,46	66	18,55			
	597	20,8	3	13	15	2,55		3,42	4,62	31	4,62			

Type	Protein 1	Protein 2	Residue 1	Residue 2	Å	Spectral count			Score _{max}			Total spectral count	Best Score _{max}
						Set 1	Set 2	Set 3	Set 1	Set 2	Set 3		
			1589	19,2	8	11	72	16,27	6,25	10,71	91	16,27	
			1896	14,9		4	6		3,36	5,90	10	5,90	
			2070	2115	12,7	6	8		6,52	10,99	14	10,99	
			2108	1		1			0,54		1	0,54	
			2115	2070	12,7	6	8		6,52	10,99	14	10,99	
			2121	2121	17,3	5	4		2,09	2,43	9	2,43	
			2116	1437	16,9		3			6,61	3	6,61	
			2121	1437	16,5	7	14	74	14,39	7,39	13,36	95	14,39
			1441	1441	19,1		2			15,61	2	15,61	
			2115	2115	17,3		5	4		2,09	2,43	9	2,43
Bud13/Cwc26	Bud13/Cwc26	2	101				1			3,08	1	3,08	
		15	19		1				0,21		1	0,21	
			21		1				5,91		1	5,91	
		19	15		1				0,21		1	0,21	
			41				1			1,56	1	1,56	
		21	15		1				5,91		1	5,91	
		24	35				3			3,80	3	3,80	
			41				1			3,47	1	3,47	
			53				1			2,49	1	2,49	
		25	35		1	1	2	1,20	0,84	5,34	4	5,34	
			41				1			2,07	1	2,07	
		28	41		1		8	6,18		14,29	9	14,29	
			53				6			6,54	6	6,54	
		35	24				3			3,80	3	3,80	
			25		1	1	2	1,20	0,84	5,34	4	5,34	
			53				3			8,98	3	8,98	
			61				1			3,56	1	3,56	
		41	19				1			1,56	1	1,56	
			24				1			3,47	1	3,47	
			25				1			2,07	1	2,07	
			28		1		8	6,18		14,29	9	14,29	
			53			4	9		3,09	12,17	13	12,17	
			61		3	3			3,34	7,69	6	7,69	
			64			1				1,88	1	1,88	
			68		1	1	2	4,67		7,43	4	7,43	
		53	24				1			3,22	1	3,22	
			28				6			2,49	1	2,49	
			35				3			6,54	6	6,54	
			41			4	9			8,98	3	8,98	
			68		1	3				3,09	13	12,17	
			115				1			3,34	6	7,69	
		61	35				1			2,39	1	2,39	
			41		3	3				3,56	1	3,56	
			66		1					7,69	6	7,69	
			68		2		7	7,24		5,57	9	7,24	
			72				1			3,68	1	3,68	
			115				3			4,79	3	4,79	
		64	41			1				1,88	1	1,88	
			68		1	5	3	2,98	1,90	3,80	9	3,80	
			97				1			2,58	1	2,58	
			66	61	1				3,45		1	3,45	
			68	41	1	1	2	4,67	1,93	7,43	4	7,43	
				53		1	3			1,13	4	5,85	
				61	2		7	7,24		5,57	9	7,24	
				64	1	5	3	2,98	1,90	3,80	9	3,80	
				97			1			7,93	1	7,93	
		72	41				1			3,22	1	3,22	
			61				1			3,68	1	3,68	
		97	64				1			2,58	1	2,58	
			68				1			7,93	1	7,93	
			120				1			5,85	1	5,85	
		101	2				1			3,08	1	3,08	
			115		2		5	16,70		6,15	7	16,70	
			120			2	1			1,30	3	4,37	
		115	53				1			2,39	1	2,39	
			61				3			4,79	3	4,79	
			101		2		5	16,70		6,15	7	16,70	
			120		6	10	20	2,96	9,61	6,67	36	9,61	
			130		1	2	12	3,08	6,06	9,19	15	9,19	
			136		3		7	7,16		9,97	10	9,97	
		120	97				1			5,85	1	5,85	
			101			2	1			1,30	3	4,37	
			115		6	10	20	2,96	9,61	6,67	36	9,61	
			130		3	13	36	11,28	6,89	10,21	52	11,28	
			136		3	3	3	7,47	3,22	2,54	9	7,47	
			146		1	2		8,97	5,49		3	8,97	
			151		4			10,35			4	10,35	
		130	115		1	2	12	3,08	6,06	9,19	15	9,19	
			120		3	13	36	11,28	6,89	10,21	52	11,28	
			146				2			7,00	2	7,00	
		136	115		3		7	7,16		9,97	10	9,97	
			120		3	3	3	7,47	3,22	2,54	9	7,47	

Type	Protein 1	Protein 2	Residue 1	Residue 2	Å	Spectral count			Score _{max}			Total spectral count	Best Score _{max}
						Set 1	Set 2	Set 3	Set 1	Set 2	Set 3		
			146				1	13	0,49	11,34	14	11,34	
			151			4		2	8,47	2,60	6	8,47	
			146	120		1	2		8,97	5,49	3	8,97	
			130					2		7,00	2	7,00	
			136				1	13	0,49	11,34	14	11,34	
			151	120		4			10,35		4	10,35	
			136			4		2	8,47		6	8,47	
			179	181			5	2		4,64	5,41	7	5,41
			201					1		5,33	1	5,33	
			206			5	6	13	6,72	8,97	24	8,97	
			256				1	4	0,05	9,52	5	9,52	
			180	206				1		7,72	1	7,72	
			256					1		4,92	1	4,92	
			181	179			5	2		4,64	5,41	7	5,41
			206			6	9	34	19,87	5,70	49	19,87	
			256					5		8,73			
			201	179				1		7,16	5	7,16	
			206			3	6	24	17,55	10,00	33	17,55	
			213					7		9,31	7	9,31	
			217					2		8,21	2	8,21	
			206	179		5	6	13	6,72	8,97	24	8,97	
			180					1		7,72	1	7,72	
			181			6	9	34	19,87	5,70	49	19,87	
			201			3	6	24	17,55	10,00	33	17,55	
			213	201				2		5,58	4	6,81	
			213	201				2		6,81	2	8,21	
			217				3	8		4,81	8,80	11	8,80
			256	179			1	4		0,05	9,52	5	9,52
			180					1		4,92	1	4,92	
			181					5		7,16	5	7,16	
Bud31	Bud31	5	20			1			2,53		1	2,53	
		10	20			1			1,92		1	1,92	
		20	5			1			2,53		1	2,53	
			10			1			1,92		1	1,92	
		37	44	10,2			1			0,28		1	0,28
		44	37	10,2		1			0,28		1	0,28	
		69	71	5,8		1			0,53		1	0,53	
		71	69	5,8		1			0,53		1	0,53	
Cef1	Cef1	22	59	12,4		1	3		2,22	6,24	4	6,24	
		59	22	12,4		1	3		2,22	6,24	4	6,24	
		180	187					1		7,80	1	7,80	
		187	180					1		7,80	1	7,80	
		201				2			1,81		2	1,81	
		201	187			2			1,81		2	1,81	
		239	247	13,0		1		1	0,64		2	3,78	
		251	247	19,0				1		6,43	1	6,43	
		240	247	11,0		7	10	11	6,18	3,89	28	6,18	
		251	251	16,9		2	6	2	11,13	5,98	10	11,13	
		247	239	13,0		1		1	0,64		2	3,78	
		240	240	11,0		7	10	11	6,18	3,89	28	6,18	
		251	251	6,2			2			1,16	2	1,16	
		257	257	15,3		1				0,06	1	0,06	
		259	259	18,5		1				0,19	1	0,19	
		251	239	19,0				1		6,43	1	6,43	
		240	240	16,9		2	6	2	11,13	5,98	10	11,13	
		247	247	6,2			2			1,16	2	1,16	
		257	247	15,3		1				0,06	1	0,06	
		259	247	18,5		1				0,19	1	0,19	
		293	296			10	2	33	19,98	1,64	45	19,98	
		296	293			10	2	33	19,98	1,64	45	19,98	
		308	308				1			0,26	1	0,26	
		305	312			2			4,54		2	4,54	
			314			4			12,62		4	12,62	
			318				2			6,69	2	6,69	
			353			1	2		1,94	1,90	3	1,94	
			356					1		4,33	1	4,33	
			359				1	2		2,73	3	2,73	
		308	296			1			0,26		1	0,26	
		321						1		3,27	1	3,27	
		353		1			1		6,11		2	6,11	
		359		1					2,23		1	2,23	
		312	305			2			4,54		2	4,54	
			314			2			3,18		2	3,18	
			318			4		5	5,43		9	6,08	
			353					2		8,80	2	8,80	
			356			1			0,73		1	0,73	
			359			1	1		1,80	1,09	2	1,80	
		314	305			4			12,62		4	12,62	
			312			2			3,18		2	3,18	
			321			5		1	7,68		6	7,68	

Type	Protein 1	Protein 2	Residue 1	Residue 2	Å	Spectral count			Score _{max}			Total spectral count	Best Score _{max}	
						Set 1	Set 2	Set 3	Set 1	Set 2	Set 3			
Clf1	Clf1	318	305				4		2	5,43	3,63	6,69	2	6,69
			312			2	1	4	1,63			6,08	9	6,08
			321					1			4,01	7	4,01	
			335					1			1,76	1	1,76	
			353					1			3,81	1	3,81	
		321	308					1			3,27	1	3,27	
			314			5		1	7,68			4,29	6	7,68
			318			2	1	4	1,63	3,63	4,01	1,76	7	4,01
		335	318			1	2		1,94	1,90	1,76	1	1,76	
		353	305			1			6,11			3,15	3	1,94
			308			1		1			8,80	2	8,80	
			312					2			3,81	1	3,81	
			318					1			2,42	3	2,42	
			359			1	1	1	0,24	1,79	2,42	1,96	7	1,96
			364			2	2	3	0,84	0,85	1,96	4,33	1	4,33
		356	305					1				1,53	1	0,73
			312			1			0,73			1,53	1	0,73
			364					1				2,73	3	2,73
		359	305				1	2		0,23		2,73	1	2,23
			308			1			2,23			2,23	2	1,80
			312			1	1		1,80	1,09		2,42	3	2,42
			353			1	1	1	0,24	1,79	2,42	1,96	7	1,96
		364	353			2	2	3	0,84	0,85	1,96	4,33	1	4,33
			356					1				1,53	1	1,53
		24	28					5				2,75	5	2,75
		25	111			1		1	0,47			3,22	2	3,22
		28	24					5				2,75	5	2,75
		111	25			1		1	0,47			3,22	2	3,22
		281	304			1		1	0,19			4,13	2	4,13
		304	281			1		1	0,19			4,13	2	4,13
		352	399					2				5,61	2	5,61
		399	352					2				5,61	2	5,61
		529	532			11	4	9	5,44	3,71	4,44	24	54,44	
		532	529			11	4	9	5,44	3,71	4,44	24	54,44	
		605	679			1			1,17			1	1,17	
		635	640					3				6,37	3	6,37
		640	635					3				6,37	3	6,37
			668					1				2,54	1	2,54
		679	640			2		2	5,39			7,80	4	7,80
			673			5	3	26	11,23	4,56	9,23	34	11,23	
		673	668			5	3	26	11,23	4,56	9,23	34	11,23	
		679	605			1			1,17			1	1,17	
			640			2		2	5,39			7,80	4	7,80
			668					2				4,00	2	4,00
		670	679			3		2	0,80			3,82	5	3,82
			680					1				0,47	1	0,47
		673	668			5	3	26	11,23	4,56	9,23	34	11,23	
		679	605			1			1,17			1	1,17	
			640			2		2	5,39			7,80	4	7,80
			668					2				4,00	2	4,00
		670	679			3		2	0,80			3,82	5	3,82
			680			4	3	1	5,77	2,48	2,21	8	5,77	
		682	679			4	3	1	5,77	2,48	2,21	8	5,77	
		2	58			1			0,87			1	0,87	
Cus1	Cus1	39	41			4	11	22	2,49	4,59	6,67	37	6,67	
			48			2	5	18	0,94	4,56	8,19	25	8,19	
			50				2		0,43			2	0,43	
			53			1	3	7	1,97	1,07	5,10	11	5,10	
		40	53					1				5,61	1	5,61
		41	39			4	11	22	2,49	4,59	6,67	37	6,67	
			50					1				0,80	1	0,80
			53			1	7	16	5,65	4,56	7,37	24	7,37	
		48	39			2	5	18	0,94	4,56	8,19	25	8,19	
			53			6	3	22	2,64	5,74	11,98	31	11,98	
			58			1	5	1	1,95	1,58	2,06	7	2,06	
			61				1		0,49			1	0,49	
		50	39				2					3,01	3	3,01
			41					1				0,80	1	0,80
			58			1	9		0,41	3,33		10	3,33	
			64			1			0,30			1	0,30	
		53	39			1	3	7	1,97	1,07	5,10	11	5,10	
			40					1				5,61	1	5,61
			41			1	7	16	5,65	4,56	7,37	24	7,37	
			48			6	3	22	2,64	5,74	11,98	31	11,98	
			61			5	11	74	11,82	2,66	9,67	90	11,82	
			64			5	9	19	8,61	7,23	9,56	33	9,56	
		58	2			1			0,87			1	0,87	
			48			1	5	1	1,95	1,58	2,06	7	2,06	
			50			1	9		0,41	3,33		10	3,33	
			64			6	9	10	5,40	4,87	9,31	25	9,31	
			83					1				2,06	1	2,06
		61	48			5	11	74	11,82	0,49	2,66	9,67	90	0,49
			53									9,67	90	11,82

Type	Protein 1	Protein 2	Residue 1	Residue 2	Å	Spectral count			Score _{max}			Total spectral count	Best Score _{max}
						Set 1	Set 2	Set 3	Set 1	Set 2	Set 3		
Cwc15	Cwc15	79						2			6,33	2	6,33
		64	48					3			3,01	3	3,01
		50					1			0,30	1	0,30	
		53				5	9	19	8,61	7,23	9,56	33	9,56
		58				6	9	10	5,40	4,87	9,31	25	9,31
		79						2			8,20	2	8,20
		83						4			6,60	4	6,60
		79	61					2			6,33	2	6,33
		64						2			8,20	2	8,20
		86				8	1	44	7,02	5,02	9,78	53	9,78
Cwc2	Cwc2	95						3			11,01	3	11,01
		83	58					1			2,06	1	2,06
		64						4			6,60	4	6,60
		95					3	5		1,03	3,62	8	3,62
		86	79			8	1	44	7,02	5,02	9,78	53	9,78
		95	79					3			11,01	3	11,01
		83						5			1,03	3,62	8
		102	102				3	5	4	16,44	3,76	11,26	12
		95				3	5	4	16,44	3,76	11,26	12	16,44
		202	226				1	2			3,89	9,01	3
Cwc2	Cwc2	246				12	17	41	22,72	14,98	14,75	70	22,72
		379						2			7,64	2	7,64
		223	236					2			2,17	2	2,17
		226	202				1	2			3,89	9,01	3
		236					8	6			5,33	4,01	14
		236	223					2			2,17	2	2,17
		226					8	6			5,33	4,01	14
		246	246				5	2			9,36	10,64	7
		246	202			12	17	41	22,72	14,98	14,75	70	22,72
		236					5	2			9,36	10,64	7
Cwc2	Cwc2	317	347					3			3,78	3	3,78
		329	347			1	4			3,04	4,83	5	4,83
		347	317				3				3,78	3	3,78
		329				1	4			3,04	4,83	5	4,83
		358	347			3	2			2,00	0,20	5	2,00
		358				3	2			2,00	0,20	5	2,00
		379	202					2			7,64	2	7,64
		38	41			2	2		7,21	2,26		4	7,21
		43					1			0,03		1	0,03
		41	38			2	2		7,21	2,26		4	7,21
Cwc2	Cwc2	43	38				1			0,03		1	0,03
		88	102			1	2		2,13	1,13		3	2,13
		91	104				1			0,77		1	0,77
		102	88			1	2		2,13	1,13		3	2,13
		108				2	2	4	1,08	4,06	6,02	8	6,02
		118						1			2,99	1	2,99
		104	91				1			0,77		1	0,77
		129						2			7,19	2	7,19
		108	102			2	2	4	1,08	4,06	6,02	8	6,02
		118				6	5	11	8,14	7,16	9,75	22	9,75
Cwc2	Cwc2	118	102			1	1		1,09	2,63		2	2,63
		129						1			2,99	1	2,99
		140				1	1				2,63	2	2,63
		129	104					2			7,19	2	7,19
		104						2			8,61	2	8,61
		108				2					8,61	2	8,61
		118				6	5	11	8,14	7,16	9,75	22	9,75
		137				3	1			8,29	0,85	4	8,29
		140	140			4	6	5	6,64	9,52	7,70	15	9,52
		145					1				3,95	1	3,95
Cwc2	Cwc2	145	129				3	1			8,29	0,85	4
		137				2				3,46		2	3,46
		145	145					2			3,46	2	3,46
		140	118			1	1			1,09	2,63	2	2,63
		129				4	6	5	6,64	9,52	7,70	15	9,52
		151					2	2		2,07	5,16	4	5,16
		145	129				1				3,95	1	3,95
		137				2				3,46		2	3,46
		151				1	2	4	4,45	3,80	6,62	7	6,62
		151	140				2	2		2,07	5,16	4	5,16
Cwc2	Cwc2	145				1	2	4	4,45	3,80	6,62	7	6,62
		2	10				1			2,02		1	2,02
		10	2				1			2,02		1	2,02
		86	13,6					1			3,30	1	3,30
		61	86	10,5				1			1,98	1	1,98
		86	10	13,6				1			3,30	1	3,30
		61		10,5				1			1,98	1	1,98
		116	152				3				3,54	3	3,54
		135	152				1				1,28	1	1,28
		152	116				3				3,54	3	3,54
Cwc2	Cwc2	135					1				1,28	1	1,28
		179	152					2			2,12	2	2,12
		236		28,0				2			2,12	2	2,12
		185	236	15,4			2				1,73	2	1,73
		11,38										2	11,38
		11,38										2	1,73

Type	Protein 1	Protein 2	Residue 1	Residue 2	Å	Spectral count			Score _{max}			Total spectral count	Best Score _{max}
						Set 1	Set 2	Set 3	Set 1	Set 2	Set 3		
Cwc21	Cwc21	236	179	28,0	15,4		2	2	1,73	11,38	2	2	11,38
		185				3	4	7	3,22	5,82	5,67	2	1,73
		310	320			3	4	7	3,22	5,82	5,67	14	5,82
		320	310									14	5,82
		47	53			3	2	4	4,27	1,64	5,88	9	5,88
		53	47			3	2	4	4,27	1,64	5,88	9	5,88
		62				1	3		0,66	3,71		4	3,71
		62	53									4	3,71
		97	105			19	9	97	13,12	10,74	20,89	125	20,89
		98	105			35	34	89	11,32	6,04	16,07	158	16,07
Cwc22	Cwc22	105	97			19	9	97	13,12	10,74	20,89	125	20,89
		98										125	20,89
		98				35	34	89	11,32	6,04	16,07	158	16,07
		294	316	12,8			2					2	10,65
		316	294	12,8			2					2	10,65
		406	444	6,3			1					1	9,70
		444	406	6,3			1					1	9,70
		495	505				5					5	3,07
		496	505				1					1	2,78
		505	495				5					5	3,07
Cwc24	Cwc24	496					1					1	2,78
		508		6				2,05				6	2,05
		508	505	6				2,05				6	2,05
		520	530	6	5	7	6,60	1,97	3,93	18		18	6,60
		530	520	6	5	7	6,60	1,97	3,93			18	6,60
		63	67	2	2		4,00	3,97				4	4,00
		67	63	2	2		4,00	3,97				4	4,00
		93	123	4	1	5	3,57	3,31	7,13	10		10	7,13
		123	93	4	1	5	3,57	3,31	7,13			10	7,13
		148	169	15,2		5	2		4,97	3,91		7	4,97
Cwc27	Cwc27	169	148	15,2		5	2		4,97	3,91		7	4,97
		186	232	16,5	1		1	3,36				2	5,25
		194	203	19,0	4	3	4	4,38	5,27	5,88	11		5,88
		256		1				0,08				1	0,08
		203	194	19,0	4	3	4	4,38	5,27	5,88	11		5,88
		229	18,7	1			2	3,05				3	3,05
		225	229	6,6			1					1	1,98
		229	203	18,7	1		2	3,05				3	3,05
		225		6,6			1					1	1,98
		232	186	16,5	1		1	3,36				2	5,25
Ecm2	Ecm2	256	194	1			1	0,08				1	0,08
		36	171	3				2,82				3	2,82
		56	146				1					1	2,68
		146	56				1					1	2,68
		171	36	3				2,82				3	2,82
		225	234				1					1	2,94
		234	225				1					1	2,94
		278	289	3			6	7,00				9	7,00
		289	278	3			6	7,00				9	7,00
		295		1				0,27				1	0,27
Ecm2	Ecm2	297		4		6	14	5,00	4,97	6,99	24		6,99
		295	289	1				0,27				1	0,27
		297	289	4	6	14	5,00	4,97	6,99	24		6,99	
		47	57	9,0			3					3	4,44
		57	47	9,0			3					3	4,44
		116	138				1					1	2,97
		157					1					1	1,82
		119	157				5					5	7,84
		138	116				1					1	2,97
		157					5					5	5,28
Ecm2	Ecm2	164	138				1					1	1,77
		164	140				1					1	7,61
		140	164				1					1	5,66
		157	116				1					1	1,82
		116					5					5	7,84
		119					5					5	5,28
		138					5					5	5,28
		167	138				1					16	12,22
		157		4	2	10	8,34	3,76	12,22			16	12,22
		173					3					3	4,01
167	167	247					1					1	1,49
		277		1				0,27				1	0,27
		164	138				1					1	1,77
		140					1					1	1,77
		173					5					5	6,16
		337					1					5	5,06
		167	138				1					1	7,61
		157		4	2	10	8,34	3,76	12,22			16	12,22
173	173	247		3	3	1	5,86	4,25	5,43	7		7	5,86
		311					2					2	10,95
		318					1					1	5,27
		337					1					1	8,56
		157	157				3					3	4,01
		164					5					5	6,16
		245	18,2		1		1					1	4,58
		247	14,2		1		2					3	5,85

Type	Protein 1	Protein 2	Residue 1	Residue 2	Å	Spectral count			Score _{max}			Total spectral count	Best Score _{max}
						Set 1	Set 2	Set 3	Set 1	Set 2	Set 3		
Hsh155	Hsh155	311	245	12,3		1	3	1	0,94	4,38	5,13	1	5,13
		177	274			1			2,93			1	0,94
		188	265			5	5	5	28,24	10,98	8,48	15	4,38
		189	265			1			1,19			1	2,93
		198	265									1	28,24
		277										1	1,19
		230	233			4	3		4,11	4,96		7	4,96
		265	265	20,3		19	12	33	32,27	6,16	10,72	64	32,27
		233	230			4	3		4,11	4,96		7	4,96
		265							0,06			1	0,06
		245	173	18,2		1		1			4,58	1	4,58
		177	177	12,3		1			0,94			1	0,94
		247	157			3	3	1	5,86	4,25	5,43	7	1,49
		167										1	5,86
		173	173	14,2		1		2	3,56		5,85	3	5,85
		265	189			1				2,93		1	2,93
		198				5	5	5	28,24	10,98	8,48	15	28,24
		230	230	20,3		19	12	33	32,27	6,16	10,72	64	32,27
		233				1			0,06			1	0,06
		274	188					3			4,38	3	4,38
		318						2			6,59	2	6,59
		331						1			2,85	1	2,85
		337						1			3,12	1	3,12
		342						1			1,44	1	1,44
		277	157			1			0,27			1	0,27
		198				1			1,19			1	1,19
		311	167					2			10,95	2	10,95
		173						1			5,13	1	5,13
		318	167					1			5,27	1	5,27
		274						2			6,59	2	6,59
		331	274					1			2,85	1	2,85
		337	164					1			5,06	1	5,06
		167						1			8,56	1	8,56
		274						1			3,12	1	3,12
		342	274					1			1,44	1	1,44
		35	45			1	1	10	2,62	5,55	7,08	12	7,08
		51				1	3			0,37	5,65	4	5,65
		66					2				4,45	2	4,45
		72					1				2,34	1	2,34
		45	35			1	1	10	2,62	5,55	7,08	12	7,08
		66				3	1			3,20	9,81	4	9,81
		51	35			1	3			0,37	5,65	4	5,65
		66				1				0,81		1	0,81
		66	35					2			4,45	2	4,45
		45				3	1			3,20	9,81	4	9,81
		51				1				0,81		1	0,81
		72	35			3	2				2,34	1	2,34
		237								4,63	5,77	5	5,77
		150	151					1			1,84	1	1,84
		158	158			2	6	42	2,30	5,25	11,34	50	11,34
		151	150					1			1,84	1	1,84
		158	150			2	6	42	2,30	5,25	11,34	50	11,34
		191				8	6			9,77	5,29	14	9,77
		172	191	16,0				1			1,81	1	1,81
		191	158			8	6			9,77	5,29	14	9,77
		172		16,0				1			1,81	1	1,81
		237	72			3	2			4,63	5,77	5	5,77
		276	10,8	12		1			8,55	1,25		13	8,55
		237	10,8	12		1			8,55	1,25		13	8,55
		410	455			1				2,56		1	2,56
		455	410			1						1	2,56
		473	521	16,9				3			5,34	3	5,34
		521	473	16,9				3			5,34	3	5,34
		696	699	9,3		1					1,39	1	1,39
		699	696	9,3		1					1,39	1	1,39
Hsh49	Hsh49	1	2					1			3,97	1	3,97
		2	1					1			3,97	1	3,97
		22	39			11	5	16	3,26	0,85	1,87	32	3,26
		42				4	2	2	1,36	0,20	2,19	8	2,19
		39	22			11	5	16	3,26	0,85	1,87	32	3,26
		42	22			4	2	2	1,36	0,20	2,19	8	2,19
		101	133			1	1			0,40	4,53	2	4,53
		113	193					1			4,87	1	4,87
		126	133					1			0,45		
		130	160					1			1,53	2,99	4
		166				2	17	2	3,42	3,45	2,68	21	3,45
		133	101					1			0,40	4,53	2
		126						1			0,45		4,53
		213						1			5,74	1	5,74
		160	130					1			1,53	2,99	4
		166	130			2	17	2	3,42	3,45	2,68	21	3,45
		193	113					1			4,87	1	4,87
		204	213					1			5,08	1	5,08

Type	Protein 1	Protein 2	Residue 1	Residue 2	Å	Spectral count			Score _{max}			Total spectral count	Best Score _{max}
						Set 1	Set 2	Set 3	Set 1	Set 2	Set 3		
Isy1	Isy1	Isy1	213	133				1		5,74	1	5,74	
			204					1		5,08	1	5,08	
			7	27		3	2	6	11,09	5,81	12,96	11	12,96
			42				2	1	0,70	1,60		3	1,60
			45			1	3		0,86	3,71		4	3,71
			59			1			0,47			1	0,47
			27	7		3	2	6	11,09	5,81	12,96	11	12,96
			40			7	3	2	4,61	1,77	2,80	12	4,61
			42				1	2		2,63	1,73	3	2,63
			45			3	2	4	8,36	6,79	10,44	9	10,44
			56			2	3	11	1,01	2,43	4,30	16	4,30
			59				1		0,35			1	0,35
			61					1		1,94		1	1,94
			40	27		7	3	2	4,61	1,77	2,80	12	4,61
			42				2	1		0,70	1,60	3	1,60
Lea1	Lea1	Lea1	27				1	2		2,63	1,73	3	2,63
			45			1	3		0,86	3,71		4	3,71
			56			2	3	11	1,01	2,43	4,30	16	4,30
			61					3		5,35		3	5,35
			59	7		1			0,47			1	0,47
			27				1			0,35		1	0,35
			61	27				1		1,94		1	1,94
			56					3		5,35		3	5,35
			121	139		9	9	11	5,87	5,51	6,68	29	6,68
			143			1	1		2,06	0,58		2	2,06
			139	121		9	9	11	5,87	5,51	6,68	29	6,68
			143	121		1	1		2,06	0,58		2	2,06
			194	215		2	6	6	4,07	0,65	4,87	14	4,87
			205			2	2	10	5,00	3,61	4,08	14	5,00
Msl1	Msl1	Msl1	215				3	1		0,95	1,30	4	1,30
			205	215			3	6		4,59	4,67	9	4,67
			232			2	6	6	4,07	0,65	4,87	14	4,87
			215	194		3	1		0,95	1,30		4	1,30
			205				1			1,74		1	1,74
			232	194		2	2	10	5,00	3,61	4,08	14	5,00
			205			3	6		4,59	4,67		9	4,67
			215					1			1,74		1,74
			2	7			3	1			1,99	1	1,99
			8				2			1,72	3,22	5	3,22
			7	2			1				1,99	1	1,99
			8	2		3	2			1,72	3,22	5	3,22
Ntc20	Ntc20	Ntc20	85	94			1				5,31	1	5,31
			94				1				5,31	1	5,31
Prp11	Prp11	Prp11	11	28		2	6		4,08	11,92		8	11,92
			36				3			9,36		3	9,36
			60				1			9,75		1	9,75
			192				3			6,66		3	6,66
			28	11		2	6		4,08	11,92		8	11,92
			48			2				9,07		2	9,07
			60			1				2,84		1	2,84
			192			1				9,70		1	9,70
			36	11			3			9,36		3	9,36
			60				5			8,01		5	8,01
			126			1				3,24		1	3,24
			192			3				4,78		3	4,78
			48	28			2			9,07		2	9,07
			126			1				6,08		1	6,08
			192			2				3,54		2	3,54
Prp17	Prp17	Prp17	60	11		1				9,75		1	9,75
			28				1			2,84		1	2,84
			36				5			8,01		5	8,01
			103	126		6	8		3,96	9,95		14	9,95
			121	144		1			0,21			1	0,21
			173				1			2,81		1	2,81
			126	36			1			3,24		1	3,24
			48				1			6,08		1	6,08
			103			6	8		3,96	9,95		14	9,95
			144			1			0,15			1	0,15
			144	121			1			0,21		1	0,21
			126				1			0,15		1	0,15
			175			1			0,40			1	0,40
			173	121			1				2,81	1	2,81
			175	144		1		3		0,40		1	0,40
			192	11			1				6,66	3	6,66
			28				1				9,70	1	9,70
			36				3				4,78	3	4,78
			48				2				3,54	2	3,54
			121	239		4	5	6	6,28	5,94	4,87	15	6,28
			239	121		4	5	6	6,28	5,94	4,87	15	6,28
			307	366			1			0,79		1	0,79
			366	307		1			0,79			1	0,79
			404	422		13	17	7	5,19	4,49	3,07	37	5,19

Type	Protein 1	Protein 2	Residue 1	Residue 2	Å	Spectral count			Score _{max}			Total spectral count	Best Score _{max}
						Set 1	Set 2	Set 3	Set 1	Set 2	Set 3		
Prp19	Prp19		427			13	17	7	5,19	4,49	3,07	1	0,20
			422	404		1			0,20			37	5,19
			427	404		8	6	24	16,47	10,59	13,52	1	0,20
			450			8	6	24	16,47	10,59	13,52	38	16,47
			450	427		0,09						38	16,47
			1	1		2			0,53			2	0,09
			107	275		2						2	0,53
			108	120		7	13	36	10,19	12,01	10,04	56	12,01
			139			4	2	1	8,19	9,46	4,06	7	9,46
			170			1	4		0,75	2,58		5	2,58
			202			1			1,74			1	1,74
			275			1			1,30			1	1,30
			404			1			1,37			1	1,37
			120	108		7	13	36	10,19	12,01	10,04	56	12,01
			135			3	3	10	2,42	3,57	5,07	16	5,07
			139			2			5,92			2	5,92
			130	139		2			6,22			2	6,22
			135	120		3	3	10	2,42	3,57	5,07	16	5,07
			139			1	1		1,67	0,39		2	1,67
			272			1	1		0,12	3,74		2	3,74
			275			1	2		1,52	0,16		3	1,52
			139	108		4	2	1	8,19	9,46	4,06	7	9,46
			120			2			5,92			2	5,92
			130			2			6,22			2	6,22
			135			1	1		1,67	0,39		2	1,67
			139			2			1,94	3,41		4	3,41
			275			1	1		3,68	0,16		2	3,68
			168	433		6				3,63		6	3,63
			452			3			0,33	1,26		5	1,26
			170	108		1	4		0,75	2,58		5	2,58
			202			6	9	3	9,23	2,87		18	9,23
			275			1			1,54			1	1,54
			452			1	1	6	1,59	3,49	4,13	8	4,13
			173	202		1			1,49			1	1,49
			229			3	5	6	7,09	6,18	5,53	14	7,09
			433			3	1	15	4,59	1,24	4,51	19	4,59
			452			3			1,90			3	1,90
			455			1	1		14,22	3,43		2	14,22
			202	108		1			1,74			1	1,74
			170			6	9	3	9,23	2,56	2,87	18	9,23
			173			1			1,49			1	1,49
			226			4	6	2	13,94	4,89	6,26	12	13,94
			229			2	5	4	2,01	8,09	8,68	11	8,68
			272			2	3	1	1,91	4,52	4,51	6	4,52
			226	202		4	6	2	13,94	4,89	6,26	12	13,94
			229	173		3	5	6	7,09	6,18	5,53	14	7,09
			202			2	5	4	2,01	8,09	8,68	11	8,68
			272	135		1			0,12	3,74		2	3,74
			202			2	3	1	1,91	4,52	4,51	6	4,52
			275	107		2			0,53			2	0,53
			108			1			1,30			1	1,30
			135			1	2		1,52	0,16		3	1,52
			139			1	1		3,68	0,16		2	3,68
			170			1			1,54			1	1,54
			404			1			1,22			1	1,22
			404	108		1			1,37			1	1,37
			275			1			1,22			1	1,22
			452			1			0,61			1	0,61
			455			10	7	1	1,72	2,98	1,86	18	2,98
			433	168		6				3,63		6	3,63
			173			3	1	15	4,59	1,24	4,51	19	4,59
			455			3	10	25	2,74	4,45	4,69	38	4,69
			452	168		2			0,33	1,26		5	1,26
			170			1	1	6	1,59	3,49	4,13	8	4,13
			173			3			1,90			3	1,90
			404			1			0,61			1	0,61
			455			1			0,08			1	0,08
Prp2	Prp2	2	40			13				12,82		13	12,82
			43			6				10,23		6	10,23
			52			14				13,80		14	13,80
			60			12				18,06		12	18,06
			71			1				9,34		1	9,34
			75			8				14,79		8	14,79
			83			10				16,56		10	16,56
			87			3				3,67		3	3,67
			91			3				10,76		3	10,76
			101			6				11,26		6	11,26
			102			3				11,70		3	11,70
			113			3				14,59		3	14,59

Type	Protein 1	Protein 2	Residue 1	Residue 2	Å	Spectral count			Score _{max}			Total spectral count	Best Score _{max}
						Set 1	Set 2	Set 3	Set 1	Set 2	Set 3		
			120					5		8,80	5	8,80	
			128					2		14,67	2	14,67	
			133					1		3,34	1	3,34	
			211					6		13,57	6	13,57	
			311					3		7,66	3	7,66	
			454					1		5,92	1	5,92	
			560					1		4,74	1	4,74	
			718					2		3,94	2	3,94	
			732					8		6,84	8	6,84	
			756					7		17,20	7	17,20	
			820					1		3,90	1	3,90	
10	14							3		3,67	3	3,67	
	45							3		7,09	3	7,09	
	52							2		8,08	2	8,08	
	60							1		4,28	1	4,28	
	75							1		2,04	1	2,04	
	87							1		6,49	1	6,49	
	101							1		4,08	1	4,08	
	102							3		3,09	3	3,09	
	756							1		1,81	1	1,81	
14	10							3		3,67	3	3,67	
40	2							13		12,82	13	12,82	
	45							28		11,49	28	11,49	
	52				2		15		1,49	9,58	17	9,58	
	87						1			2,65	1	2,65	
43	2						6			10,23	6	10,23	
	52				3		11		0,82	8,87	14	8,87	
	84						1			4,92	1	4,92	
45	10						3			7,09	3	7,09	
	40						28			11,49	28	11,49	
	60						6			12,75	6	12,75	
	71						2			5,80	2	5,80	
	75						2			4,02	2	4,02	
	87						2			4,54	2	4,54	
52	2						14			13,80	14	13,80	
	10						2			8,08	2	8,08	
	40				2		15		1,49	9,58	17	9,58	
	43				3		11		0,82	8,87	14	8,87	
	60				8		49		12,05	9,88	57	12,05	
	71				3		6		5,22	6,45	9	6,45	
	75						8			8,26	8	8,26	
	83						1			2,87	1	2,87	
	84				1		3		0,62	5,66	4	5,66	
	87						5			8,35	5	8,35	
	91						3			5,24	3	5,24	
	101						5			9,32	5	9,32	
	102						2			7,20	2	7,20	
	130						1			3,97	1	3,97	
	718				1				1,79		1	1,79	
60	2						12			18,06	12	18,06	
	10						1			4,28	1	4,28	
	45						6			12,75	6	12,75	
	52				8		49		12,05	9,88	57	12,05	
	75				3		34		8,01	18,94	37	18,94	
	83				1		6		1,00	9,85	7	9,85	
	84						1			2,78	1	2,78	
	87						5			7,52	5	7,52	
	91						3			18,89	3	18,89	
	101						3			3,96	3	3,96	
	102				1		7		1,63	10,86	8	10,86	
	113						2			6,15	2	6,15	
	211						1			2,25	1	2,25	
	718				1				1,82		1	1,82	
	756						1			6,52	1	6,52	
71	2						1			9,34	1	9,34	
	45						2			5,80	2	5,80	
	52				3		6		5,22	6,45	9	6,45	
	83				4		7		3,81	8,07	11	8,07	
	84						4			3,69	4	3,69	
	87				1		8		2,44	7,38	9	7,38	
	91						6			5,36	6	5,36	
	102						2			9,28	2	9,28	
	137						1			2,42	1	2,42	
	560						1			1,75	1	1,75	
	718				1				0,88		1	0,88	
75	2						8			14,79	8	14,79	
	10						1			2,04	1	2,04	
	45						2			4,02	2	4,02	
	52						8			8,26	8	8,26	
	60				3		34		8,01	18,94	37	18,94	
	84						2			9,22	2	9,22	
	87						19			7,46	19	7,46	
	91				2		11		3,86	9,65	13	9,65	

Type	Protein 1	Protein 2	Residue 1	Residue 2	Å	Spectral count			Score _{max}			Total spectral count	Best Score _{max}
						Set 1	Set 2	Set 3	Set 1	Set 2	Set 3		
83	101							5		6,24		5	6,24
	102							2		12,54		2	12,54
	120							2		8,13		2	8,13
	128							1		2,49		1	2,49
	130							1		1,92		1	1,92
	756							3		5,75		3	5,75
	2							10		16,56		10	16,56
	52							1		2,87		1	2,87
	60					1		6	1,00	9,85		7	9,85
	71					4		7	3,81	8,07		11	8,07
84	87					3		47	5,82	10,73		50	10,73
	91					1		22	8,15	14,13		23	14,13
	101							9		6,84		9	6,84
	102							8		14,02		8	14,02
	113							2		1,82		2	1,82
	130							4		6,05		4	6,05
	137							2		4,51		2	4,51
	211							1		3,67		1	3,67
	718					1			0,95			1	0,95
	756							1		3,86		1	3,86
87	43							1		4,92		1	4,92
	52					1		3	0,62	5,66		4	5,66
	60							1		2,78		1	2,78
	71							4		3,69		4	3,69
	75							2		9,22		2	9,22
	91					1			1,71			1	1,71
	101					1		10	0,64	14,24		11	14,24
	102							4		2,53		4	2,53
	128							1		3,59		1	3,59
	137							1		4,46		1	4,46
91	211							1		10,64		1	10,64
	2							3		3,67		3	3,67
	10							1		6,49		1	6,49
	40							1		2,65		1	2,65
	45							2		4,54		2	4,54
	52							5		8,35		5	8,35
	60							5		7,52		5	7,52
	71					1		8	2,44	7,38		9	7,38
	75							19		7,46		19	7,46
	83					3		47	5,82	10,73		50	10,73
101	101					2		10	3,21	8,67		12	8,67
	102							13		8,10		13	8,10
	113							1		4,56		1	4,56
	120							2		4,07		2	4,07
	128							2		8,92		2	8,92
	130							1		4,39		1	4,39
	211							2		8,33		2	8,33
	756							1		5,21		1	5,21
	2							3		10,76		3	10,76
	52							3		5,24		3	5,24
102	60							3		18,89		3	18,89
	71							6		5,36		6	5,36
	75					2		11	3,86	9,65		13	9,65
	83					1		22	8,15	14,13		23	14,13
	84					1			1,71			1	1,71
	102							38	4,76	24,32		40	24,32
	113							6		10,94		6	10,94
	120							1		7,13		1	7,13
	128							1		2,94		1	2,94
	130							1		1,56		1	1,56
102	133							2		4,48		2	4,48
	756							2		6,74		2	6,74
	2							6		11,26		6	11,26
	10							1		4,08		1	4,08
	52							5		9,32		5	9,32
	60							3		3,96		3	3,96
	75							5		6,24		5	6,24
	83							9		6,84		9	6,84
	84					1		10	0,64	14,24		11	14,24
	87					2		10	3,21	8,67		12	8,67
102	113					1			0,28	5,95		7	5,95
	120							2	1,17	5,59		3	5,59
	128					1		1	1,99	6,88		2	6,88
	130							8		4,46		8	4,46
	133							12		10,63		12	10,63
	137							11		7,91		11	7,91
	454							1		2,37		1	2,37
	560							2		4,85		2	4,85
	718					1			1,08			1	1,08
	732							4		7,01		4	7,01
102	756							1		3,76		1	3,76
	2							3		11,70		3	11,70
	10							3		3,09		3	3,09

Type	Protein 1	Protein 2	Residue 1	Residue 2	Å	Spectral count			Score _{max}			Total spectral count	Best Score _{max}
						Set 1	Set 2	Set 3	Set 1	Set 2	Set 3		
	52							2		7,20	2	7,20	
	60						1		7	10,86	8	10,86	
	71							2		9,28	2	9,28	
	75							2		12,54	2	12,54	
	83							8		14,02	8	14,02	
	84							4		2,53	4	2,53	
	87							13		8,10	13	8,10	
	91					2		38	4,76	24,32	40	24,32	
	120							18		12,55	18	12,55	
	128					1		2	1,45	4,50	3	4,50	
	130					1		4	0,49	2,61	5	2,61	
	133							2		5,63	2	5,63	
	137							5		5,65	5	5,65	
	211							2		11,21	2	11,21	
	732							2		4,71	2	4,71	
113	2							3		14,59	3	14,59	
	60							2		6,15	2	6,15	
	83							2		1,82	2	1,82	
	87							1		4,56	1	4,56	
	91							6		10,94	6	10,94	
	101					1		6	0,28	5,95	7	5,95	
	128					1		5	0,61	6,01	6	6,01	
	130							5		2,45	5	2,45	
	133							9		7,71	9	7,71	
	137							1		3,87	1	3,87	
	718							1		2,65	1	2,65	
	732							1		1,77	1	1,77	
120	2							5		8,80	5	8,80	
	75							2		8,13	2	8,13	
	87							2		4,07	2	4,07	
	91							1		7,13	1	7,13	
	101					1		2	1,17	5,59	3	5,59	
	102							18		12,55	18	12,55	
	130								0,64		1	0,64	
	133					1		2	4,37	4,22	3	4,37	
	137					1		2	0,12	1,69	3	1,69	
	211							1		5,08	1	5,08	
	756							2		6,73	2	6,73	
128	2							2		14,67	2	14,67	
	75							1		2,49	1	2,49	
	84							1		3,59	1	3,59	
	87							2		8,92	2	8,92	
	91							1		2,94	1	2,94	
	101					1		1	1,99	6,88	2	6,88	
	102					1		2	1,45	4,50	3	4,50	
	113					1		5	0,61	6,01	6	6,01	
	133					6		15	6,32	7,13	21	7,13	
	137					1		11	2,73	5,82	12	5,82	
130	52							1		3,97	1	3,97	
	75							1		1,92	1	1,92	
	83							4		6,05	4	6,05	
	87							1		4,39	1	4,39	
	91							1		1,56	1	1,56	
	101							8		4,46	8	4,46	
	102					1		4	0,49	2,61	5	2,61	
	113							5		2,45	5	2,45	
	120					1			0,64		1	0,64	
	137					3		9	5,88	4,22	12	5,88	
	211							9		5,07	9	5,07	
	560							1		3,67	1	3,67	
	820							1		3,03	1	3,03	
133	2							1		3,34	1	3,34	
	91							2		4,48	2	4,48	
	101							12		10,63	12	10,63	
	102							2		5,63	2	5,63	
	113							9		7,71	9	7,71	
	120					1		2	4,37	4,22	3	4,37	
	128					6		15	6,32	7,13	21	7,13	
	211							2		9,86	2	9,86	
	718							1		3,98	1	3,98	
	820							1		2,61	1	2,61	
137	71							1		2,42	1	2,42	
	83							2		4,51	2	4,51	
	84							1		4,46	1	4,46	
	101							11		7,91	11	7,91	
	102							5		5,65	5	5,65	
	113							1		3,87	1	3,87	
	120					1		2	0,12	1,69	3	1,69	
	128					1		11	2,73	5,82	12	5,82	
	130					3		9	5,88	4,22	12	5,88	
	211							3		5,38	3	5,38	
	454							6		3,78	6	3,78	
	467							1		2,10	1	2,10	

Type	Protein 1	Protein 2	Residue 1	Residue 2	Å	Spectral count			Score _{max}			Total spectral count	Best Score _{max}
						Set 1	Set 2	Set 3	Set 1	Set 2	Set 3		
	485							2		1,97		2	1,97
	718											1	2,09
	732							1		4,63		1	4,63
	820							1		2,10		1	2,10
211	2							6		13,57		6	13,57
	60							1		2,25		1	2,25
	83							1		3,67		1	3,67
	84							1		10,64		1	10,64
	87							2		8,33		2	8,33
	102							2		11,21		2	11,21
	120							1		5,08		1	5,08
	130							9		5,07		9	5,07
	133							2		9,86		2	9,86
	137							3		5,38		3	5,38
	221					14		11	10,43	9,69		25	10,43
	311							2		6,47		2	6,47
	467					1		1	5,48	1,33		2	5,48
	560					1		3	0,29	4,27		4	4,27
	756							1		3,80		1	3,80
221	211					14		11	10,43	9,69		25	10,43
270	316	10,5						7		3,20		7	3,20
300	311	10,5				17		96	12,63	8,36		113	12,63
	316	5,1				18		61	11,21	8,08		79	11,21
311	2							3		7,66		3	7,66
	211							2		6,47		2	6,47
	300	10,5				17		96	12,63	8,36		113	12,63
	732	15,3				19		32	10,39	7,35		51	10,39
316	270	10,5						7		3,20		7	3,20
	300	5,1				18		61	11,21	8,08		79	11,21
454	2							1		5,92		1	5,92
	101							1		2,37		1	2,37
	137							6		3,78		6	3,78
467	137							1		2,10		1	2,10
	211					1		1	5,48	1,33		2	5,48
485	137							2		1,97		2	1,97
	728	20,5						1		2,31		1	2,31
	732	19,4				4		18	3,26	3,88		22	3,88
560	2							1		4,74		1	4,74
	71							1		1,75		1	1,75
	101							2		4,85		2	4,85
	130							1		3,67		1	3,67
	211					1		3	0,29	4,27		4	4,27
632	640	17,0						14		9,06		14	9,06
640	632	17,0						14		9,06		14	9,06
	750	13,8				1		10	10,69	5,47		11	10,69
	756	22,0				3		58	4,80	12,53		61	12,53
718	2							2		3,94		2	3,94
	52					1			1,79			1	1,79
	60					1			1,82			1	1,82
	71					1			0,88			1	0,88
	83					1			0,95			1	0,95
	101					1			1,08			1	1,08
	113							1		2,65		1	2,65
	133							1		3,98		1	3,98
	137					1			2,09			1	2,09
728	485	20,5						1		2,31		1	2,31
732	2							8		6,84		8	6,84
	101							4		7,01		4	7,01
	102							2		4,71		2	4,71
	113							1		1,77		1	1,77
	137							1		4,63		1	4,63
	311	15,3				19		32	10,39	7,35		51	10,39
	485	19,4				4		18	3,26	3,88		22	3,88
750	640	13,8				1		10	10,69	5,47		11	10,69
756	2							7		17,20		7	17,20
	10							1		1,81		1	1,81
	60							1		6,52		1	6,52
	75							3		5,75		3	5,75
	83							1		3,86		1	3,86
	87							1		5,21		1	5,21
	91							2		6,74		2	6,74
	101							1		3,76		1	3,76
	120							2		6,73		2	6,73
	211							1		3,80		1	3,80
	640	22,0				3		58	4,80	12,53		61	12,53
	763	14,1				2		40	9,09	12,10		42	12,10
820	2							1		3,90		1	3,90
	130							1		3,03		1	3,03
	133							1		2,61		1	2,61
	137							1		2,10		1	2,10
	840							1		2,40		1	2,40
828	870							1		1,73		1	1,73

Type	Protein 1	Protein 2	Residue 1	Residue 2	Å	Spectral count			Score _{max}			Total spectral count	Best Score _{max}
						Set 1	Set 2	Set 3	Set 1	Set 2	Set 3		
Prp21	Prp21	840	820					1			2,40	1	2,40
		870	828			44	68	224	20,67	13,04	17,06	336	1,73
		60	71	16,5		4	4	22	4,27	2,96	8,71	30	8,71
		71	60	16,5		4	4	22	4,27	2,96	8,71	30	8,71
		242	265				1			3,28		1	3,28
		262	265			22	12	60	16,56	13,76	15,33	94	16,56
		274				15	2	6	16,38	4,84	11,87	23	16,38
		264	274			11	2	5	11,70	5,32	9,86	18	11,70
		265	242				1			3,28		1	3,28
		262				22	12	60	16,56	13,76	15,33	94	16,56
		274				24	14	43	11,26	12,12	13,33	81	13,33
		287						1		6,89		1	6,89
		274	262			15	2	6	16,38	4,84	11,87	23	16,38
		264				11	2	5	11,70	5,32	9,86	18	11,70
		265				24	14	43	11,26	12,12	13,33	81	13,33
Prp46	Prp46	287	265			5	4	9	11,49	6,89	9,14	18	11,49
		274				7			11,92	5,84	12,61	14	12,61
		56	67			4	3		2	4,54		4	10,59
		66	88			2				5,10		2	5,10
		67	56			4	3		7	11,92	5,84	14	12,61
		88							5,27			4	5,27
		87	56			2			2	4,54		4	10,59
		100				1				3,30		1	3,30
		434						1		7,51		1	7,51
		88	66			2				5,10		2	5,10
		67				4				5,27		4	5,27
		434						2			8,97	2	8,97
		100	87			1				3,30		1	3,30
		130	427	5,6		1				1,68		1	1,68
Prp8	Prp8	319	409	12,6		2	2	1	3,03	2,00	4,05	5	4,05
		409	319	12,6		2	2	1	3,03	2,00	4,05	5	4,05
		427		14,2		3				2,81		3	2,81
		427	130	5,6		1				1,68		1	1,68
		409		14,2		3				2,81		3	2,81
		434	87					1			7,51	1	7,51
		88						2			8,97	2	8,97
		89	96			1		3	1,18		2,86	4	2,86
		90	98			10	10	44	11,94	5,37	8,84	64	11,94
		96	89			3		3		7,29	8,18	6	8,18
		98	90			10	12	5	9,77	5,19	5,53	27	9,77
		103	90			3		3		3,04		5	3,04
		96				5					0,41	1	0,41
		121						1			1,40	3	1,40
		611						3					
Prp21	Prp46	121	103					1			0,41	1	0,41
		131	141	19,0				2			0,41	1	0,41
		141	131	19,0				2			6,72	2	6,72
		152	159	14,2		1				2,84		2	2,84
		159	152	14,2		1				2,84		1	2,84
		555		14,3				2			4,98	2	4,98
		586		12,2		1	10			6,63	11,62	11	11,62
		600		23,5		1				0,46		1	0,46
		325	334	13,8	1	3	4		3,20	7,63	6,84	8	7,63
		334	325	13,8	1	3	4		3,20	7,63	6,84	8	7,63
		351	519	13,2	1				2,41			1	2,41
		524		8,9	1	4	2		0,72	2,53	3,46	7	3,46
		517	524	10,5		2				0,76		2	0,76
		681		10,8		1	2			0,03	5,56	3	5,56
		684		11,3	32	39	14		17,30	11,19	12,75	85	17,30
Prp8	Prp8	697		16,6	7	8	1		14,38	10,61	6,39	16	14,38
		519	351	13,2	1				2,41			1	2,41
		524	351	8,9	1	4	2		0,72	2,53	3,46	7	3,46
		517		10,5		2				0,76		2	0,76
		555	159	14,3				2			4,98	2	4,98
		586	159	12,2		1	10			6,63	11,62	11	11,62
		612		8,2		1				0,76		1	0,76
		743		24,3	4	19	37		4,97	4,66	8,41	60	8,41
		600	159	23,5		1				0,46		1	0,46
		611		15,4		4				0,86		4	0,86
		743		34,6		3				0,71		3	0,71
		608	612	6,9				1			3,91	1	3,91
		611	103					3			1,40	3	1,40
		600		15,4		4				0,86		4	0,86
		612	586	8,2		1				0,76		1	0,76
		608		6,9			1			3,91		1	3,91
		681	517	10,8		1	2			0,03	5,56	3	5,56

Type	Protein 1	Protein 2	Residue 1	Residue 2	Å	Spectral count			Score _{max}			Total spectral count	Best Score _{max}
						Set 1	Set 2	Set 3	Set 1	Set 2	Set 3		
	684	517	11,3	32	39	14	17,30	11,19	12,75	85	17,30		
	697	697	13,9	5	21	8	7,47	8,93	9,86	34	9,86		
	697	517	16,6	7	8	1	14,38	10,61	6,39	16	14,38		
	684	684	13,9	5	21	8	7,47	8,93	9,86	34	9,86		
	1926	1926	24,8	1			0,85			1	0,85		
	743	586	24,3	4	19	37	4,97	4,66	8,41	60	8,41		
	600	34,6		3				0,71		3	0,71		
	847	23,9		1	3			4,19	6,45	4	6,45		
	747	847	13,7		1	3		1,66	4,97	4	4,97		
	794	819	10,7		14	4		15,35	14,19	18	15,35		
	847	847	13,1		7	3		2,50	3,65	10	3,65		
	1093	1093	10,5		9	10		14,53	11,74	19	14,53		
	810	817	10,7	1	14	15		3,52	3,42	4,05	30	4,05	
	817	810	10,7	1	14	15		3,52	3,42	4,05	30	4,05	
	819	794	10,7		14	4			15,35	14,19	18	15,35	
	847	847	15,5		9	2		2,71	2,90	11	2,90		
	842	847	8,6		2			2,62			2	2,62	
	1334	1334	17,8		1	7		1,19	6,49	8	6,49		
	846	1093	15,2		1	1		0,14	3,04	2	3,04		
	847	743	23,9		1	3		4,19	6,45	4	6,45		
	747	747	13,7		1	3		1,66	4,97	4	4,97		
	794	794	13,1		7	3		2,50	3,65	10	3,65		
	819	819	15,5		9	2		2,71	2,90	11	2,90		
	842	842	8,6		2			2,62			2	2,62	
	858	858	16,6		4	4		2,10	5,81	8	5,81		
	1093	1093	14,5	1	16	42		4,29	4,49	6,79	59	6,79	
	858	847	16,6		4	4			2,10	5,81	8	5,81	
	920	1589	25,2			6			11,44		6	11,44	
	926	1330	16,4			2				2,13	2	2,13	
	956	965	15,3		1	9			7,59	8,31	10	8,31	
	965	956	15,3		1	9			7,59	8,31	10	8,31	
	1093	794	10,5		9	10			14,53	11,74	19	14,53	
	846	846	15,2		1	1			0,14	3,04	2	3,04	
	847	847	14,5	1	16	42		4,29	4,49	6,79	59	6,79	
	1150	1294	17,6			3				4,68	3	4,68	
	1205	1310	14,1	4	5	6		3,84	7,76	5,90	15	7,76	
	1416	1416	29,2		1	3			0,73	3,40	4	3,40	
	1209	1416	23,0			7				4,45	7	4,45	
	1294	1150	17,6			3				4,68	3	4,68	
	1310	1205	14,1	4	5	6		3,84	7,76	5,90	15	7,76	
	1330	926	16,4			2				2,13	2	2,13	
	1334	842	17,8		1	7			1,19	6,49	8	6,49	
	1416	1205	29,2		1	3			0,73	3,40	4	3,40	
	1209	1209	23,0			7				4,45	7	4,45	
	1589	920	25,2			6				11,44	6	11,44	
	1807	1938	27,3			6				11,77	6	11,77	
	2080			1	1	3		1,57	4,98	10,34	5	10,34	
	2089					3				6,25	3	6,25	
	1821	2089			2	1			2,04	9,85	3	9,85	
	2097					1				6,01	1	6,01	
	1864	1903	23,2			2				9,16	2	9,16	
	2016	2016	20,0			2				8,28	2	8,28	
	2108					3				5,03	3	5,03	
	2122	2122		3	1	39		9,51	0,36	12,14	43	12,14	
	1873	1903	13,7		1	6			2,31	5,25	7	5,25	
	2122	2122				3				8,01	3	8,01	
	1892	1910	13,5			1				0,12	1	0,12	
	1892	1912	11,2		2					3,97	2	3,97	
	1903	1864	23,2			2				9,16	2	9,16	
	1873	1873	13,7		1	6			2,31	5,25	7	5,25	
	1910	1910	13,0	1	5	6			5,80	5,02	6	5,80	
	2122	2122		1	1	2			6,77	0,79	6,25	4	
	1910	1892	13,5			1				0,12	1	0,12	
	1903	13,0	1	5					5,80	5,02	6	5,80	
	1938	10,5	1	4	10				6,36	4,60	4,92	15	
	2094					1				2,66	1	2,66	
	2097					1				2,86	1	2,86	
	2108		1	3	4		0,68		1,28	2,72	8	2,72	
	2122		2	1	15		2,18		2,25	6,80	18	6,80	
	2149	27,0				1				2,68	1	2,68	
	1912	1892	11,2			2				3,97	2	3,97	
	1926	697	24,8	1							1	0,85	
	1938	1807	27,3			6					11,77	6	
	1938	1910	10,5	1	4	10					4,92	15	
	2016	2016	20,2			2					9,82	2	
	2089			1	1	7		0,97	1,24	8,39	9	8,39	
	2094					4				4,70	4	4,70	
	2097					3				8,74	3	8,74	
	2016	1864	20,0			2				8,28	2	8,28	
	1938	20,2				2				9,82	2	9,82	
	2066	13,6	37	22	181	10,94	10,87	13,52		240	13,52		
	2089		14	17	51	10,35	7,92	10,17		82	10,35		
	2094		13	5	19	13,88	2,39	9,90		37	13,88		

Type	Protein 1	Protein 2	Residue 1	Residue 2	Å	Spectral count			Score _{max}			Total spectral count	Best Score _{max}
						Set 1	Set 2	Set 3	Set 1	Set 2	Set 3		
2066	2097					7	8	53	8,40	9,47	15,21	68	15,21
	2108							50			13,74	50	13,74
	2122					13	5	176	13,68	10,45	18,77	194	18,77
	2124						1	27		1,46	10,09	28	10,09
	2016	2016			13,6	37	22	181	10,94	10,87	13,52	240	13,52
	2089					3	5	1	16,26	10,47	4,79	9	16,26
	2094							1			1,43	1	1,43
	2097						1	3	5,68	3,12	9,49	5	9,49
	2108							1			12,86	1	12,86
	2122							3			7,78	3	7,78
2089	2080	1807				1	1	3	1,57	4,98	10,34	5	10,34
	2094	1807					1			0,52		1	0,52
	1821						2	1			6,25	3	6,25
	1938					1	1	7	0,97	1,24	9,85	3	9,85
	2016	1938				14	17	51	10,35	7,92	10,17	82	10,35
	2066	2016				3	5	1	16,26	10,47	4,79	9	16,26
	2097					3	4	6	3,76	4,85	6,46	13	6,46
	2094	1910						1			2,66	1	2,66
	1938							4			4,70	4	4,70
	2016	1938				13	5	19	13,88	2,39	9,90	37	13,88
2097	2066	2066						1			1,43	1	1,43
	2080	2080					1			0,52		1	0,52
	2097	1821				1	2	3	2,50	2,28	3,09	6	3,09
	2108	2108						1			2,58	1	2,58
	2122	2122						3			3,48	3	3,48
	1821	1821						1			6,01	1	6,01
	1910	1910						1			2,86	1	2,86
	1938	1938						3			8,74	3	8,74
	2016	2016				7	8	53	8,40	9,47	15,21	68	15,21
	2066	2066				1	1	3	5,68	3,12	9,49	5	9,49
2108	2089	2089				3	4	6	3,76	4,85	6,46	13	6,46
	2094	2094				1	2	3	2,50	2,28	3,09	6	3,09
	2108	2108					3	14		8,71	13,41	17	13,41
	2154	2154						3			8,11	3	8,11
	1864	1864						3			5,03	3	5,03
	1910	1910				1	3	4	0,68	1,28	2,72	8	2,72
	2016	2016						50			13,74	50	13,74
	2066	2066						1			12,86	1	12,86
	2094	2094						1			2,58	1	2,58
	2097	2097				3	14			8,71	13,41	17	13,41
2122	2154	2154				1	4		0,40		12,04	5	12,04
	1864	1864				3	1	39	9,51	0,36	12,14	43	12,14
	1873	1873					3				8,01	3	8,01
	1903	1903				1	1	2	6,77	0,79	6,25	4	6,77
	1910	1910				2	1	15	2,18	2,25	6,80	18	6,80
	2016	2016				13	5	176	13,68	10,45	18,77	194	18,77
	2066	2066						3			7,78	3	7,78
	2094	2094						3			3,48	3	3,48
	2154	2154						1			5,88	1	5,88
	2124	2124				1	27			1,46	10,09	28	10,09
Prp9	2149	1910			27,0		1	1			2,68	1	2,68
	2154	2154			11,1			1			3,72	1	3,72
	2154	2097						3			8,11	3	8,11
	2108	2108				1	4		0,40		12,04	5	12,04
	2122	2122					1				5,88	1	5,88
	2149	2149			11,1			1			3,72	1	3,72
	2	115					9				8,22	9	8,22
	89	140				3	21		7,09		12,66	24	12,66
	95	107					8				5,74	8	5,74
	107	95					8				5,74	8	5,74
Rse1	115	115			19	18	106	15,02	10,77	15,60	143	15,60	
	107	107			19	18	106	15,02	10,77	15,60	143	15,60	
	124	124			1	3	16	7,42	17,05	11,60	20	17,05	
	124	115			1	3	16	7,42	17,05	11,60	20	17,05	
	140	89			1	3	21		7,09	12,66	24	12,66	
	278	290					1				5,55	1	5,55
	290	278					1				5,55	1	5,55
	302	306			3	2	8	2,17	0,36	4,48	13	4,48	
	306	302			3	2	8	2,17	0,36	4,48	13	4,48	
	468	492					1				2,75	1	2,75
Rse1	492	468						1			2,75	1	2,75
	519	519			7	2	35	14,33	4,31	10,25	44	14,33	
	518	525						3			11,09	3	11,09
	519	492			7	2	35	14,33	4,31	10,25	44	14,33	
	526	526				1				1,71		1	1,71
	525	518						3			11,09	3	11,09
	526	519				1				1,71		1	1,71
	172	221		11,9			2				16,26	2	16,26
	1269	1269					1				2,32	1	2,32
	221	172		11,9			2				16,26	2	16,26
	221	1269					1				9,63	1	9,63

Type	Protein 1	Protein 2	Residue 1	Residue 2	Å	Spectral count			Score _{max}			Total spectral count	Best Score _{max}	
						Set 1	Set 2	Set 3	Set 1	Set 2	Set 3			
SmB	SmB	347	462					1			7,93	1	7,93	
		352	462			2			6,88			2	6,88	
		361	948	41,6		2			4,89			2	4,89	
			949	40,2			1	1		0,77	2,39	2	2,39	
		462	347				1	1		7,93	1	7,93		
			352			2			6,88			2	6,88	
		948	361	41,6		2			4,89			2	4,89	
		949	361	40,2			1	1		0,77	2,39	2	2,39	
			1001	32,1		4	6	15	4,50	5,93	6,24	25	6,24	
		1001	949	32,1		4	6	15	4,50	5,93	6,24	25	6,24	
		1007	1057	13,9		1	1	2	4,79	1,61	6,13	4	6,13	
		1057	1007	13,9		1	1	2	4,79	1,61	6,13	4	6,13	
		1269		172				1			2,32	1	2,32	
			221					1			9,63	1	9,63	
		1316	1342				13	3		14,76	21,63	16	21,63	
		1342	1316				13	3		14,76	21,63	16	21,63	
		2	100	5,7				1			10,51	1	10,51	
		19	100	5,7				2			3,05	2	3,05	
		55	76	8,7		8	12	40	6,64	3,56	11,39	60	11,39	
		60	65			4	4	7	4,30	3,31	5,84	15	5,84	
			68			2	3	1	1,37	5,46	4,25	6	5,46	
			76			25	18	71	9,06	11,00	15,56	114	15,56	
		65	60			4	4	7	4,30	3,31	5,84	15	5,84	
		76		76		1	1	4	1,71	2,16	3,38	6	3,38	
		68	60			2	3	1	1,37	5,46	4,25	6	5,46	
		76	55	8,7		8	12	40	6,64	3,56	11,39	60	11,39	
			60			25	18	71	9,06	11,00	15,56	114	15,56	
			65			1	1	4	1,71	2,16	3,38	6	3,38	
		100		100	25,9		5			3,05		5	3,05	
			186				1			0,89		1	0,89	
		100	2					1			10,51	1	10,51	
		19		5,7				2			3,05	2	3,05	
		76		25,9			5			3,05		5	3,05	
			117					4			2,62	4	2,62	
			186					1			4,81	1	4,81	
		105	117				1	3		3,86	3,45	4	3,86	
		114	117					1			3,62	1	3,62	
			121					4			4,11	4	4,11	
		117	100					4			2,62	4	2,62	
			105				1	3		3,86	3,45	4	3,86	
		114						1			3,62	1	3,62	
		114	114					4			2,96	4	2,96	
		127	127					5			4,67	3	4,67	
		121	114					4			4,11	4	4,11	
		121	127					5			5,72	5	5,72	
		121	131					1			3,87	1	3,87	
		124	138					1			1,87	1	1,87	
		124	117					4			2,96	4	2,96	
		124	138				2			0,87		2	0,87	
		127	121				1			0,43		1	0,43	
		131	121					5			5,72	5	5,72	
			138			2	6	16	4,95	3,88	6,45	24	6,45	
			186					2			5,10	2	5,10	
		132	138			2	5	6	1,64	0,84	3,47	13	3,47	
		132	186			1	3	7	3,47	5,07	7,22	11	7,22	
		138	117					1			2,88	1	2,88	
		138	121					2			0,87	2	0,87	
			124				2	6	16	4,95	3,88	6,45	24	6,45
		131	132			2	5	6	1,64	0,84	3,47	13	3,47	
		132	186			1	3	7	3,47	5,07	7,22	11	7,22	
		145	194					1			2,88	1	2,88	
		145	138					1			0,89	1	0,89	
		145	186				1	1	5	0,24	1,08	8,93	7	8,93
		145	76				1			0,24	1,08	8,93	7	8,93
		100						1			4,81	1	4,81	
		124					1			0,43		1	0,43	
		131						2			5,10	2	5,10	
		132					1			1,00		1	1,00	
		138				1	3	7	3,47	5,07	7,22	11	7,22	
		145				1	1	5	0,24	1,08	8,93	7	8,93	
		194	138					1			2,88	1	2,88	
SmD1	SmD1	1	111					1			7,56	1	7,56	
		2	111					1			10,15	1	10,15	
			128				1			0,40		1	0,40	
		8	111			1	1	9	0,72	2,50	6,04	11	6,04	
			128					3			7,32	3	7,32	
			129					1			2,81	1	2,81	
			140					1			1,87	1	1,87	
		9	128					3			8,18	3	8,18	
			129					1			7,12	1	7,12	
		111	1					1			7,56	1	7,56	
		111	2					1			10,15	1	10,15	

Type	Protein 1	Protein 2	Residue 1	Residue 2	Å	Spectral count			Score _{max}			Total spectral count	Best Score _{max}
						Set 1	Set 2	Set 3	Set 1	Set 2	Set 3		
SmD2	SmD2	8				1	1	9	0,72	2,50	6,04	11	6,04
		128					4	10		5,45	7,08	14	7,08
		140					1	2		0,16	3,04	3	3,04
		128	2				1			0,40		1	0,40
		8						3			7,32	3	7,32
		9						3			8,18	3	8,18
		111					4	10		5,45	7,08	14	7,08
		140				7	18	37	4,55	6,31	12,00	62	12,00
		129	8					1			2,81	1	2,81
		9						1			7,12	1	7,12
		140	8					1			1,87	1	1,87
		111					1	2		0,16	3,04	3	3,04
		128				7	18	37	4,55	6,31	12,00	62	12,00
		53	59	17,5			10				6,35	10	6,35
		73	8,0		11	35	4		6,78	6,85	5,79	50	6,85
		79	15,6			1				0,17		1	0,17
		59	53	17,5		10				6,35		10	6,35
		73	14,7			3				2,22		3	2,22
		79	31,5			4				1,61		4	1,61
		82	38,7			1				2,37		1	2,37
		93	9,7	1		4	1		3,38	6,61	6,73	6	6,73
		73	53	8,0	11	35	4		6,78	6,85	5,79	50	6,85
		59	14,7			3				2,22		3	2,22
		79	53	15,6		1				0,17		1	0,17
		59	31,5			4				1,61		4	1,61
		82	7,8	3		8	12		9,75	7,33	9,77	23	9,77
		82	59	38,7		1				2,37		1	2,37
		79	7,8	3		8	12		9,75	7,33	9,77	23	9,77
		93	9,7	1		4	1		3,38	6,61	6,73	6	6,73
		82	33,8			1				2,75		1	2,75
SmD3	SmD3	2	85			2	2	7	11,37	3,17	5,24	11	11,37
		86				2	3	12	1,53	4,23	4,37	17	4,37
		9	85	13,0			1				3,31	1	3,31
		86					2				2,13	2	2,13
		79	86			1		1	0,24		1,67	2	1,67
		85	2			2	2	7	11,37	3,17	5,24	11	11,37
		9	13,0				1				3,31	1	3,31
		86	2			2	3	12	1,53	4,23	4,37	17	4,37
		9					2				2,13	2	2,13
		79				1		1	0,24		1,67	2	1,67
SmG	SmG	8	13	10,0	2	5	23	4,60	4,73	5,69	30	5,69	
		13	8	10,0	2	5	23	4,60	4,73	5,69	30	5,69	
		14	24	13,0	2	2	3	6,97	11,25	12,31	7	12,31	
		24	14	13,0	2	2	3	6,97	11,25	12,31	7	12,31	
Snt309	Snt309	46	48			3				1,72		3	1,72
		48	46			3				1,72		3	1,72
		67	94		2	3	8	4,52	1,90	3,38	13	4,52	
		72	94				1				0,61	1	0,61
		94	67		2	3	8	4,52	1,90	3,38	13	4,52	
		72					1				0,61	1	0,61
		59	72				1				0,91	1	0,91
		60	81				3				5,77	3	5,77
Snu114	Snu114	72	59				1				0,91	1	0,91
		81	60				3				5,77	3	5,77
		99	111				1				0,91	1	0,91
		494				2	5	15	4,52	7,48	6,92	22	7,48
		111	99				1				1,75	1	1,75
		115	159	6,1		3	1			1,76	3,29	4	3,29
		159	115	6,1		3	1			1,76	3,29	4	3,29
		494	99		2	5	15	4,52	7,48	6,92	22	7,48	
		581	14,0	1	3	9	1,83	5,39	14,42		13	14,42	
		520	583	15,2			1				2,21	1	2,21
		558	581	15,1			1				2,51	1	2,51
		581	494	14,0	1	3	9	1,83	5,39	14,42		13	14,42
		558	15,1				1				2,51	1	2,51
		583	520	15,2			1				2,21	1	2,21
		617	665	9,5	2	2	6	2,29	3,34	4,49	10	4,49	
		665	617	9,5	2	2	6	2,29	3,34	4,49	10	4,49	
		730	749			2	4			0,50	3,11	6	3,11
		890			1	3		1,96	1,07			4	1,96
		749	730			2	4			0,50	3,11	6	3,11
Snu17/Ist3	Snu17/Ist3	804	843	10,2	3	1			1,35	0,60		4	1,35
		843	804	10,2	3	1			1,35	0,60		4	1,35
		991	991	17,0	1	1	3	0,36	1,97	2,28	5	2,28	
		890	730		1	3		1,96	1,07			4	1,96
		947	955	18,0			4				4,69	4	4,69
		955	947	18,0			4				4,69	4	4,69
		991	843	17,0	1	1	3	0,36	1,97	2,28	5	2,28	
		96	103		4	3	7	10,92	7,53	10,43	14	10,92	
		103	96		4	3	7	10,92	7,53	10,43	14	10,92	
		123	133	17,9	2		30	0,60		9,88	32	9,88	
		138					1			2,41	1	2,41	

Type	Protein 1	Protein 2	Residue 1	Residue 2	Å	Spectral count			Score _{max}			Total spectral count	Best Score _{max}
						Set 1	Set 2	Set 3	Set 1	Set 2	Set 3		
Spp2	Spp2	133	123		17,9	2	4	30	0,60	2,22	9,88	32	9,88
			143			2			2,87			6	2,87
		138	123				2	1			2,41	1	2,41
			144						0,88			2	0,88
		143	133			2	4		2,87	2,22		6	2,87
		144	138				2			0,88		2	0,88
		7	15			1			7,65			1	7,65
		11	15			1			0,59			1	0,59
		15	7			1			7,65			1	7,65
			11			1			0,59			1	0,59
		38	52				3			13,55		3	13,55
			58				1			7,55		1	7,55
			68				1			3,42		1	3,42
			74				1			9,31		1	9,31
			83				2			4,37		2	4,37
			95				1			5,46		1	5,46
		52	38				3			13,55		3	13,55
		58	38				1			7,55		1	7,55
		68	38				1			3,42		1	3,42
			70				9			17,04		9	17,04
		70	68				9			17,04		9	17,04
			133				1			2,95		1	2,95
		74	38				1			9,31		1	9,31
		82	95				4			3,94		4	3,94
		83	38				2			4,37		2	4,37
		95	38				1			5,46		1	5,46
Syf1	Syf1		82				4			3,94		4	3,94
		124	133				1			0,10		1	0,10
		127	133				4			7,30		4	7,30
		133	70				1			2,95		1	2,95
			124				1			0,10		1	0,10
			127				4			7,30		4	7,30
			154				1			13,98		1	13,98
		154	133				1			13,98		1	13,98
		168	181				2			2,64		2	2,64
		181	168				2			2,64		2	2,64
		192	367				1			4,84		1	4,84
		220	249			2	3	3	5,33	5,17	3,14	8	5,33
		249	220			2	3	3	5,33	5,17	3,14	8	5,33
		367	192				1			4,84		1	4,84
		413	419	10,4		2	5	7	3,53	3,25	5,41	14	5,41
			424	21,1			1			0,40		1	0,40
		419	413	10,4		2	5	7	3,53	3,25	5,41	14	5,41
		424	413	21,1			1			0,40		1	0,40
		439	424				1			2,72		1	2,72
			531			9	3	23	9,89	6,16	9,55	35	9,89
		524	531			8	4	6	4,68	4,30	15,22	18	15,22
		531	439			9	3	23	9,89	6,16	9,55	35	9,89
			524			8	4	6	4,68	4,30	15,22	18	15,22
Syf2	Syf2	770	802				4			1,78		4	1,78
		790	798				2			5,42		2	5,42
		798	790				2			5,42		2	5,42
		802	770				4			1,78		4	1,78
		23	26			9	11	16	3,47	6,27	8,99	36	8,99
		26	23			9	11	16	3,47	6,27	8,99	36	8,99
		121	159				2			5,88		2	5,88
		132	142				1			1,66		1	1,66
		136	142				4			4,15		4	4,15
			145				1			3,27		1	3,27
		142	132				1			1,66		1	1,66
			136				4			4,15		4	4,15
		145	136				1			3,27		1	3,27
			151			11	4	8	5,16	3,30	4,10	23	5,16
		151	145			11	4	8	5,16	3,30	4,10	23	5,16
		159	121				2			5,88		2	5,88
		199	206			2	2	4	0,86	0,65	4,86	8	4,86
		206	199			2	2	4	0,86	0,65	4,86	8	4,86
Yju2/Cwc16	Yju2/Cwc16	5	68				1			3,01		1	3,01
		22	26			1			1,17		2,07	2	2,07
		26	22			1			1,17		2,07	2	2,07
		32	68			2				2,62		2	2,62
		36	68			3	7	8	5,78	3,70	6,46	18	6,46
			74				4			3,95		4	3,95
			80			1	4		0,96	2,88		5	2,88
		60	120			2	2	5	3,33	1,27	8,10	9	8,10
		63	68			1	2	2	3,05	4,29	5,41	5	5,41
		68	5				1			3,01		1	3,01

Type	Protein 1	Protein 2	Residue 1	Residue 2	Å	Spectral count			Score _{max}			Total spectral count	Best Score _{max}
						Set 1	Set 2	Set 3	Set 1	Set 2	Set 3		
			74	36			4		3,95			4	3,95
				68			1		1,18			1	1,18
			80	36		1	4		0,96	2,88		5	2,88
				68		18	9	20	14,57	3,40	6,29	47	14,57
			120	60		2	2	5	3,33	1,27	8,10	9	8,10
			168	172		2			2,42			2	2,42
			172	168		2			2,42			2	2,42
			242	253		1			2,43			1	2,43
			253	242		1			2,43			1	2,43
				259		1	4	4	8,00	5,45	6,27	9	8,00
				255			1	1		1,22	2,43	2	2,43
			259	253		1	4	4	8,00	5,45	6,27	9	8,00
				255			1	1		1,22	2,43	2	2,43
			272	275			1	1		0,24	6,37	2	6,37
			275	272			1	1		0,24	6,37	2	6,37
Ysf3	Ysf3		12	17	7,9		3			1,89		3	1,89
			17	12	7,9		3			1,89		3	1,89

Table S3: MolProbity validation of the final RNA model of the yeast B^{act} complex

Validation	All RNA	%	Pre-mRNA	%	U6	%	U2	%	U5	%
All-Atom Contacts										
Clash score	5	94	3.45	97	3	98	6	91	6	90
Nucleic Acid Geometry										
Probably wrong sugar puckers:	12	3.2	0	0	6	5.9	2	2.5	4	3
Bad backbone conformations:	121	32	28	51	41	40.2	21	26	31	22
Bad bonds:	0 / 8965	0	0 / 1286	0	0 / 2427	0	0 / 1902	0	0 / 335	0
Bad angles:	0 / 13938	0	0 / 1995	0	0 / 3778	0	0 / 2956	0	0 / 5209	0

References and Notes

1. M. C. Wahl, C. L. Will, R. Lührmann, The spliceosome: Design principles of a dynamic RNP machine. *Cell* **136**, 701–718 (2009). [Medline doi:10.1016/j.cell.2009.02.009](#)
2. P. Fabrizio, J. Dannenberg, P. Dube, B. Kastner, H. Stark, H. Urlaub, R. Lührmann, The evolutionarily conserved core design of the catalytic activation step of the yeast spliceosome. *Mol. Cell* **36**, 593–608 (2009). [Medline doi:10.1016/j.molcel.2009.09.040](#)
3. Z. Warkocki, C. Schneider, S. Mozaffari-Jovin, J. Schmitzová, C. Höbartner, P. Fabrizio, R. Lührmann, The G-patch protein Spp2 couples the spliceosome-stimulated ATPase activity of the DEAH-box protein Prp2 to catalytic activation of the spliceosome. *Genes Dev.* **29**, 94–107 (2015). [Medline doi:10.1101/gad.253070.114](#)
4. T. Ohrt, M. Prior, J. Dannenberg, P. Odenwälder, O. Dybkov, N. Rasche, J. Schmitzová, I. Gregor, P. Fabrizio, J. Enderlein, R. Lührmann, Prp2-mediated protein rearrangements at the catalytic core of the spliceosome as revealed by dcFCCS. *RNA* **18**, 1244–1256 (2012). [Medline doi:10.1261/rna.033316.112](#)
5. S. H. Kim, R. J. Lin, Spliceosome activation by PRP2 ATPase prior to the first transesterification reaction of pre-mRNA splicing. *Mol. Cell. Biol.* **16**, 6810–6819 (1996). [Medline doi:10.1128/MCB.16.12.6810](#)
6. R. M. Lardelli, J. X. Thompson, J. R. Yates 3rd, S. W. Stevens, Release of SF3 from the intron branchpoint activates the first step of pre-mRNA splicing. *RNA* **16**, 516–528 (2010). [Medline doi:10.1261/rna.2030510](#)
7. S. M. Fica, M. A. Mefford, J. A. Piccirilli, J. P. Staley, Evidence for a group II intron-like catalytic triplex in the spliceosome. *Nat. Struct. Mol. Biol.* **21**, 464–471 (2014). [Medline doi:10.1038/nsmb.2815](#)
8. H. D. Madhani, C. Guthrie, A novel base-pairing interaction between U2 and U6 snRNAs suggests a mechanism for the catalytic activation of the spliceosome. *Cell* **71**, 803–817 (1992). [Medline doi:10.1016/0092-8674\(92\)90556-R](#)
9. J. P. Staley, C. Guthrie, Mechanical devices of the spliceosome: Motors, clocks, springs, and things. *Cell* **92**, 315–326 (1998). [Medline doi:10.1016/S0092-8674\(00\)80925-3](#)
10. C. Yan, J. Hang, R. Wan, M. Huang, C. C. Wong, Y. Shi, Structure of a yeast spliceosome at 3.6-angstrom resolution. *Science* **349**, 1182–1191 (2015). [Medline doi:10.1126/science.aac7629](#)
11. W. P. Galej, C. Oubridge, A. J. Newman, K. Nagai, Crystal structure of Prp8 reveals active site cavity of the spliceosome. *Nature* **493**, 638–643 (2013). [Medline doi:10.1038/nature11843](#)
12. R. J. Grainger, J. D. Beggs, Prp8 protein: At the heart of the spliceosome. *RNA* **11**, 533–557 (2005). [Medline doi:10.1261/rna.2220705](#)
13. T. H. Nguyen, W. P. Galej, X. C. Bai, C. Oubridge, A. J. Newman, S. H. Scheres, K. Nagai, Cryo-EM structure of the yeast U4/U6.U5 tri-snRNP at 3.7 Å resolution. *Nature* **530**, 298–302 (2016). [Medline doi:10.1038/nature16940](#)

14. T. H. Nguyen, W. P. Galej, X. C. Bai, C. G. Savva, A. J. Newman, S. H. Scheres, K. Nagai, The architecture of the spliceosomal U4/U6.U5 tri-snRNP. *Nature* **523**, 47–52 (2015). [Medline doi:10.1038/nature14548](#)
15. R. Wan, C. Yan, R. Bai, L. Wang, M. Huang, C. C. Wong, Y. Shi, The 3.8 Å structure of the U4/U6.U5 tri-snRNP: Insights into spliceosome assembly and catalysis. *Science* **351**, 466–475 (2016). [Medline doi:10.1126/science.aad6466](#)
16. D. E. Agafonov, B. Kastner, O. Dybkov, R. V. Hofele, W. T. Liu, H. Urlaub, R. Lührmann, H. Stark, Molecular architecture of the human U4/U6.U5 tri-snRNP. *Science* **351**, 1416–1420 (2016). [Medline doi:10.1126/science.aad2085](#)
17. Z. Warkocki, P. Odenwälder, J. Schmitzová, F. Platzmann, H. Stark, H. Urlaub, R. Ficner, P. Fabrizio, R. Lührmann, Reconstitution of both steps of *Saccharomyces cerevisiae* splicing with purified spliceosomal components. *Nat. Struct. Mol. Biol.* **16**, 1237–1243 (2009). [Medline doi:10.1038/nsmb.1729](#)
18. B. Sander, M. M. Golas, E. M. Makarov, H. Brahms, B. Kastner, R. Lührmann, H. Stark, Organization of core spliceosomal components U5 snRNA loop I and U4/U6 Di-snRNP within U4/U6.U5 Tri-snRNP as revealed by electron cryomicroscopy. *Mol. Cell* **24**, 267–278 (2006). [Medline doi:10.1016/j.molcel.2006.08.021](#)
19. E. Absmeier, J. Wollenhaupt, S. Mozaffari-Jovin, C. Becke, C. T. Lee, M. Preussner, F. Heyd, H. Urlaub, R. Lührmann, K. F. Santos, M. C. Wahl, The large N-terminal region of the Brr2 RNA helicase guides productive spliceosome activation. *Genes Dev.* **29**, 2576–2587 (2015). [Medline](#)
20. T. H. Nguyen, J. Li, W. P. Galej, H. Oshikane, A. J. Newman, K. Nagai, Structural basis of Brr2-Prp8 interactions and implications for U5 snRNP biogenesis and the spliceosome active site. *Structure* **21**, 910–919 (2013). [Medline doi:10.1016/j.str.2013.04.017](#)
21. S. Bessonov, M. Anokhina, A. Krasauskas, M. M. Golas, B. Sander, C. L. Will, H. Urlaub, H. Stark, R. Lührmann, Characterization of purified human Bact spliceosomal complexes reveals compositional and morphological changes during spliceosome activation and first step catalysis. *RNA* **16**, 2384–2403 (2010). [Medline doi:10.1261/rna.2456210](#)
22. K. S. Keating, N. Toor, P. S. Perlman, A. M. Pyle, A structural analysis of the group II intron active site and implications for the spliceosome. *RNA* **16**, 1–9 (2010). [Medline doi:10.1261/rna.1791310](#)
23. N. Toor, K. S. Keating, S. D. Taylor, A. M. Pyle, Crystal structure of a self-spliced group II intron. *Science* **320**, 77–82 (2008). [Medline doi:10.1126/science.1153803](#)
24. S. M. Fica, N. Tuttle, T. Novak, N. S. Li, J. Lu, P. Koodathingal, Q. Dai, J. P. Staley, J. A. Piccirilli, RNA catalyses nuclear pre-mRNA splicing. *Nature* **503**, 229–234 (2013). [Medline](#)
25. J. Hang, R. Wan, C. Yan, Y. Shi, Structural basis of pre-mRNA splicing. *Science* **349**, 1191–1198 (2015). [Medline doi:10.1126/science.aac8159](#)
26. T. A. Steitz, J. A. Steitz, A general two-metal-ion mechanism for catalytic RNA. *Proc. Natl. Acad. Sci. U.S.A.* **90**, 6498–6502 (1993). [Medline doi:10.1073/pnas.90.14.6498](#)

27. R. T. Chan, A. R. Robart, K. R. Rajashankar, A. M. Pyle, N. Toor, Crystal structure of a group II intron in the pre-catalytic state. *Nat. Struct. Mol. Biol.* **19**, 555–557 (2012). [Medline](#) [doi:10.1038/nsmb.2270](#)
28. M. Marcia, A. M. Pyle, Visualizing group II intron catalysis through the stages of splicing. *Cell* **151**, 497–507 (2012). [Medline](#) [doi:10.1016/j.cell.2012.09.033](#)
29. E. J. Sontheimer, J. A. Steitz, The U5 and U6 small nuclear RNAs as active site components of the spliceosome. *Science* **262**, 1989–1996 (1993). [Medline](#) [doi:10.1126/science.8266094](#)
30. A. J. Newman, C. Norman, U5 snRNA interacts with exon sequences at 5' and 3' splice sites. *Cell* **68**, 743–754 (1992). [Medline](#) [doi:10.1016/0092-8674\(92\)90149-7](#)
31. A. L. Steckelberg, V. Boehm, A. M. Gromadzka, N. H. Gehring, CWC22 connects pre-mRNA splicing and exon junction complex assembly. *Cell Reports* **2**, 454–461 (2012). [Medline](#) [doi:10.1016/j.celrep.2012.08.017](#)
32. T. C. Yeh, H. L. Liu, C. S. Chung, N. Y. Wu, Y. C. Liu, S. C. Cheng, Splicing factor Cwc22 is required for the function of Prp2 and for the spliceosome to escape from a futile pathway. *Mol. Cell. Biol.* **31**, 43–53 (2011). [Medline](#) [doi:10.1128/MCB.00801-10](#)
33. G. Buchwald, S. Schüssler, C. Basquin, H. Le Hir, E. Conti, Crystal structure of the human eIF4AIII-CWC22 complex shows how a DEAD-box protein is inhibited by a MIF4G domain. *Proc. Natl. Acad. Sci. U.S.A.* **110**, E4611–E4618 (2013). [Medline](#) [doi:10.1073/pnas.1314684110](#)
34. L. A. Lindsey-Boltz, G. Chawla, N. Srinivasan, U. Vijayraghavan, M. A. Garcia-Blanco, The carboxy terminal WD domain of the pre-mRNA splicing factor Prp17p is critical for function. *RNA* **6**, 1289–1305 (2000). [Medline](#) [doi:10.1017/S1355838200000327](#)
35. C. Schneider, D. E. Agafonov, J. Schmitzová, K. Hartmuth, P. Fabrizio, R. Lührmann, Dynamic Contacts of U2, RES, Cwc25, Prp8 and Prp45 Proteins with the Pre-mRNA Branch-Site and 3' Splice Site during Catalytic Activation and Step 1 Catalysis in Yeast Spliceosomes. *PLOS Genet.* **11**, e1005539 (2015). [Medline](#) [doi:10.1371/journal.pgen.1005539](#)
36. D. S. McPheeters, P. Muhlenkamp, Spatial organization of protein-RNA interactions in the branch site-3' splice site region during pre-mRNA splicing in yeast. *Mol. Cell. Biol.* **23**, 4174–4186 (2003). [Medline](#) [doi:10.1128/MCB.23.12.4174-4186.2003](#)
37. C. Cretu *et al.*, Molecular architecture of SF3b and structural consequences of its cancer-related mutations. *Mol. Cell*, PDB ID: 5IFE (2016).
38. C. L. Will, C. Schneider, A. M. MacMillan, N. F. Katopodis, G. Neubauer, M. Wilm, R. Lührmann, C. C. Query, A novel U2 and U11/U12 snRNP protein that associates with the pre-mRNA branch site. *EMBO J.* **20**, 4536–4546 (2001). [Medline](#) [doi:10.1093/emboj/20.16.4536](#)
39. C. C. Query, S. A. Strobel, P. A. Sharp, Three recognition events at the branch-site adenine. *EMBO J.* **15**, 1392–1402 (1996). [Medline](#)

40. G. Edwalds-Gilbert, D. H. Kim, E. Silverman, R. J. Lin, Definition of a spliceosome interaction domain in yeast Prp2 ATPase. *RNA* **10**, 210–220 (2004). [Medline](#) [doi:10.1261/rna.5151404](#)
41. A. M. Wlodaver, J. P. Staley, The DExD/H-box ATPase Prp2p destabilizes and proofreads the catalytic RNA core of the spliceosome. *RNA* **20**, 282–294 (2014). [Medline](#) [doi:10.1261/rna.042598.113](#)
42. H. L. Liu, S. C. Cheng, The interaction of Prp2 with a defined region of the intron is required for the first splicing reaction. *Mol. Cell. Biol.* **32**, 5056–5066 (2012). [Medline](#) [doi:10.1128/MCB.01109-12](#)
43. R. B. Darman, M. Seiler, A. A. Agrawal, K. H. Lim, S. Peng, D. Aird, S. L. Bailey, E. B. Bhavsar, B. Chan, S. Colla, L. Corson, J. Feala, P. Fekkes, K. Ichikawa, G. F. Keaney, L. Lee, P. Kumar, K. Kunii, C. MacKenzie, M. Matijevic, Y. Mizui, K. Myint, E. S. Park, X. Puyang, A. Selvaraj, M. P. Thomas, J. Tsai, J. Y. Wang, M. Warmuth, H. Yang, P. Zhu, G. Garcia-Manero, R. R. Furman, L. Yu, P. G. Smith, S. Buonamici, Cancer-Associated SF3B1 Hotspot Mutations Induce Cryptic 3' Splice Site Selection through Use of a Different Branch Point. *Cell Reports* **13**, 1033–1045 (2015). [Medline](#) [doi:10.1016/j.celrep.2015.09.053](#)
44. S. Alsafadi, A. Houy, A. Battistella, T. Popova, M. Wassem, E. Henry, F. Tirode, A. Constantinou, S. Piperno-Neumann, S. Roman-Roman, M. Dutertre, M. H. Stern, Cancer-associated SF3B1 mutations affect alternative splicing by promoting alternative branchpoint usage. *Nat. Commun.* **7**, 10615 (2016). [Medline](#) [doi:10.1038/ncomms10615](#)
45. S. Bonnal, L. Vigevani, J. Valcárcel, The spliceosome as a target of novel antitumour drugs. *Nat. Rev. Drug Discov.* **11**, 847–859 (2012). [Medline](#) [doi:10.1038/nrd3823](#)
46. B. C. Rymond, M. Rosbash, Cleavage of 5' splice site and lariat formation are independent of 3' splice site in yeast mRNA splicing. *Nature* **317**, 735–737 (1985). [Medline](#) [doi:10.1038/317735a0](#)
47. C. Kappel, U. Zachariae, N. Dölker, H. Grubmüller, An unusual hydrophobic core confers extreme flexibility to HEAT repeat proteins. *Biophys. J.* **99**, 1596–1603 (2010). [Medline](#) [doi:10.1016/j.bpj.2010.06.032](#)
48. E. Conti, C. W. Müller, M. Stewart, Karyopherin flexibility in nucleocytoplasmic transport. *Curr. Opin. Struct. Biol.* **16**, 237–244 (2006). [Medline](#) [doi:10.1016/j.sbi.2006.03.010](#)
49. A. G. Cook, E. Conti, Nuclear export complexes in the frame. *Curr. Opin. Struct. Biol.* **20**, 247–252 (2010). [Medline](#) [doi:10.1016/j.sbi.2010.01.012](#)
50. C. Yan, R. Wan, R. Bai, G. Huang, Y. Shi, Structure of a yeast catalytically activated spliceosome at 3.5 Å resolution. *Science* 10.1126/science.aag0291 10.1126/science.aag0291 (2016). [Medline](#) [doi:10.1126/science.aag0291](#)
51. A. Yokoi, Y. Kotake, K. Takahashi, T. Kadokawa, Y. Matsumoto, Y. Minoshima, N. H. Sugi, K. Sagane, M. Hamaguchi, M. Iwata, Y. Mizui, Biological validation that SF3b is a target of the antitumor macrolide pladienolide. *FEBS J.* **278**, 4870–4880 (2011). [Medline](#) [doi:10.1111/j.1742-4658.2011.08387.x](#)

52. T. W. Chiang, S. C. Cheng, A weak spliceosome-binding domain of Yju2 functions in the first step and bypasses Prp16 in the second step of splicing. *Mol. Cell. Biol.* **33**, 1746–1755 (2013). [Medline](#) [doi:10.1128/MCB.00035-13](#)
53. S. L. Yean, R. J. Lin, U4 small nuclear RNA dissociates from a yeast spliceosome and does not participate in the subsequent splicing reaction. *Mol. Cell. Biol.* **11**, 5571–5577 (1991). [Medline](#) [doi:10.1128/MCB.11.11.5571](#)
54. A. Chari, D. Haselbach, J. M. Kirves, J. Ohmer, E. Paknia, N. Fischer, O. Ganichkin, V. Möller, J. J. Frye, G. Petzold, M. Jarvis, M. Tietzel, C. Grimm, J. M. Peters, B. A. Schulman, K. Tittmann, J. Markl, U. Fischer, H. Stark, ProteoPlex: Stability optimization of macromolecular complexes by sparse-matrix screening of chemical space. *Nat. Methods* **12**, 859–865 (2015). [Medline](#) [doi:10.1038/nmeth.3493](#)
55. G. Edwalds-Gilbert, D. H. Kim, S. H. Kim, Y. H. Tseng, Y. Yu, R. J. Lin, Dominant negative mutants of the yeast splicing factor Prp2 map to a putative cleft region in the helicase domain of DExD/H-box proteins. *RNA* **6**, 1106–1119 (2000). [Medline](#) [doi:10.1017/S1355838200992483](#)
56. A. Leitner, T. Walzthoeni, R. Aebersold, Lysine-specific chemical cross-linking of protein complexes and identification of cross-linking sites using LC-MS/MS and the xQuest/xProphet software pipeline. *Nat. Protoc.* **9**, 120–137 (2014). [Medline](#) [doi:10.1038/nprot.2013.168](#)
57. B. Yang, Y. J. Wu, M. Zhu, S. B. Fan, J. Lin, K. Zhang, S. Li, H. Chi, Y. X. Li, H. F. Chen, S. K. Luo, Y. H. Ding, L. H. Wang, Z. Hao, L. Y. Xiu, S. Chen, K. Ye, S. M. He, M. Q. Dong, Identification of cross-linked peptides from complex samples. *Nat. Methods* **9**, 904–906 (2012). [Medline](#) [doi:10.1038/nmeth.2099](#)
58. M. van Heel, G. Harauz, E. V. Orlova, R. Schmidt, M. Schatz, A new generation of the IMAGIC image processing system. *J. Struct. Biol.* **116**, 17–24 (1996). [Medline](#) [doi:10.1006/jsb.1996.0004](#)
59. J. A. Mindell, N. Grigorieff, Accurate determination of local defocus and specimen tilt in electron microscopy. *J. Struct. Biol.* **142**, 334–347 (2003). [Medline](#) [doi:10.1016/S1047-8477\(03\)00069-8](#)
60. S. H. Scheres, RELION: Implementation of a Bayesian approach to cryo-EM structure determination. *J. Struct. Biol.* **180**, 519–530 (2012). [Medline](#) [doi:10.1016/j.jsb.2012.09.006](#)
61. E. F. Pettersen, T. D. Goddard, C. C. Huang, G. S. Couch, D. M. Greenblatt, E. C. Meng, T. E. Ferrin, UCSF Chimera—a visualization system for exploratory research and analysis. *J. Comput. Chem.* **25**, 1605–1612 (2004). [Medline](#) [doi:10.1002/jcc.20084](#)
62. P. Emsley, B. Lohkamp, W. G. Scott, K. Cowtan, Features and development of Coot. *Acta Crystallogr. D Biol. Crystallogr.* **66**, 486–501 (2010). [Medline](#) [doi:10.1107/S0907444910007493](#)
63. P. D. Adams, P. V. Afonine, G. Bunkóczki, V. B. Chen, I. W. Davis, N. Echols, J. J. Headd, L. W. Hung, G. J. Kapral, R. W. Grosse-Kunstleve, A. J. McCoy, N. W. Moriarty, R. Oeffner, R. J. Read, D. C. Richardson, J. S. Richardson, T. C. Terwilliger, P. H. Zwart, PHENIX: A comprehensive Python-based system for macromolecular structure solution.

Acta Crystallogr. D Biol. Crystallogr. **66**, 213–221 (2010). [Medline](#)
[doi:10.1107/S0907444909052925](#)

64. I. W. Davis, A. Leaver-Fay, V. B. Chen, J. N. Block, G. J. Kapral, X. Wang, L. W. Murray, W. B. Arendall 3rd, J. Snoeyink, J. S. Richardson, D. C. Richardson, MolProbity: All-atom contacts and structure validation for proteins and nucleic acids. *Nucleic Acids Res.* **35** (Web Server), W375 (2007). [Medline](#) [doi:10.1093/nar/gkm216](#)
65. D. E. Agafonov, J. Deckert, E. Wolf, P. Odenwälder, S. Bessonov, C. L. Will, H. Urlaub, R. Lührmann, Semiquantitative proteomic analysis of the human spliceosome via a novel two-dimensional gel electrophoresis method. *Mol. Cell. Biol.* **31**, 2667–2682 (2011). [Medline](#) [doi:10.1128/MCB.05266-11](#)
66. P. C. Lin, R. M. Xu, Structure and assembly of the SF3a splicing factor complex of U2 snRNP. *EMBO J.* **31**, 1579–1590 (2012). [Medline](#) [doi:10.1038/emboj.2012.7](#)
67. E. Absmeier, L. Rosenberger, L. Apelt, C. Becke, K. F. Santos, U. Stelzl, M. C. Wahl, A noncanonical PWI domain in the N-terminal helicase-associated region of the spliceosomal Brr2 protein. *Acta Crystallogr. D Biol. Crystallogr.* **71**, 762–771 (2015). [Medline](#) [doi:10.1107/S1399004715001005](#)
68. A. M. van Roon, J. C. Yang, D. Mathieu, W. Bermel, K. Nagai, D. Neuhaus, ^{113}Cd NMR experiments reveal an unusual metal cluster in the solution structure of the yeast splicing protein Bud31p. *Angew. Chem. Int. Ed. Engl.* **54**, 4861–4864 (2015). [Medline](#) [doi:10.1002/anie.201412210](#)
69. M. Albers, A. Diment, M. Muraru, C. S. Russell, J. D. Beggs, Identification and characterization of Prp45p and Prp46p, essential pre-mRNA splicing factors. *RNA* **9**, 138–150 (2003). [Medline](#) [doi:10.1261/rna.211903](#)
70. A. Dziembowski, A. P. Ventura, B. Rutz, F. Caspary, C. Faux, F. Halgand, O. Laprévote, B. Séraphin, Proteomic analysis identifies a new complex required for nuclear pre-mRNA retention and splicing. *EMBO J.* **23**, 4847–4856 (2004). [Medline](#) [doi:10.1038/sj.emboj.7600482](#)
71. P. Wysoczański, C. Schneider, S. Xiang, F. Munari, S. Trowitzsch, M. C. Wahl, R. Lührmann, S. Becker, M. Zweckstetter, Cooperative structure of the heterotrimeric pre-mRNA retention and splicing complex. *Nat. Struct. Mol. Biol.* **21**, 911–918 (2014). [Medline](#) [doi:10.1038/nsmb.289](#)
72. M. A. Brooks, A. Dziembowski, S. Quevillon-Cheruel, V. Henriot, C. Faux, H. van Tilburgh, B. Séraphin, Structure of the yeast Pml1 splicing factor and its integration into the RES complex. *Nucleic Acids Res.* **37**, 129–143 (2009). [Medline](#) [doi:10.1093/nar/gkn894](#)
73. S. Trowitzsch, G. Weber, R. Lührmann, M. C. Wahl, Crystal structure of the Pml1p subunit of the yeast precursor mRNA retention and splicing complex. *J. Mol. Biol.* **385**, 531–541 (2009). [Medline](#) [doi:10.1016/j.jmb.2008.10.087](#)
74. H. Walbott, S. Mouffok, R. Capeyrou, S. Lebaron, O. Humbert, H. van Tilburgh, Y. Henry, N. Leulliot, Prp43p contains a processive helicase structural architecture with a specific regulatory domain. *EMBO J.* **29**, 2194–2204 (2010). [Medline](#) [doi:10.1038/emboj.2010.102](#)